Higgs and Vector Boson Decays to a Meson and a Photon at the ATLAS experiment

Robert Ward

University of Hamburg

DESY Particle Physics Seminar

25th March 2024

This project has received funding from the European Research Council (ERC) under the European Union's Horizon 2020 research and innovation programme under grant agreement no 714893 (ExclusiveHiggs)

The Higgs Boson

- Higgs boson coupling strength to fermions ∝ mass in the SM
  - Only observed Higgs-quark couplings to-date are for t- and b-quarks
  - Large QCD backgrounds at the LHC make $H \rightarrow q\bar{q}$ inclusive searches challenging

Fermion couplings

$$g_f^{SM} = \frac{m_f}{v}\sqrt{2}$$

$v \approx 246$ GeV

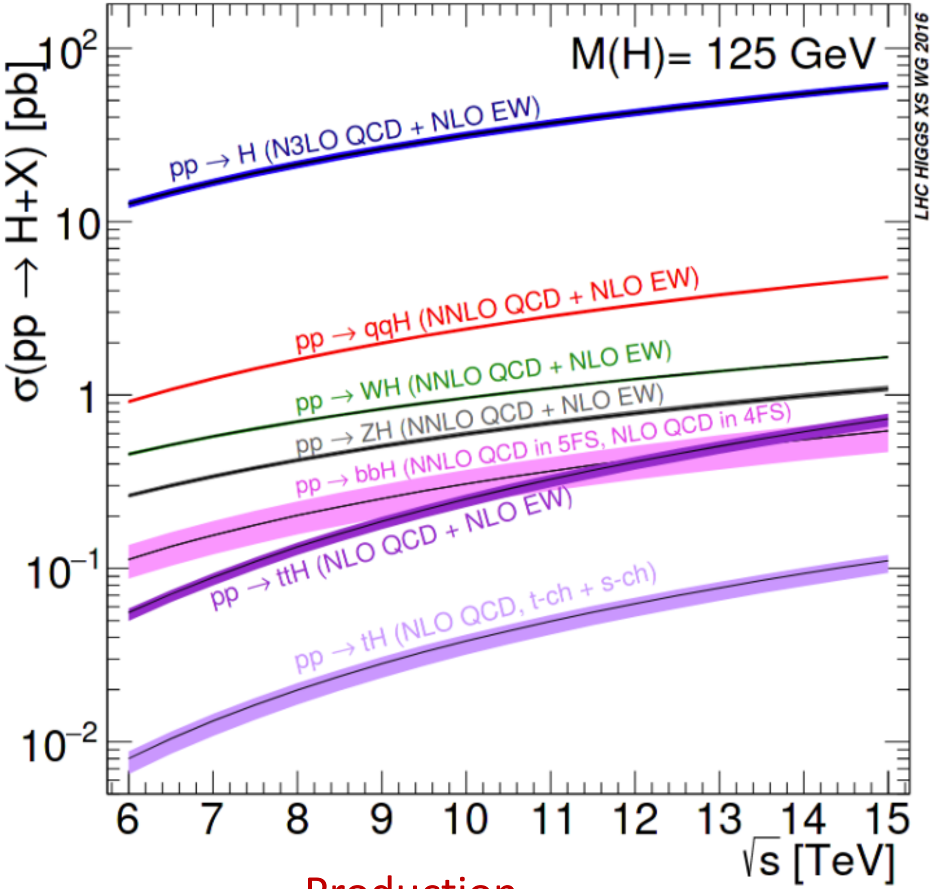

Production

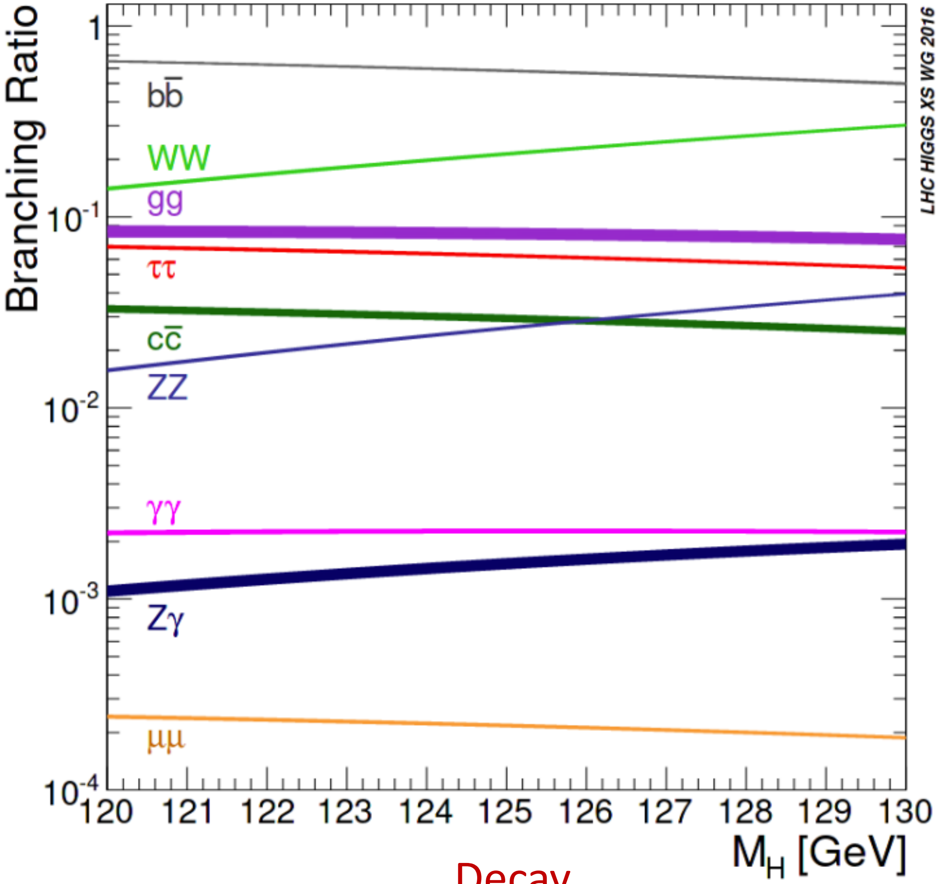

Decay

CERN-2017-002 (2016)

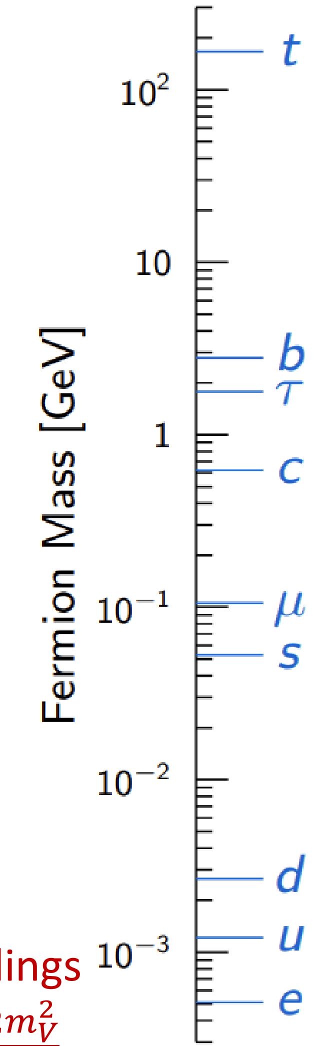

W/Z couplings

$$g_V^{SM} = \frac{2m_V^2}{v}$$

$H(Z) \to \mathcal{M}\gamma$: Motivation

- Search for exclusive $H(Z) \to \mathcal{M}\gamma$ decays: $\mathcal{M}$ = vector mesons ($q\bar{q}; J^{PC} = 1^{--}$)
  - Two destructively interfering contributions to decay amplitude

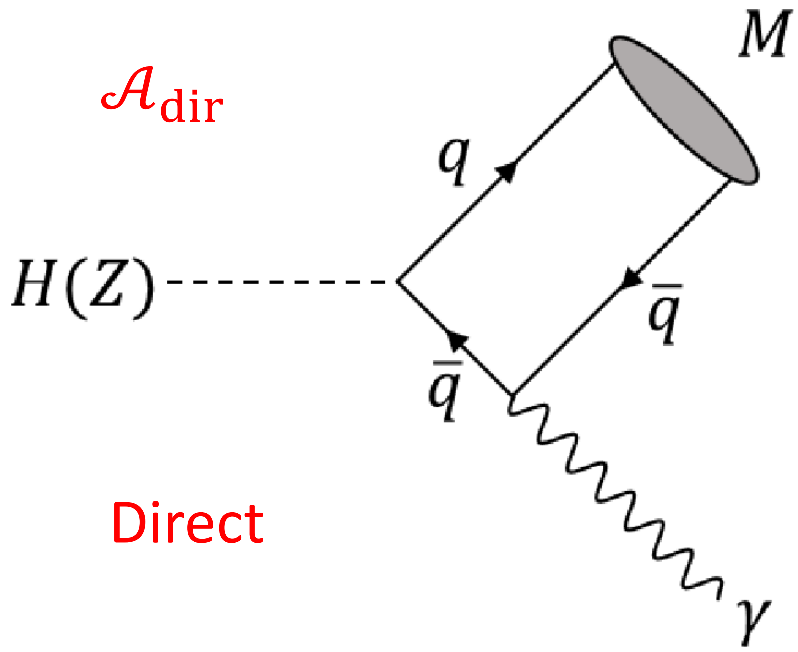

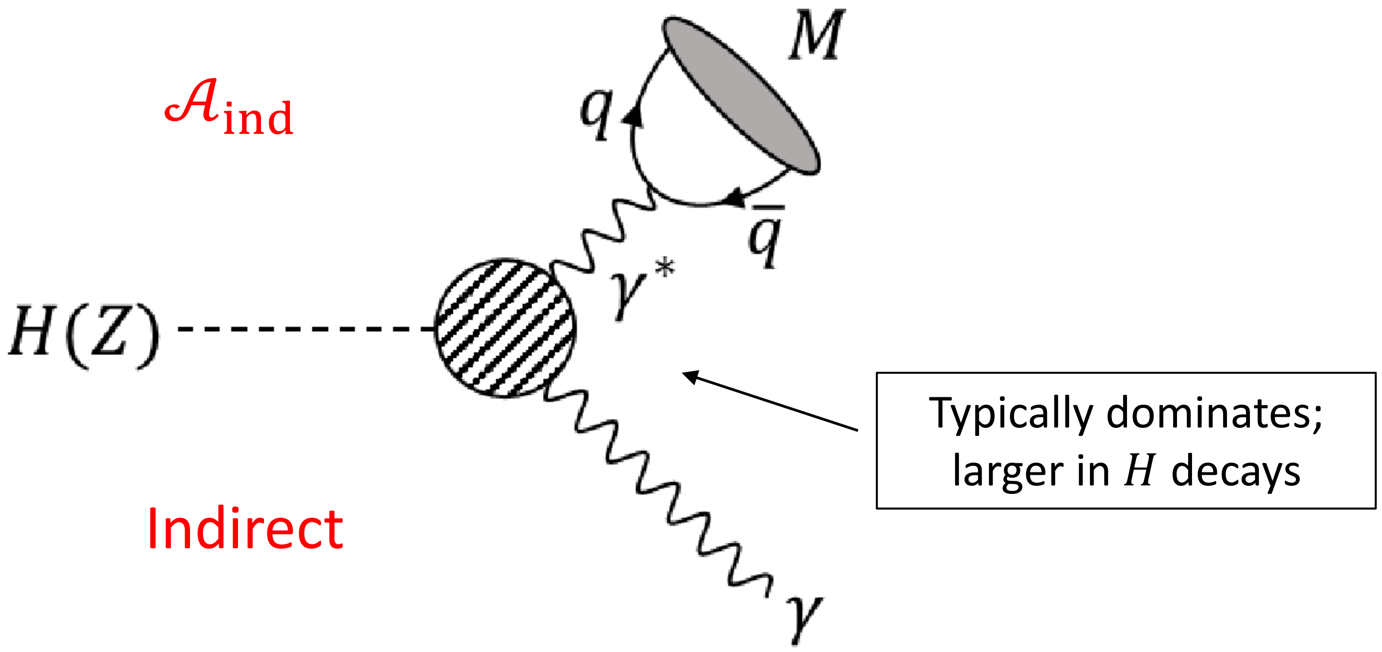

- ***H* decays:** probe magnitude and sign of quark Yukawa couplings – $\mathcal{O}(10^{-6})$ BRs
  - Distinct signatures reduce large QCD backgrounds
- ***Z* decays:** provide reference channels and tests of QCD factorisation – $\mathcal{O}(10^{-8})$ BRs
  - $1000 \times$ higher production rate of Z bosons at LHC compared to Higgs bosons: probe rarer decays

$H(Z) \rightarrow \mathcal{M}\gamma$: SM Expectations

Heavy mesons (quarkonia) $q = b, c$: J/ψ, $\psi(2S)$, $\Upsilon(1S)$, $\Upsilon(2S)$, $\Upsilon(3S)$

Light mesons $q = s, d, u$: ϕ, ρ, ω

SM expected branching fraction $\mathcal{B}(H/Z \rightarrow \mathcal{M}\gamma)$			
Meson $\mathcal{M}$	H	Z	References
J/ψ	$(2.99^{+0.16}_{-0.15}) \times 10^{-6}$	$(8.96^{+1.51}_{-1.38}) \times 10^{-8}$	[27–29]
$\psi(2S)$	$(1.03 \pm 0.06) \times 10^{-6}$	–	[28][1]
$\Upsilon(1S)$	$(5.22^{+2.02}_{-1.70}) \times 10^{-9}$	$(4.80^{+0.26}_{-0.25}) \times 10^{-8}$	[27–29]
$\Upsilon(2S)$	$(1.42^{+0.72}_{-0.57}) \times 10^{-9}$	$(2.44^{+0.14}_{-0.13}) \times 10^{-8}$	[27–29]
$\Upsilon(3S)$	$(0.91^{+0.48}_{-0.38}) \times 10^{-9}$	$(1.88^{+0.11}_{-0.10}) \times 10^{-8}$	[27–29]
ϕ	$(2.31 \pm 0.11) \times 10^{-6}$	$(1.04 \pm 0.12) \times 10^{-8}$	[25, 30]
ρ	$(1.68 \pm 0.08) \times 10^{-5}$	$(4.19 \pm 0.47) \times 10^{-9}$	[25, 30]
ω	$(1.48 \pm 0.08) \times 10^{-6}$	$(2.82 \pm 0.40) \times 10^{-8}$	[25, 30]

Theory Refs: 25: JHEP 08 (2015) 012, 27: PRD 95 (2017) 054018, 28: PRD 96 (2017) 116014, 29: PRD 97 (2018) 016009, 30: JHEP 04 (2015) 101

- $H \rightarrow \Upsilon(nS)\gamma$ particularly sensitive to BSM physics (e.g arXiv:2209.01200)

ATL-PHYS-PUB-2023-004

Flavour-Violating Decays of the Higgs and Z Bosons into $\mathcal{M}\gamma$

- Choosing "flavoured" $\mathcal{M}$ $(q\bar{q}')$ probes flavour-violating couplings
  - Forbidden at tree-level within the SM
- Any observation would imply new physics
  - Similar signatures to the rare SM decays

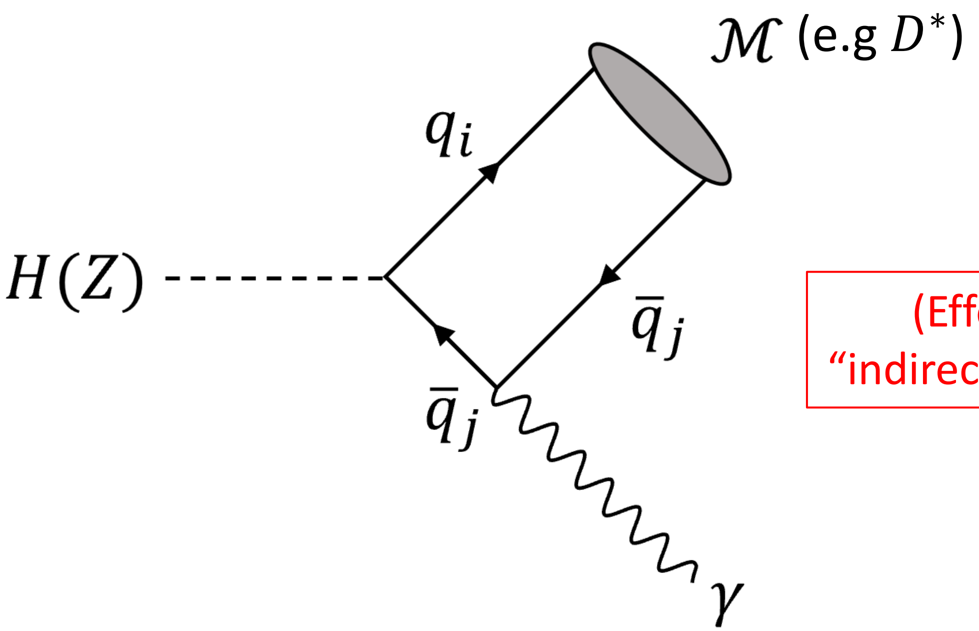

$H(Z) \to \mathcal{M}\gamma$ with flavour violation

(Effectively) no "indirect" contribution!

J. Phys. G 47 (2020) 12, 125001

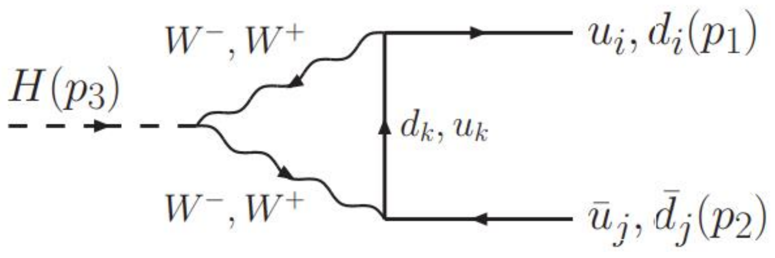

(For example)

$H \to q_i q_j$	Br
$H \to uc$	5.00×10^{-20}
$H \to ds$	1.19×10^{-11}
$H \to db$	5.16×10^{-9}
$H \to sb$	1.15×10^{-7}

SM contributions to $H \to q_i\bar{q}_j$

SM Expected Branching Fractions	
$H \to K^*\gamma$	1.0×10^{-19}
$H \to D^*\gamma$	7.0×10^{-27}
$Z \to K_s^0\gamma$	3.3×10^{-20}
$Z \to D^0\gamma$	1.4×10^{-25}

Recent SM $H(Z) \to \mathcal{M}\gamma$ predictions: arXiv:2312.11211

$W^{\pm} \to \mathcal{M}^{\pm}\gamma$: Motivation

- ***W* decays:** novel tests of QCD factorisation and quark couplings – $\mathcal{O}(10^{-9})$ BRs
  - Potential new probe for W mass measurement through fully reconstructed decays

Direct

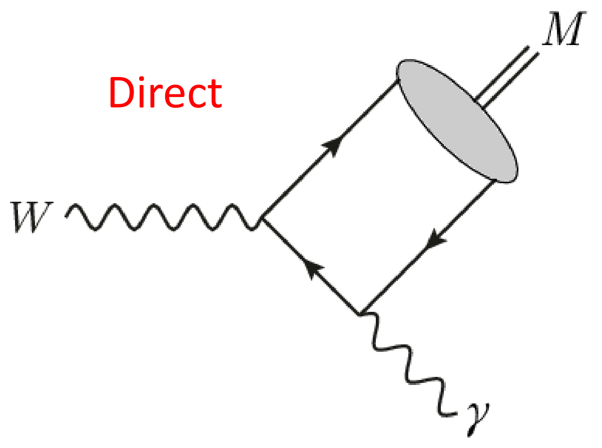

Indirect

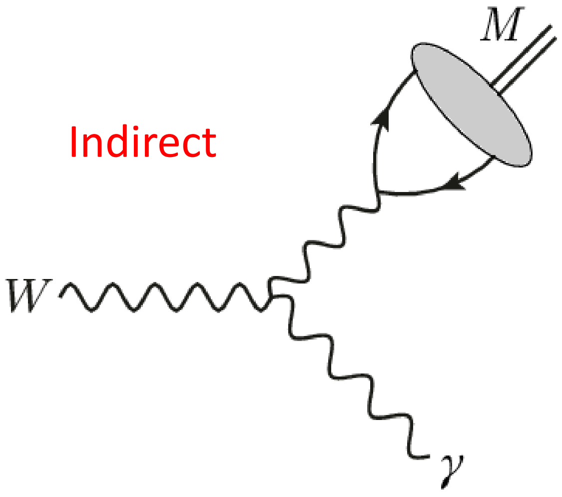

SM expected branching fraction $\mathcal{B}(W^{\pm} \to \mathcal{M}\gamma)$	
Meson $\mathcal{M}$	$W^{\pm}$
$\pi^{\pm}$	$(3.25 \pm 0.68) \times 10^{-9}$
$\rho^{\pm}$	$(8.74 \pm 1.90) \times 10^{-9}$
$K^{\pm}$	$(2.31 \pm 0.82) \times 10^{-10}$

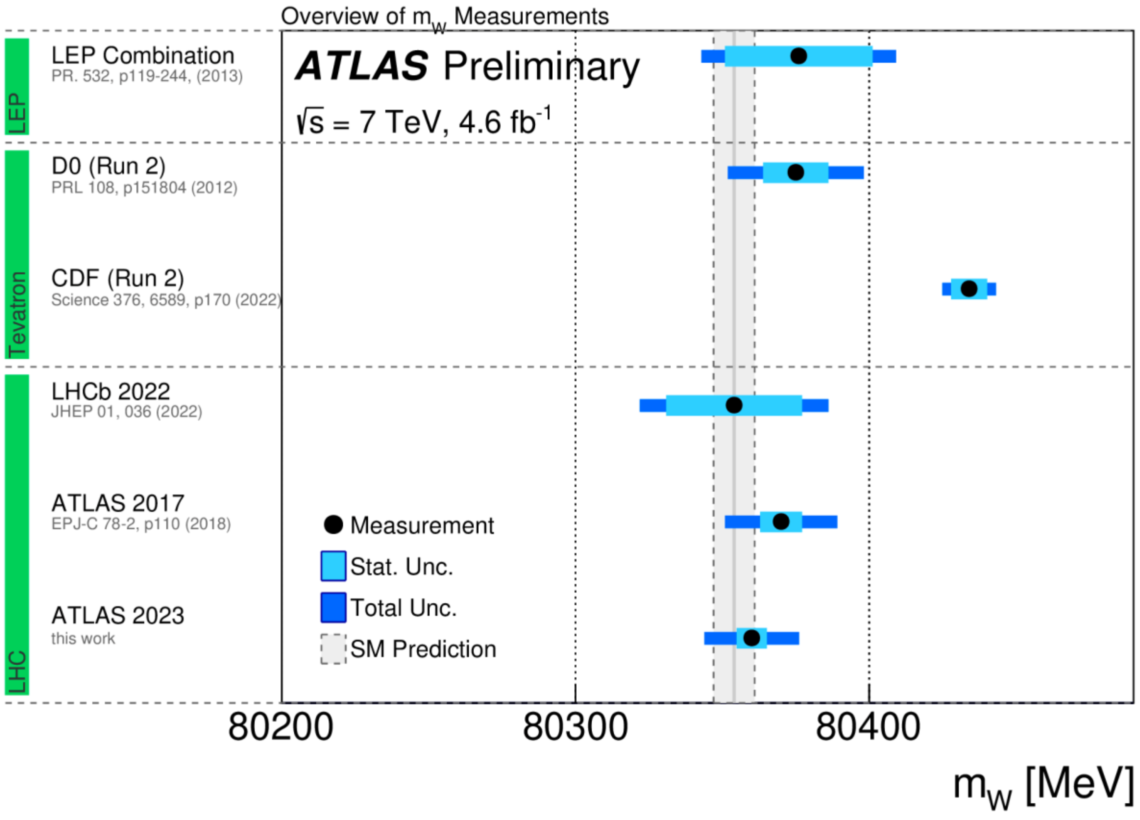

ATLAS-PHOTO-2023-022

The ATLAS Experiment

- General-purpose particle physics experiment at the LHC
  - 3k authors across 182 institutions in 42 countries

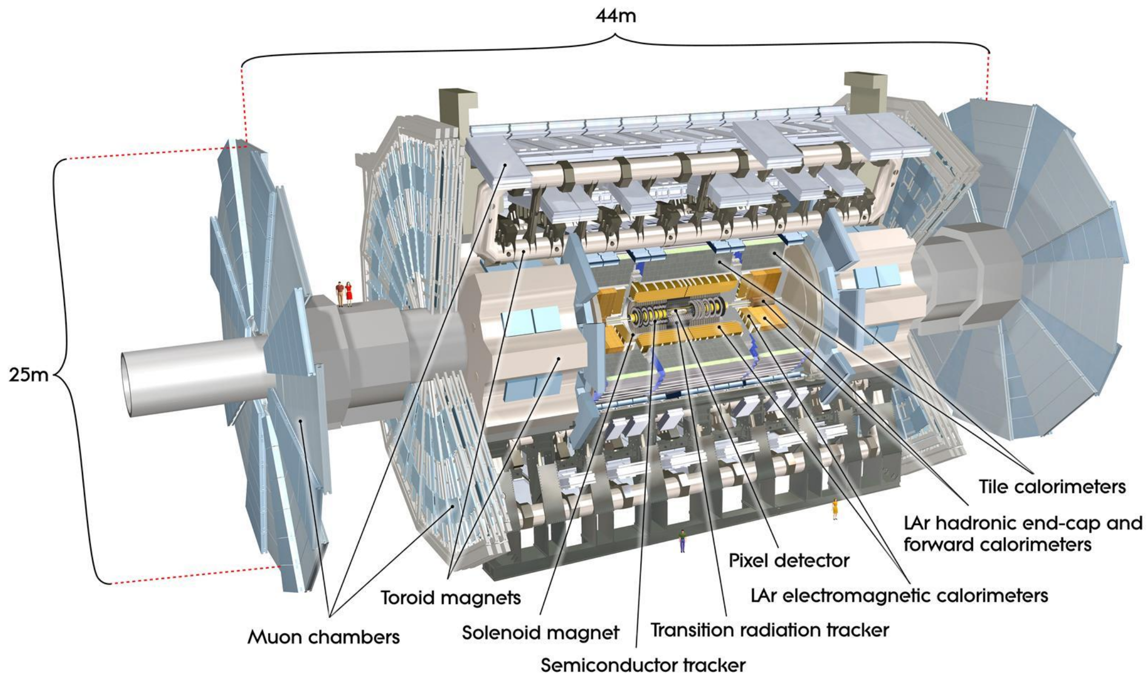

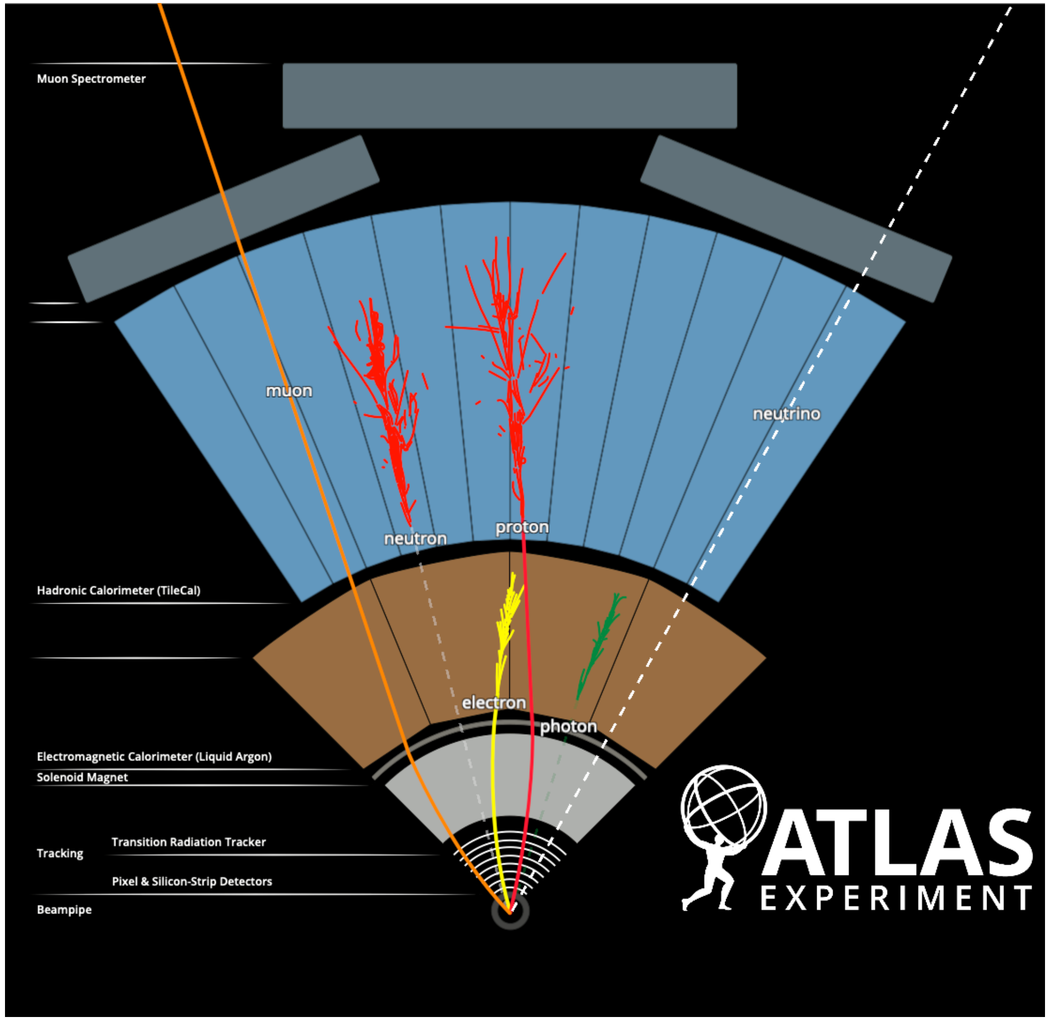

- Event rate ≈ 40 MHz – capture interesting interactions with a two-level trigger system
  - Level-1 (L1): Hardware based (→ 100 kHz)
  - Level-2/High-level Trigger (HLT): Software based (→ 1 kHz)

Public Results

- ATLAS has set limits on a multitude of these exclusive decay channels
  - Employ dedicated triggers and novel background model methods

Bold = Latest Result

Decay Channels	$\sqrt{s}$ (TeV)	Lumi. (fb^{-1})	Publication
$H(Z) \to (J/\psi, \Upsilon(nS, n = 1,2,3))\gamma$	8	20	PRL 114 (2015) 12, 121801
$H(Z) \to \phi\gamma$	13	2.7	PRL 117 (2016) 11, 111802
$H(Z) \to (\phi, \rho)\gamma$	**13**	**36**	**JHEP 07 (2018) 127**
$H(Z) \to (J/\psi, \psi(2S), \Upsilon(nS))\gamma$	13	36	PLB 786 (2018) 134-155
$H(Z) \to (J/\psi, \psi(2S), \Upsilon(nS))\gamma$	**13**	**139**	**EPJC 83 (2023) 781**
$H(Z) \to \omega\gamma$ & $H \to K^*\gamma$	**13**	**90 (134)**	**PLB 847 (2023) 138292**
$W^\pm \to (\pi^\pm, K^\pm, \rho^\pm)\gamma$	**13**	**137 (140)**	**arXiv:2309.15887**
$H \to D^*\gamma$ & $Z \to (D^0, K_s^0)\gamma$	**13**	**136**	**arXiv:2402.18731**

Time

Published last year!

Searches for exclusive Higgs boson decays into $D^*\gamma$ and Z boson decays into $D^0\gamma$ and $K_s^0\gamma$ in pp collisions at $\sqrt{s}$ = 13 TeV with the ATLAS detector

Submitted to PLB

Search for the exclusive W boson hadronic decays $W^\pm \to \pi^\pm\gamma$, $W^\pm \to K^\pm\gamma$ and $W^\pm \to \rho^\pm\gamma$ with the ATLAS detector

Submitted to PRL

$H(Z) \rightarrow (\phi, \rho)\gamma$: Overview

- $H \rightarrow \phi(K^+K^-)\gamma$: s-quark coupling
- $H \rightarrow \rho(\pi^+\pi^-)\gamma$: u- & d-quark couplings

JHEP 07 (2018) 127

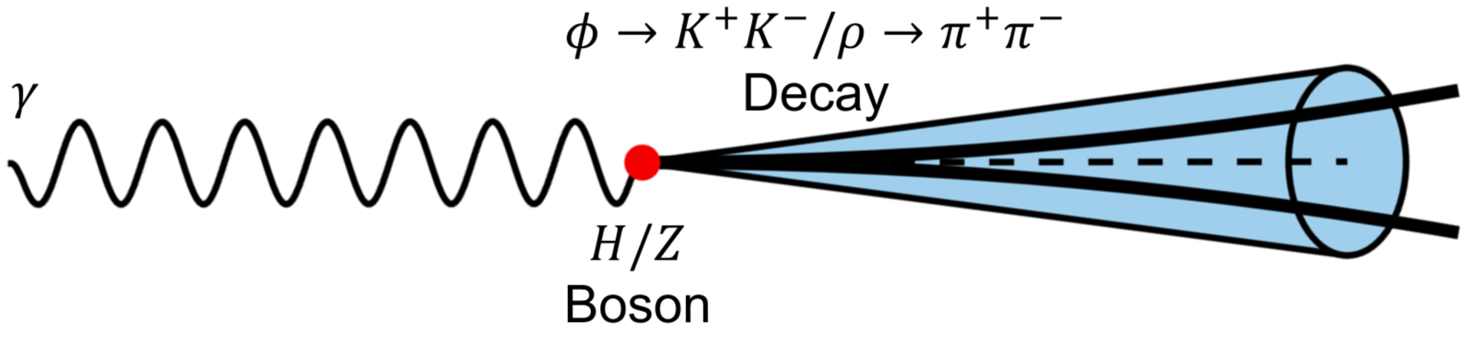

Event Signature

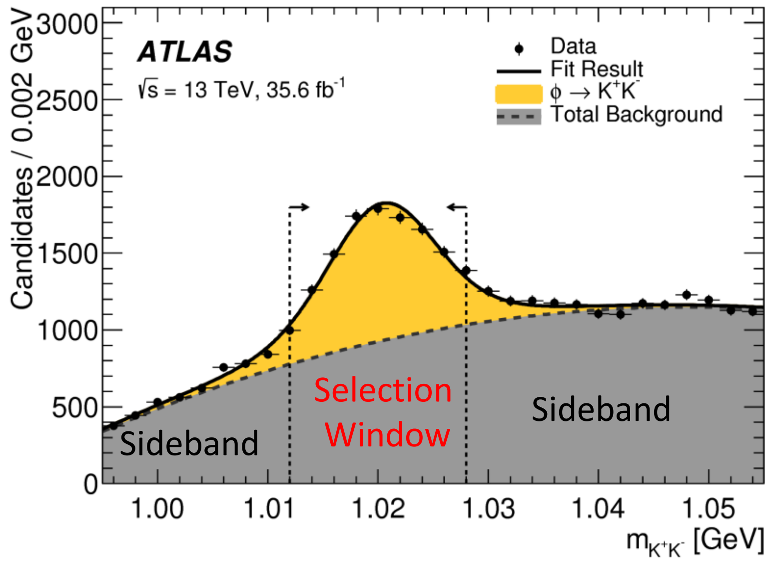

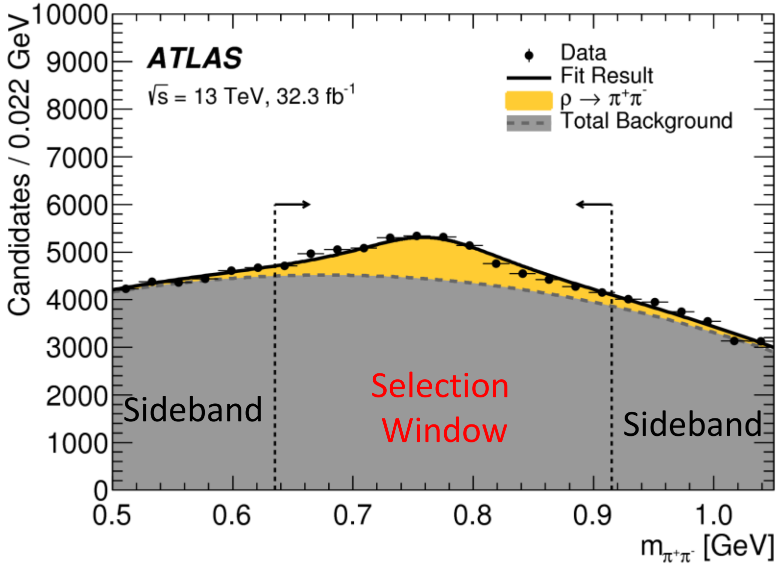

- **Dedicated** triggers based on single photon + modified τ-lepton algorithms
- Background from multi-jet and γ + jet sources
  - Non-parametric data-driven background model

$H(Z) \to (\phi, \rho)\gamma$: Trigger Strategy

- L1: Isolated EM object
  - Lowest p_T unprescaled trigger
- HLT: Collimated high-p_T track-pair consistent with ϕ/ρ mass recoiling against high-p_T photon
  - Adapted τ-lepton algorithms

Up to 83% efficiency w.r.t offline selection

Photon provides handle at L1

Capture meson decay using modified HLT τ-algorithms

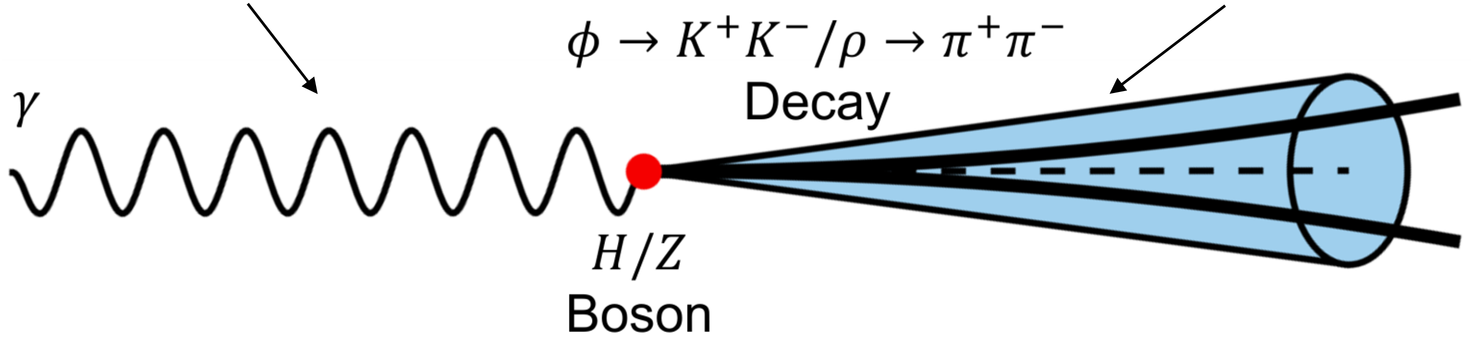

EPJC 77 (2017) 317

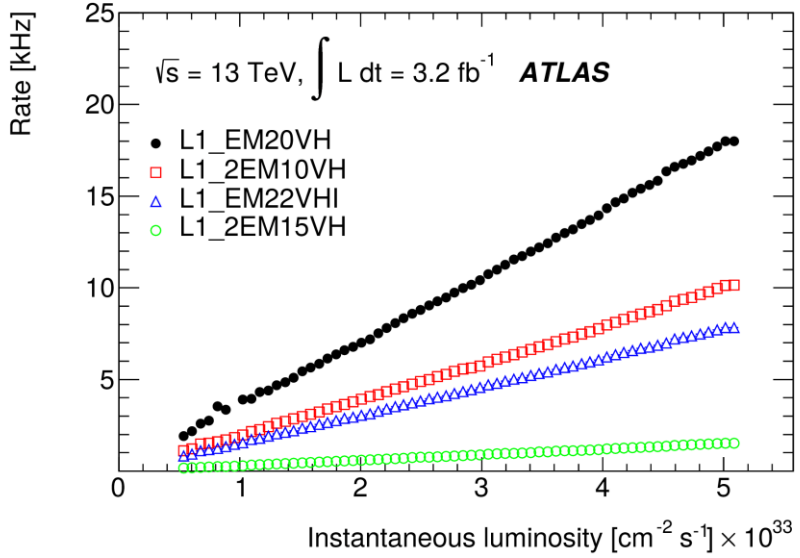

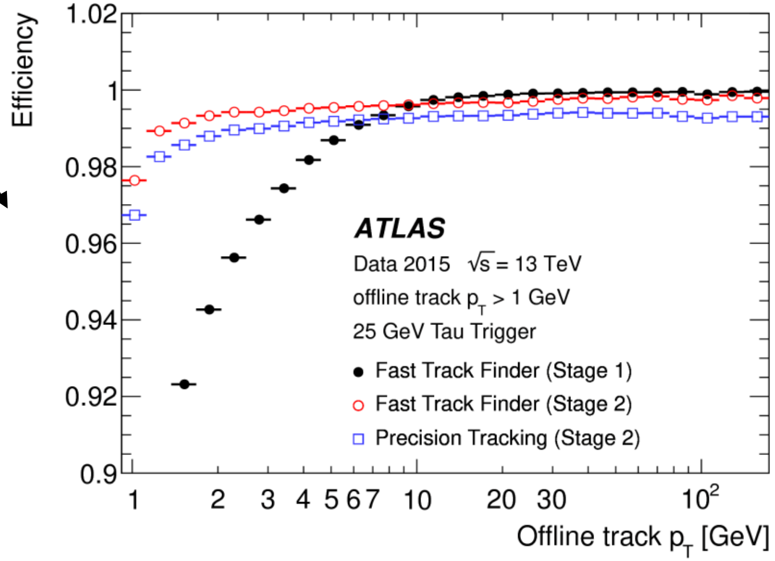

- Employ analogous triggers in other exclusive searches with hadronic final states
  - Adapt to target e.g K^*/D^0 decay instead

$H(Z) \to (\phi,\rho)\gamma$: Signal Properties

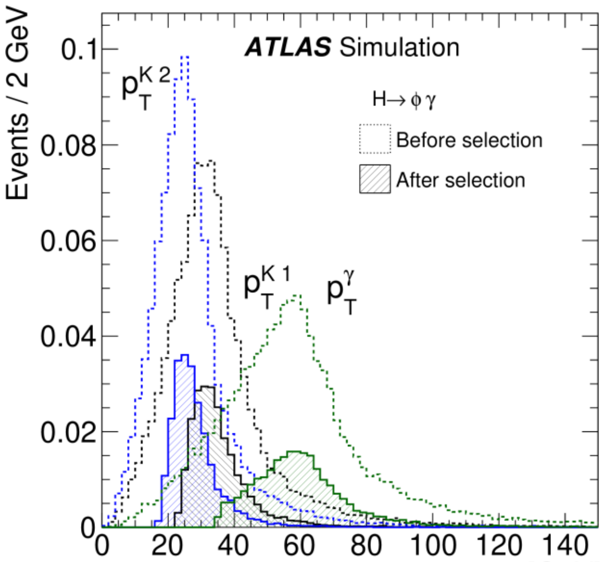

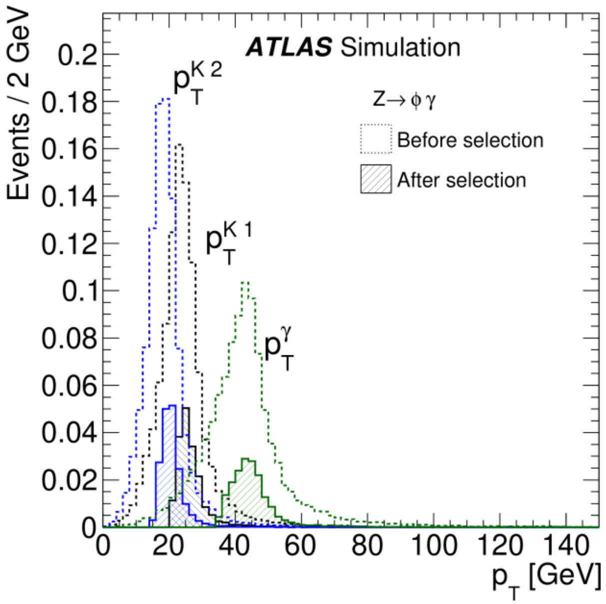

[JHEP 07 (2018) 127]

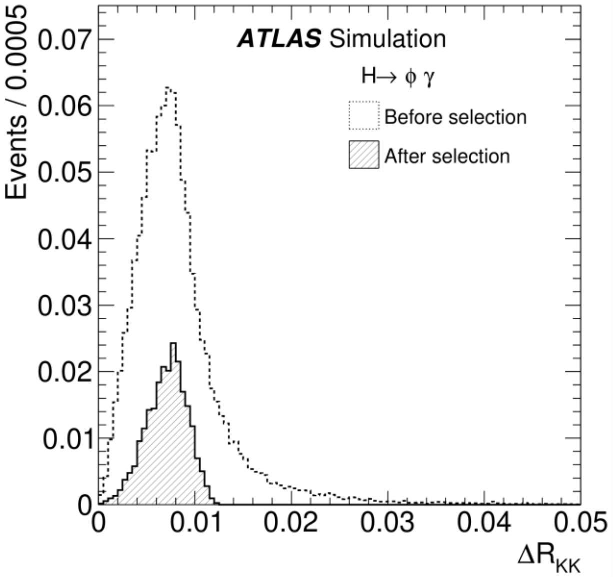

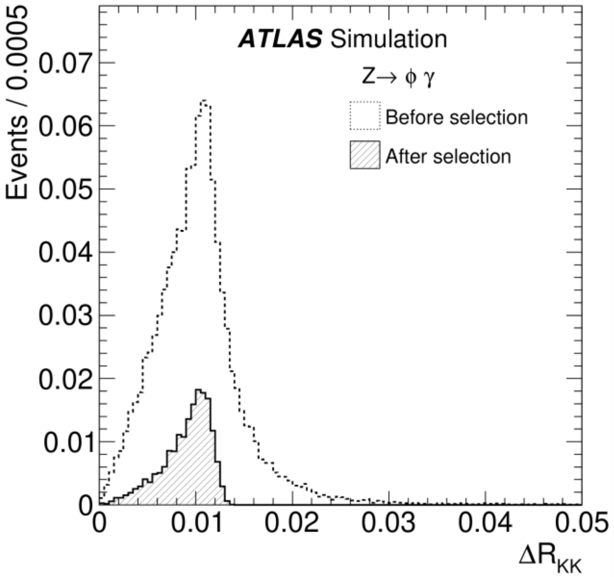

- Larger photon and track p_{T} in H decays leads to larger signal efficiencies than for Z decays

Total Signal Efficiency		
Channel	Z Signal	H Signal
$\phi\gamma$	10%	17%
$\rho\gamma$	2.4%	8%

- Small opening angles between decay products
  - Particularly for $\phi \to K^+K^-$: tracking in dense environments

[EPJC 77 (2017) 673]

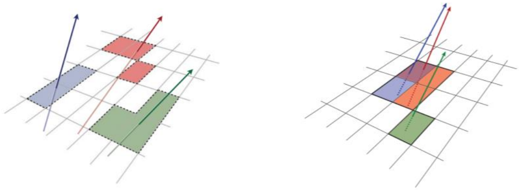

Single-Particle Clusters

Merged Clusters

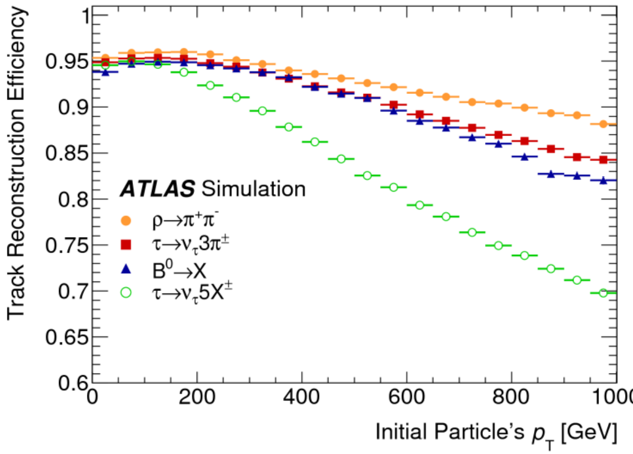

$H(Z) \rightarrow (\phi, \rho)\gamma$: Signal Modelling

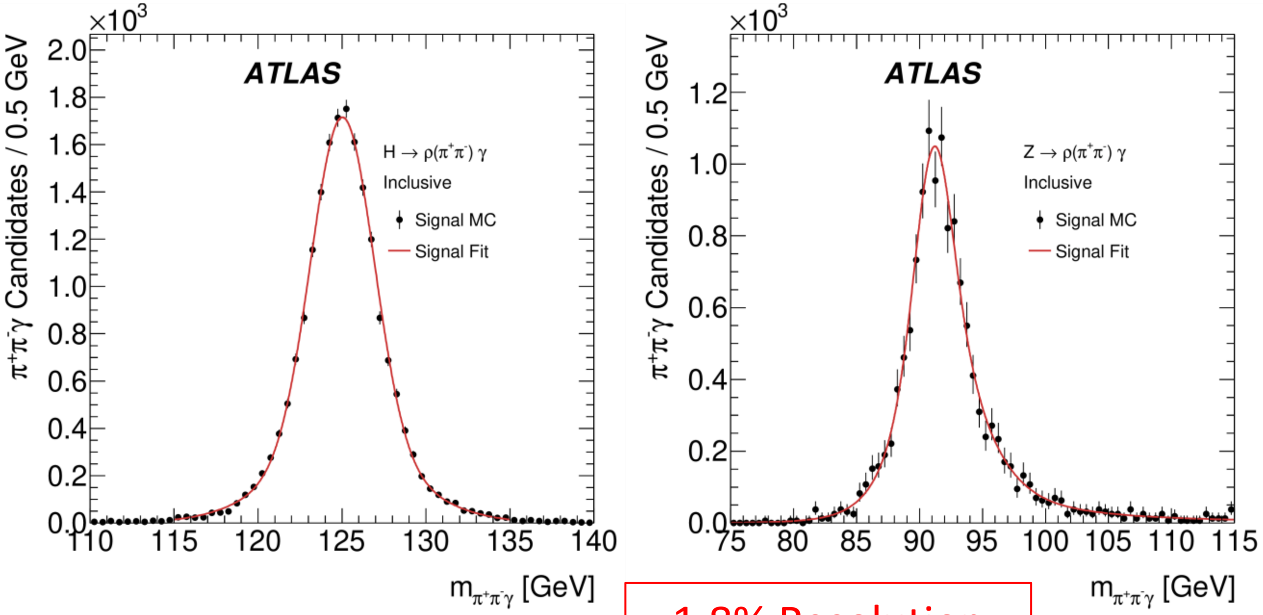

1.8% Resolution

Source of systematic uncertainty	Yield uncertainty
Total H cross section	6.3%
Total Z cross section	2.9%
Integrated luminosity	3.4%
Photon ID efficiency	2.5%
Trigger efficiency	2.0%
Tracking efficiency	6.0%

Uncertainties are considered, but they typically have a negligible impact on results

- Model boson mass distributions with analytical fits to simulated events
  - H decays – sum of two Gaussians with a common mean
  - Z decays - (sum of two Voigtians) × efficiency factor
    - Voigtian: convolution of Gaussian (detector resolution) and Lorentz (Z width) distributions
    - Efficiency factor: accounts for turn-on in signal efficiency with Z mass
- Analogous approach is applied in all exclusive $\mathcal{M}\gamma$ searches
  - Specific functions may vary

JHEP 07 (2018) 127

Aside: Non-Parametric Data Driven Background Modelling

- Non-parametric data-driven background model: *JHEP* 10 (2022) 001
  - Useful for non-resonant backgrounds from a mix of processes
    - Complex shape: difficult to model analytically/parametrically
    - Complex processes: difficult to simulate
- Use $H \to \phi\gamma$ with γ + jet MC as a case study
  - Discriminant variable: $m(\phi,\gamma)$ (three-body mass)

Pseudo-event: data-struct of $\mathcal{M}/\gamma$ 4-vectors + isolation variables

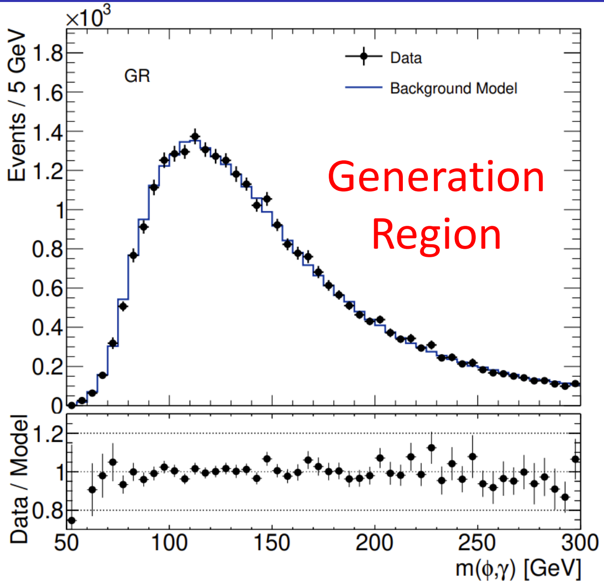

1. Model correlations in data in loose Generation Region
2. Sample many pseudo-events using model
3. Apply Validation Region selection to evaluate performance
4. Apply Signal Region selection (and smooth) for final model

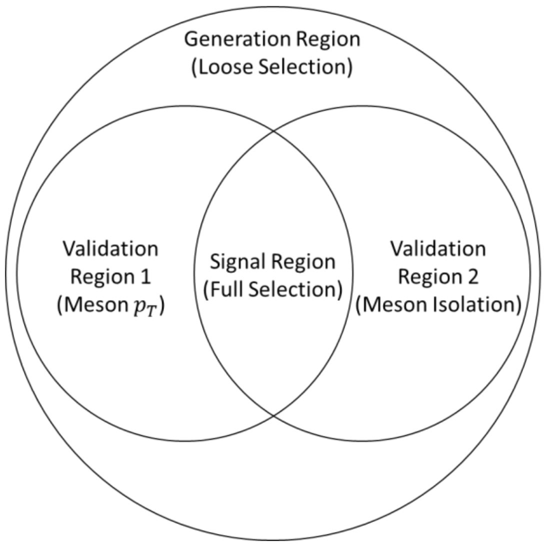

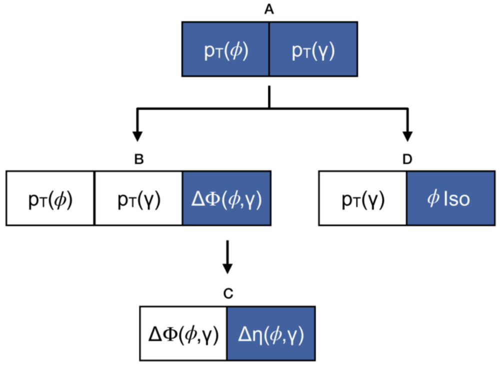

Sampling Scheme

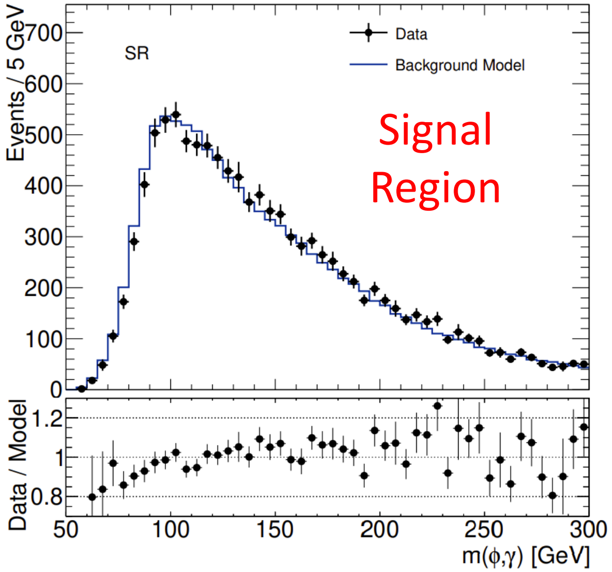

Non-Parametric Data Driven Model: Validation

➤ Many ways to evaluate performance! – validation regions, sideband selections, alternate variables

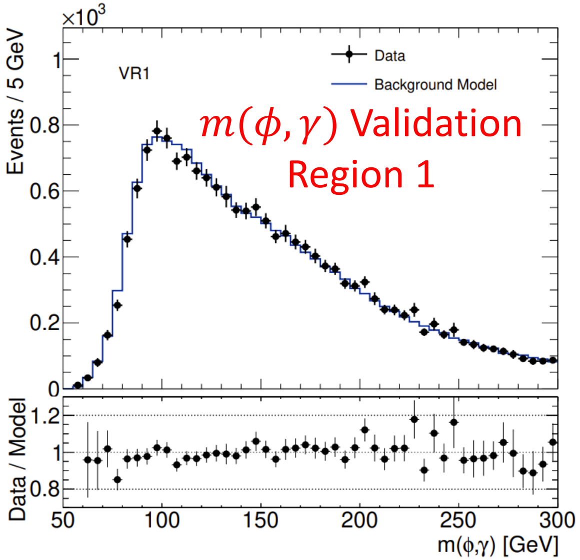

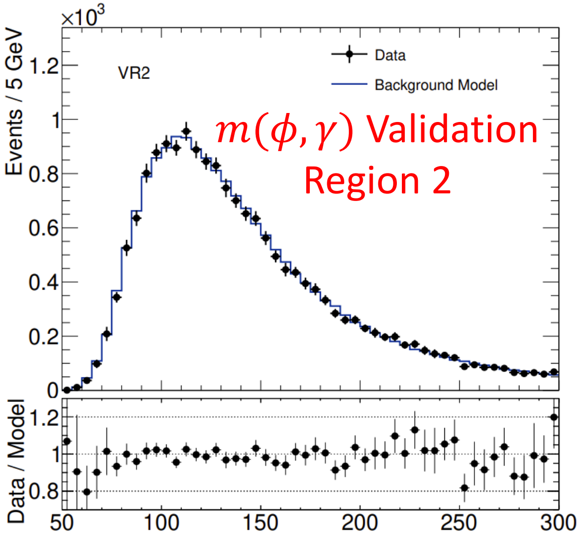

JHEP 10 (2022) 001

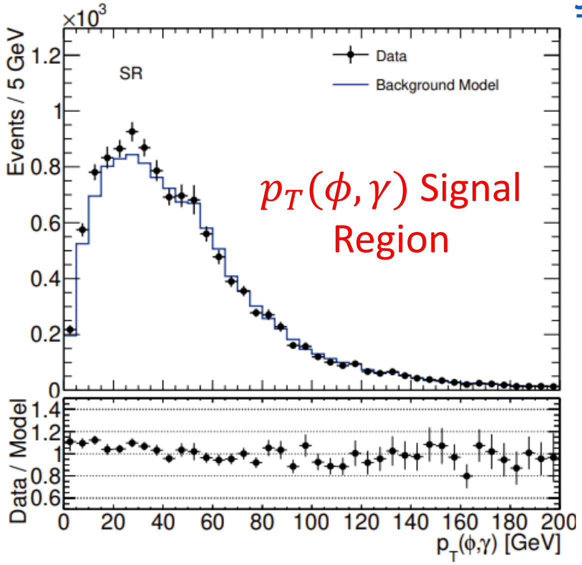

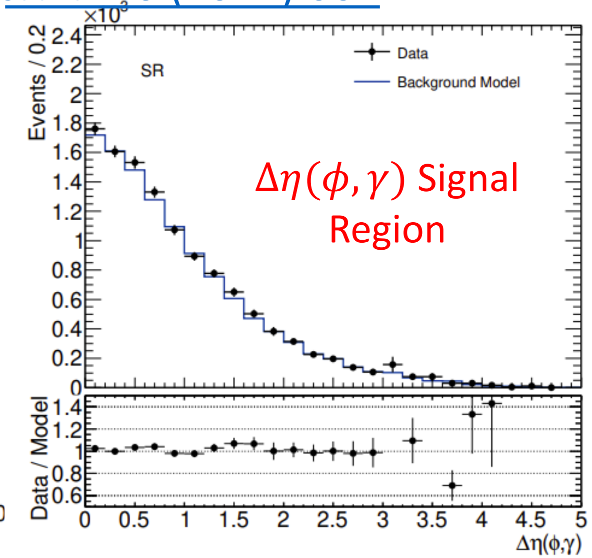

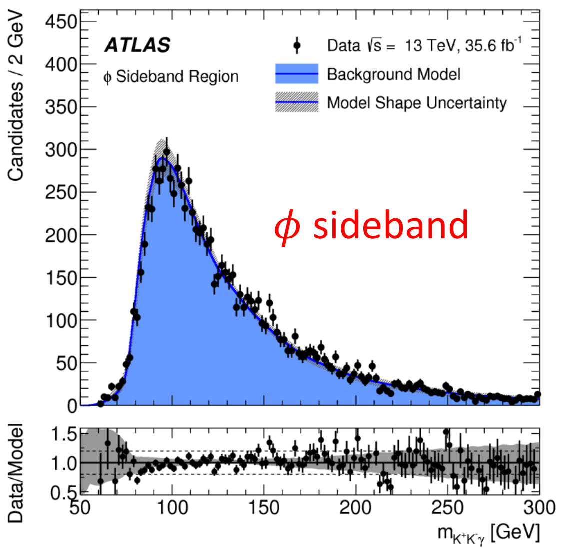

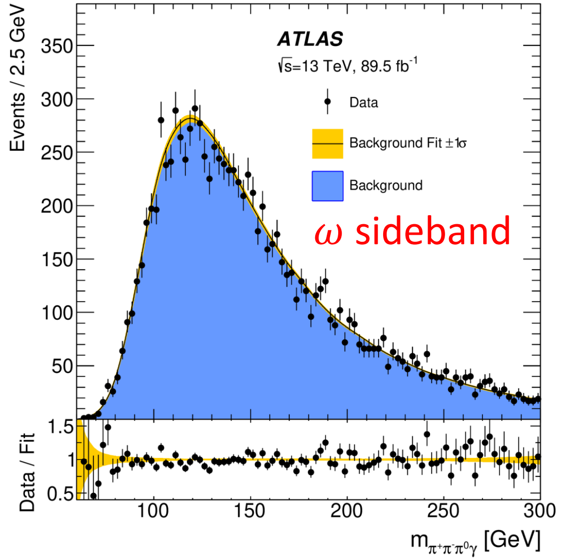

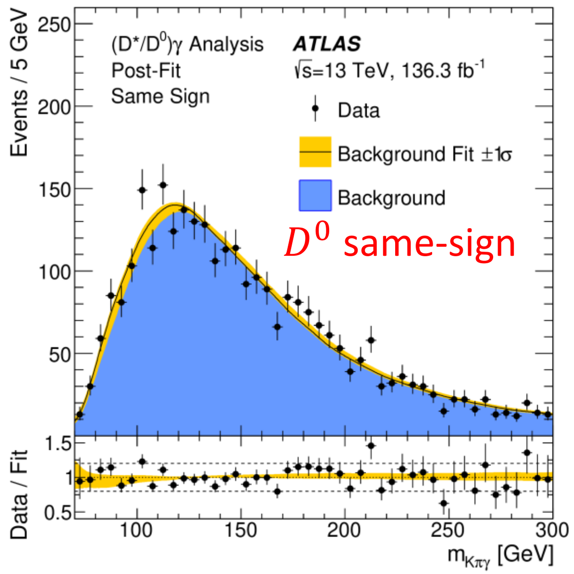

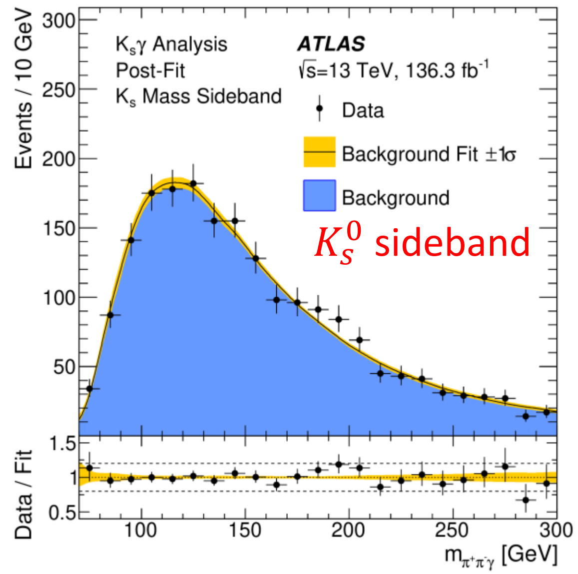

Non-Parametric Data Driven Model: Shape Systematics and Fit

- Ultimately, only the modelling of the discriminant variable in the SR is important
  - Typically define several shape uncertainties to allow model to adapt to data
    - Generate alternate templates by modifying generation procedure; data constrains nuisance parameters

- Mass tilt: reweight mass distribution with a linear function
  - Distribution can adapt to tilts in ratio
- p_{T} shift: shift generated photon p_{T} in GR
  - Distribution can shift higher/lower
- $\Delta\phi$ distortion: reweight generated $\Delta\phi$ in GR
  - Width of distribution can increase/decrease

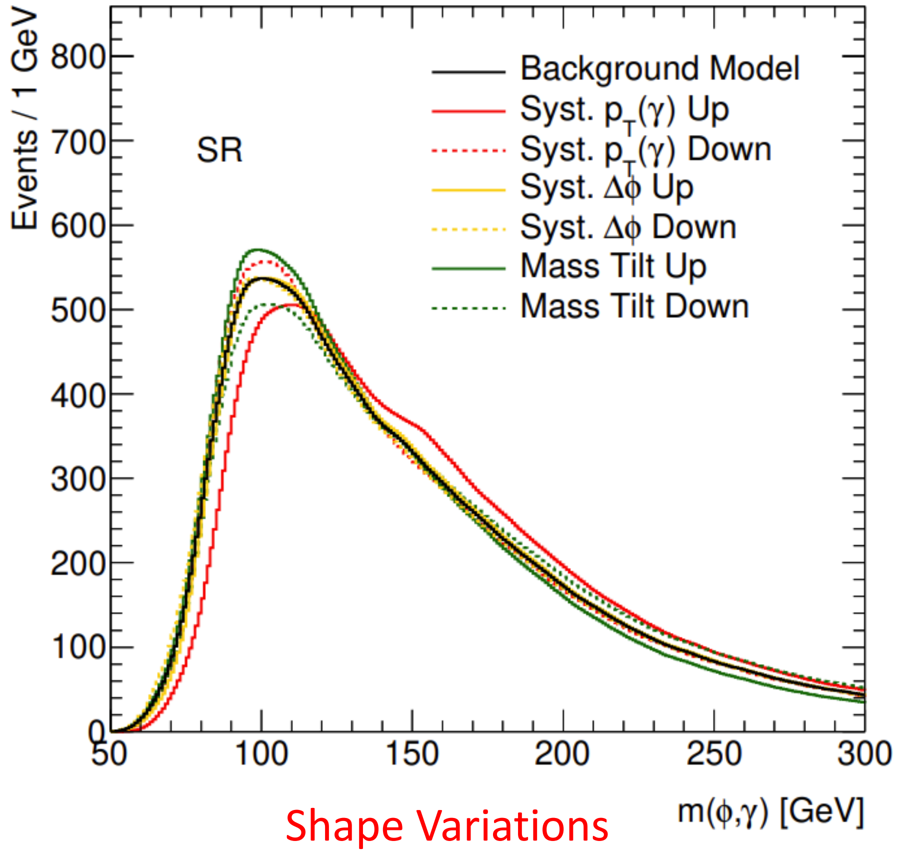

Shape Variations

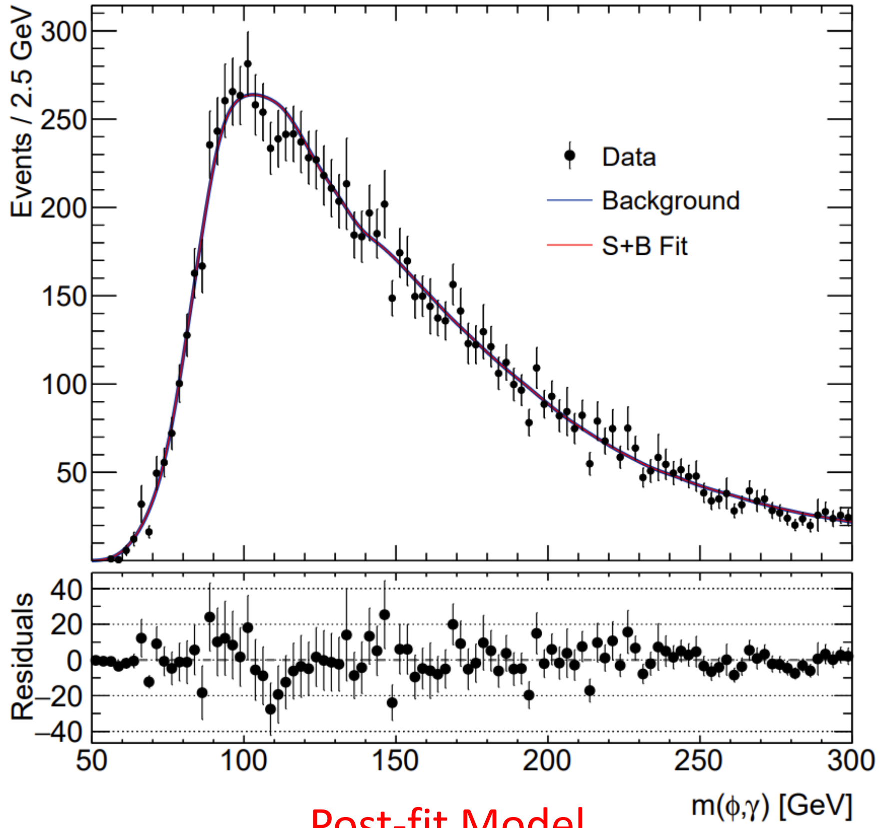

Post-fit Model

JHEP 10 (2022) 001

Non-Parametric Data Driven Model: Signal Injection

- Procedure is robust against signal contamination in Generation Region
  - Inject 5.5σ worth of signal in GR in case study – change in model prediction near H signal in SR only $\sim 2\%$

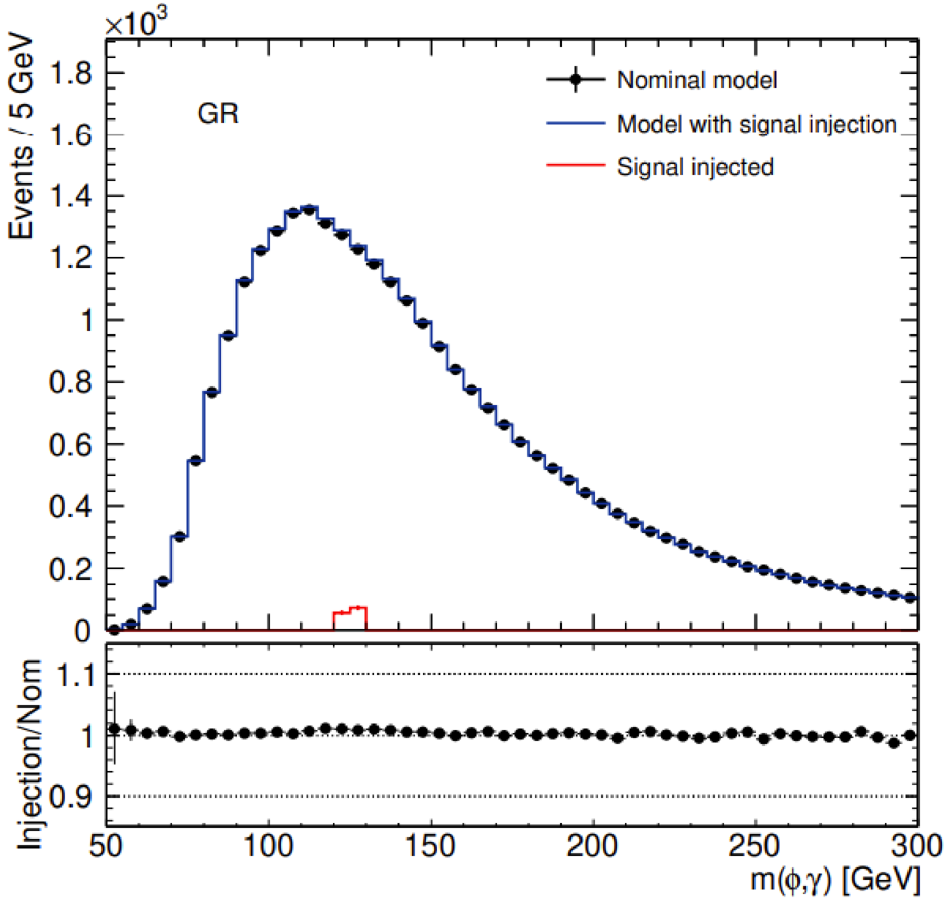

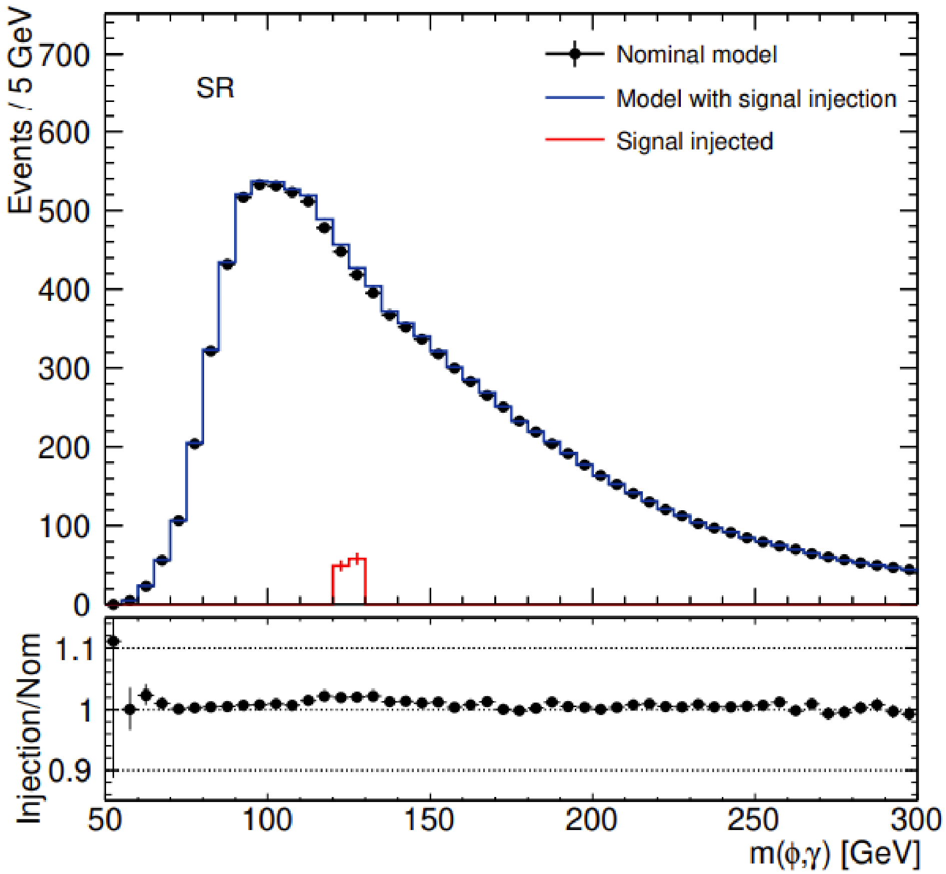

JHEP 10 (2022) 001

$H(Z) \rightarrow (\phi, \rho)\gamma$: Background Sampling Sequence

- Specific sampling scheme is flexible – can optimise based on correlations in each search
  - Blue = modelled in $\phi\gamma$; red = modelled in $\rho\gamma$

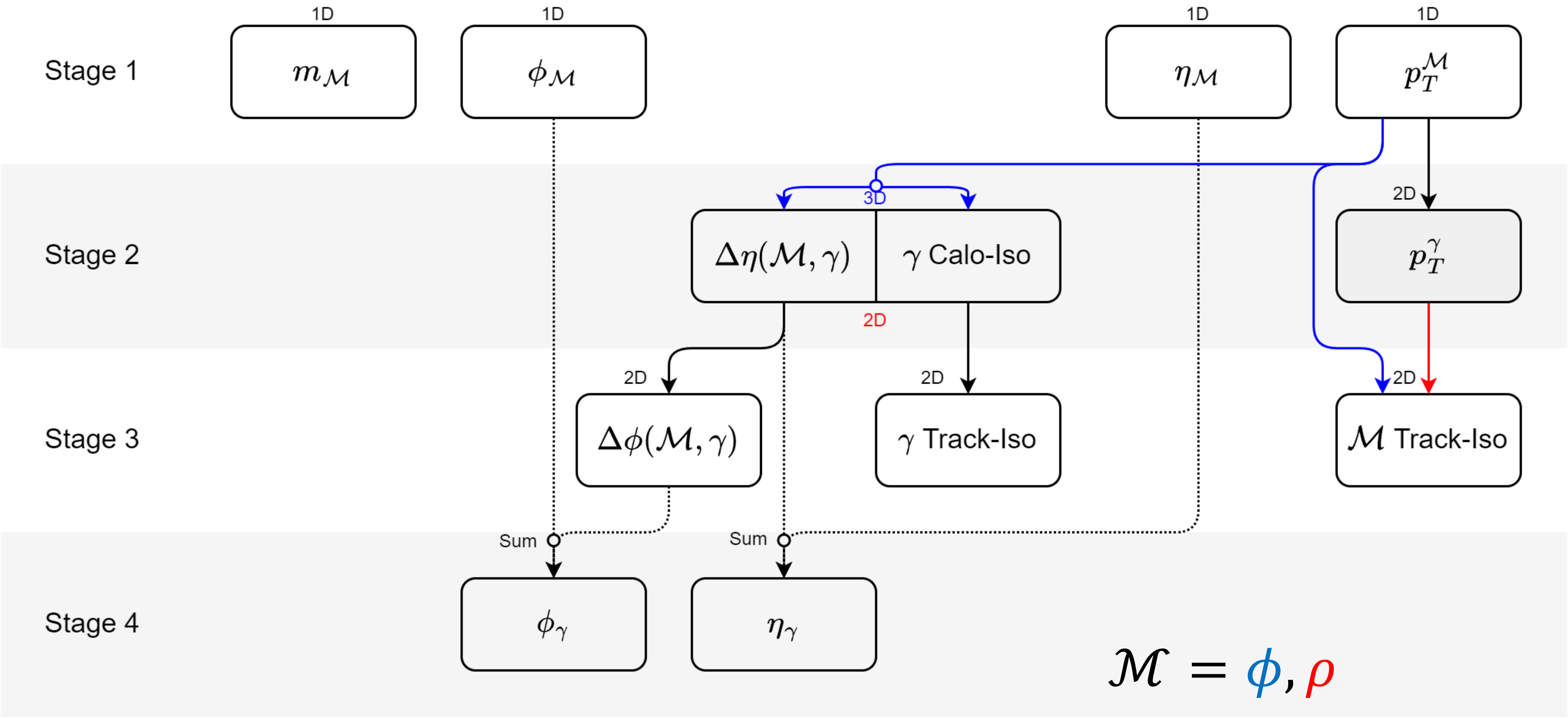

JHEP 07 (2018) 127

$H(Z) \rightarrow (\phi, \rho)\gamma$: Results

- Unbinned likelihood fit in $m(K^+K^-\gamma)$ and $m(\pi^+\pi^-\gamma)$
  - Non-parametric data-driven model for backgrounds; simulation for signals

JHEP 07 (2018) 127

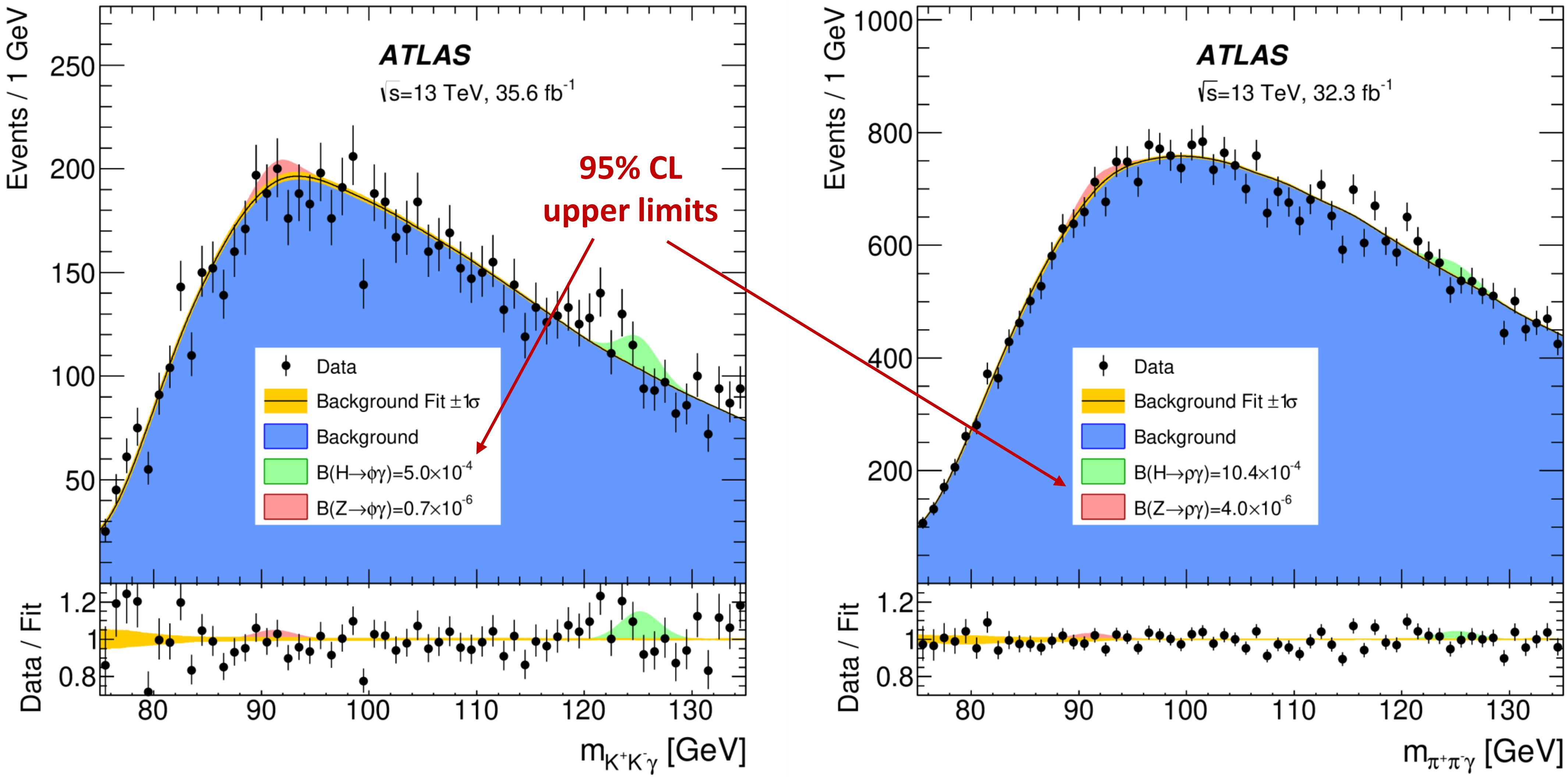

$H \to K^*\gamma$ and $H(Z) \to \omega\gamma$: Overview

- $H \to K^*(K^+\pi^-)\gamma$: d/s-quark **flavour-changing** coupling
  - Two possibilities for K/π mass hypothesis – choose closest to K^*
- $H(Z) \to \omega(\pi^+\pi^-\pi^0)\gamma$: u- & d-quark couplings
  - Use τ algorithms to reconstruct π^0 close to track-pair
  - π^0 requirement aids background rejection

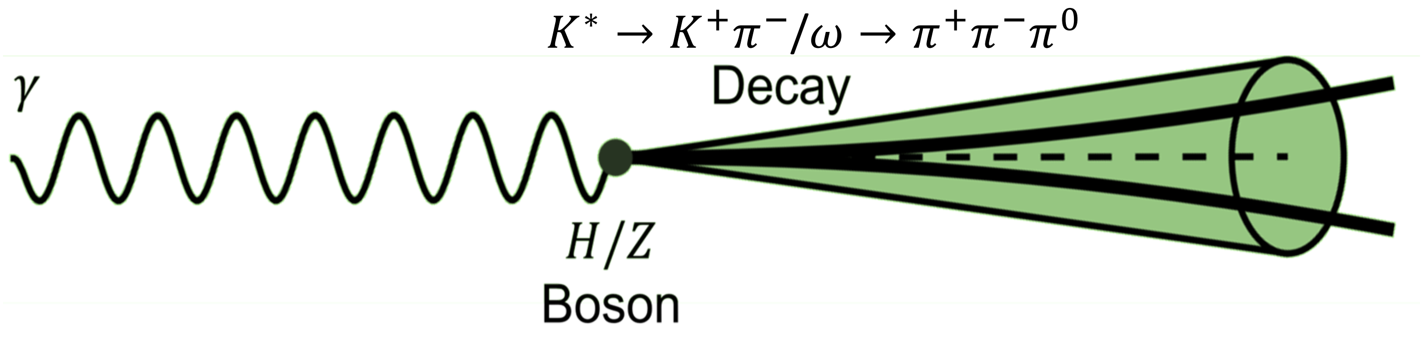

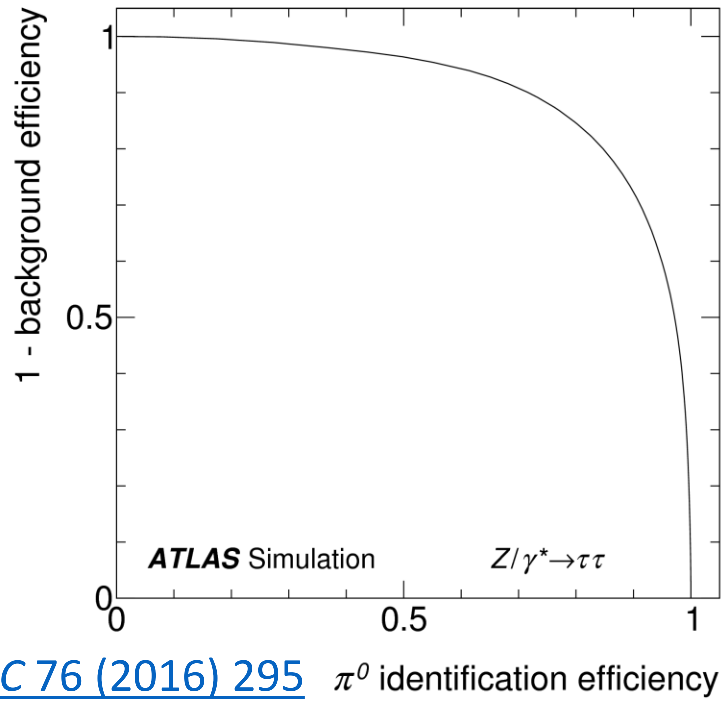

EPJC 76 (2016) 295

- **Dedicated** single photon + modified τ-lepton algorithm triggers
  - 78% efficiency w.r.t offline for $K^*\gamma$; 52% for $\omega\gamma$

Total Signal Efficiency		
$H \to K^*\gamma$	$H \to \omega\gamma$	$Z \to \omega\gamma$
12.1%	2.2%	0.4%

PLB 847 (2023) 138292

$H \to K^*\gamma$ and $H(Z) \to \omega\gamma$: Results

- Unbinned likelihood fit in $m(K^{\pm}\pi^{\mp}\gamma)$ and $m(\pi^+\pi^-\pi^0\gamma)$ PLB 847 (2023) 138292
  - Non-parametric data-driven model for backgrounds; simulation for signals

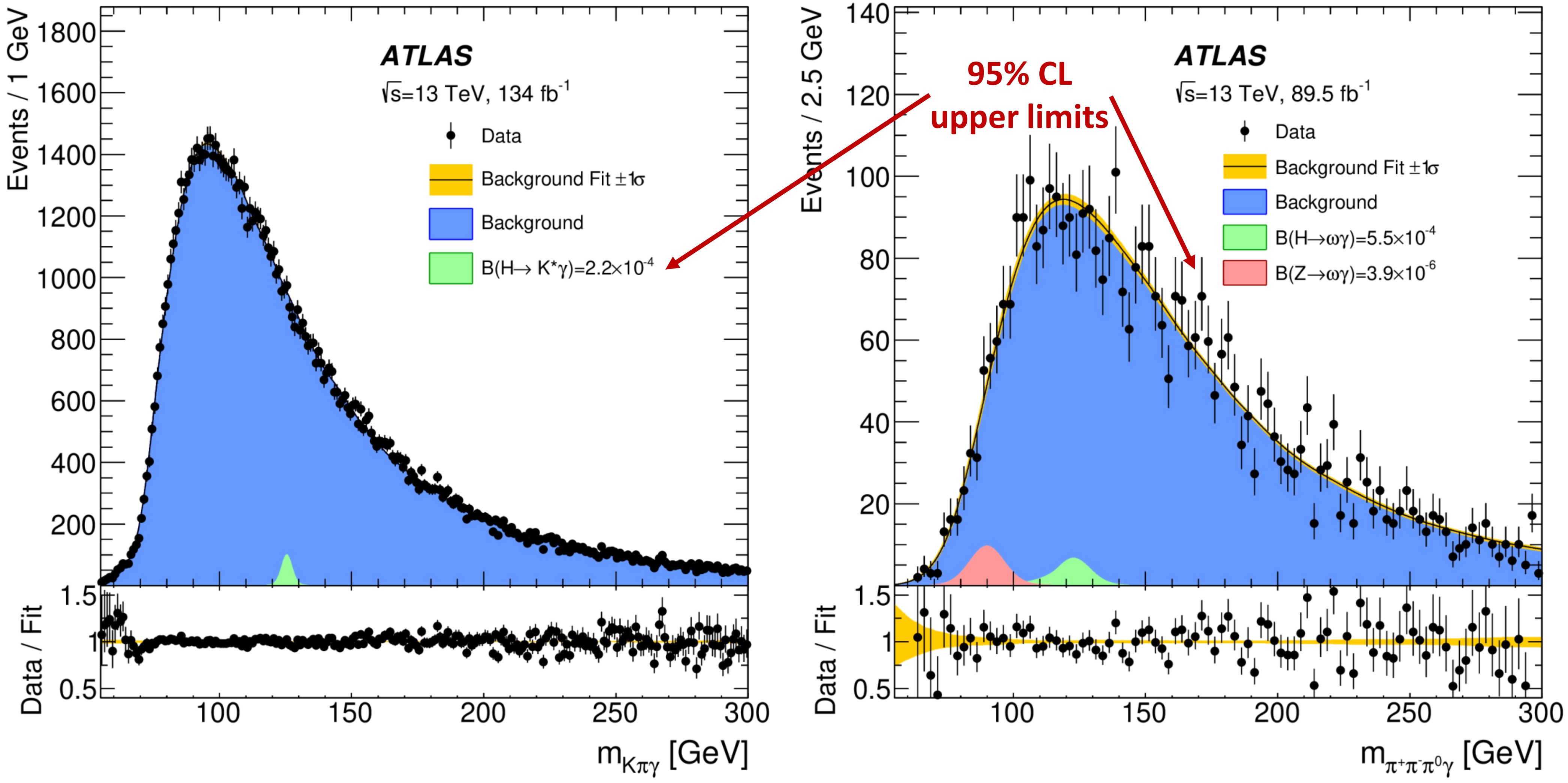

$H \to D^{*}\gamma$ & $Z \to (D^0, K_s^0)\gamma$: Overview

- $H \to D^{*}(D^0[K^-\pi^+] + \pi^0/\gamma)\gamma$ and $Z \to D^0(K^-\pi^+)\gamma$: u/c flavour-changing couplings
  - Do not reconstruct additional soft π^0/γ in D^{*} decay
  - D^0 decay is displaced - distinct from primary vertex
- $Z \to K_s^0(\pi^+\pi^-)\gamma$: d/s flavour-changing coupling
  - K_s^0 decay is particularly displaced - many occur beyond innermost ID layers

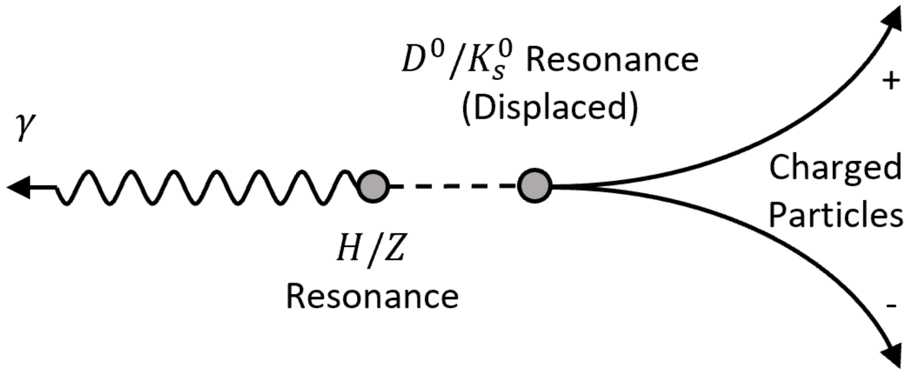

1.9 – 2.3%
Signal Resolution

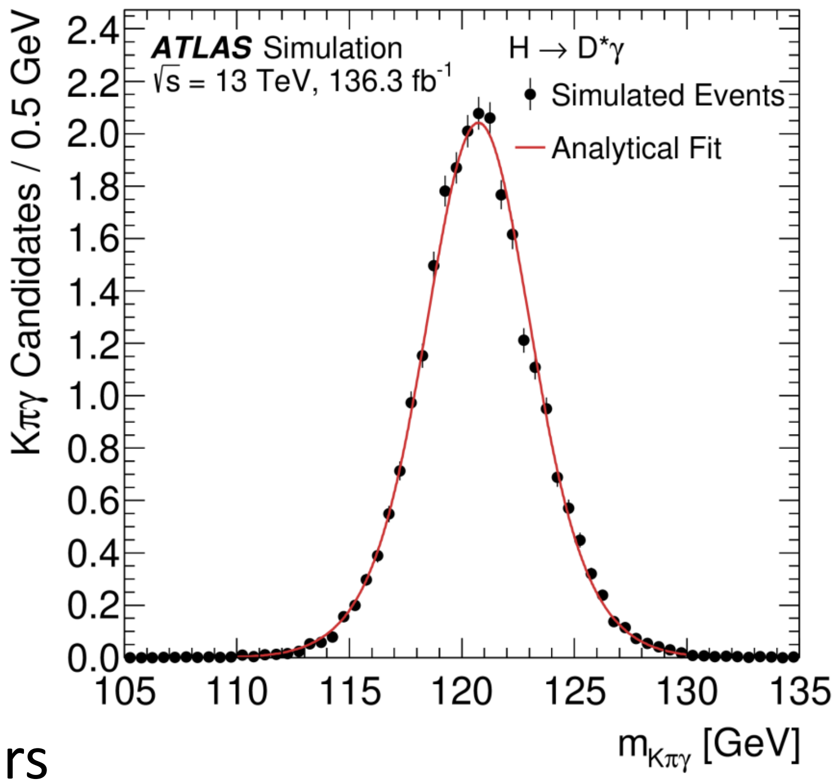

- **Dedicated** single photon + modified τ-lepton algorithm triggers
  - 69% efficiency w.r.t offline for $D^{*}\gamma$; 39% for $K_s^0\gamma$

Total Signal Efficiency		
$H \to D^{*}\gamma$	$Z \to D^0\gamma$	$Z \to K_s^0\gamma$
9%	3%	0.2%

arXiv:2402.18731

$H \to D^*\gamma$ & $Z \to (D^0, K_s^0)\gamma$: Vertex Reconstruction

- Secondary vertex reconstruction suppresses backgrounds
  - Reject prompt vertices (i.e reject values below dashed lines)
  - Vertex fit also improves meson reconstruction

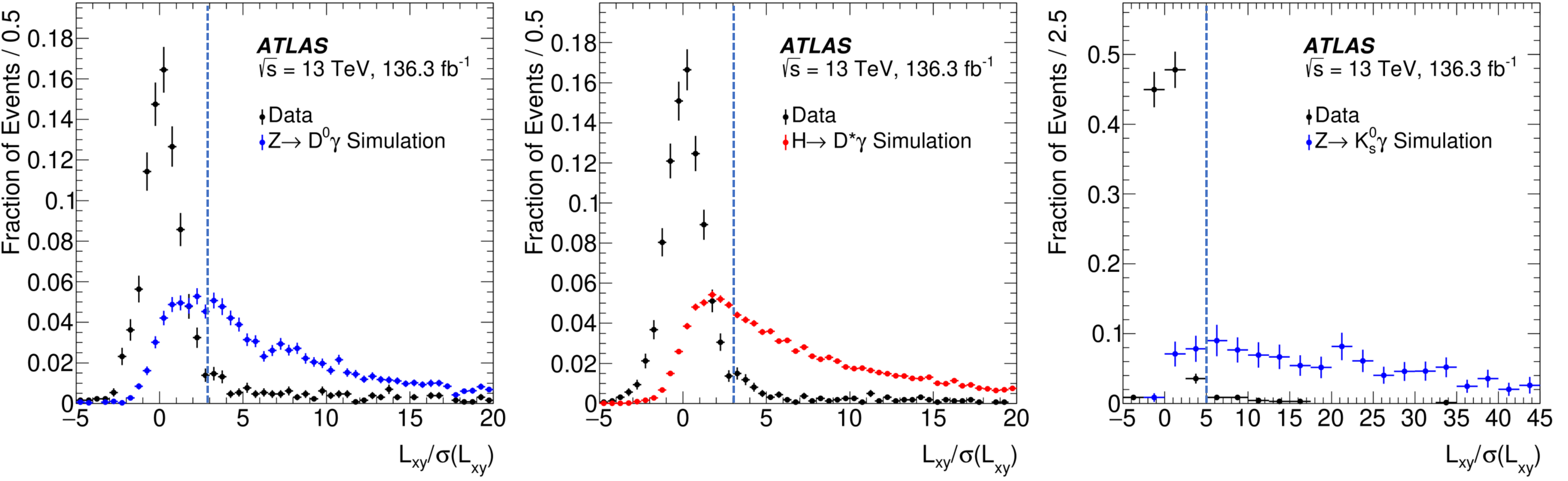

arXiv:2402.18731

$H \to D^*\gamma$ & $Z \to (D^0, K_s^0)\gamma$: Results

- Unbinned likelihood fit in $m(K\pi\gamma)$ and $m(\pi^+\pi^-\gamma)$ arXiv:2402.18731
  - Non-parametric data-driven model for backgrounds; simulation for signals

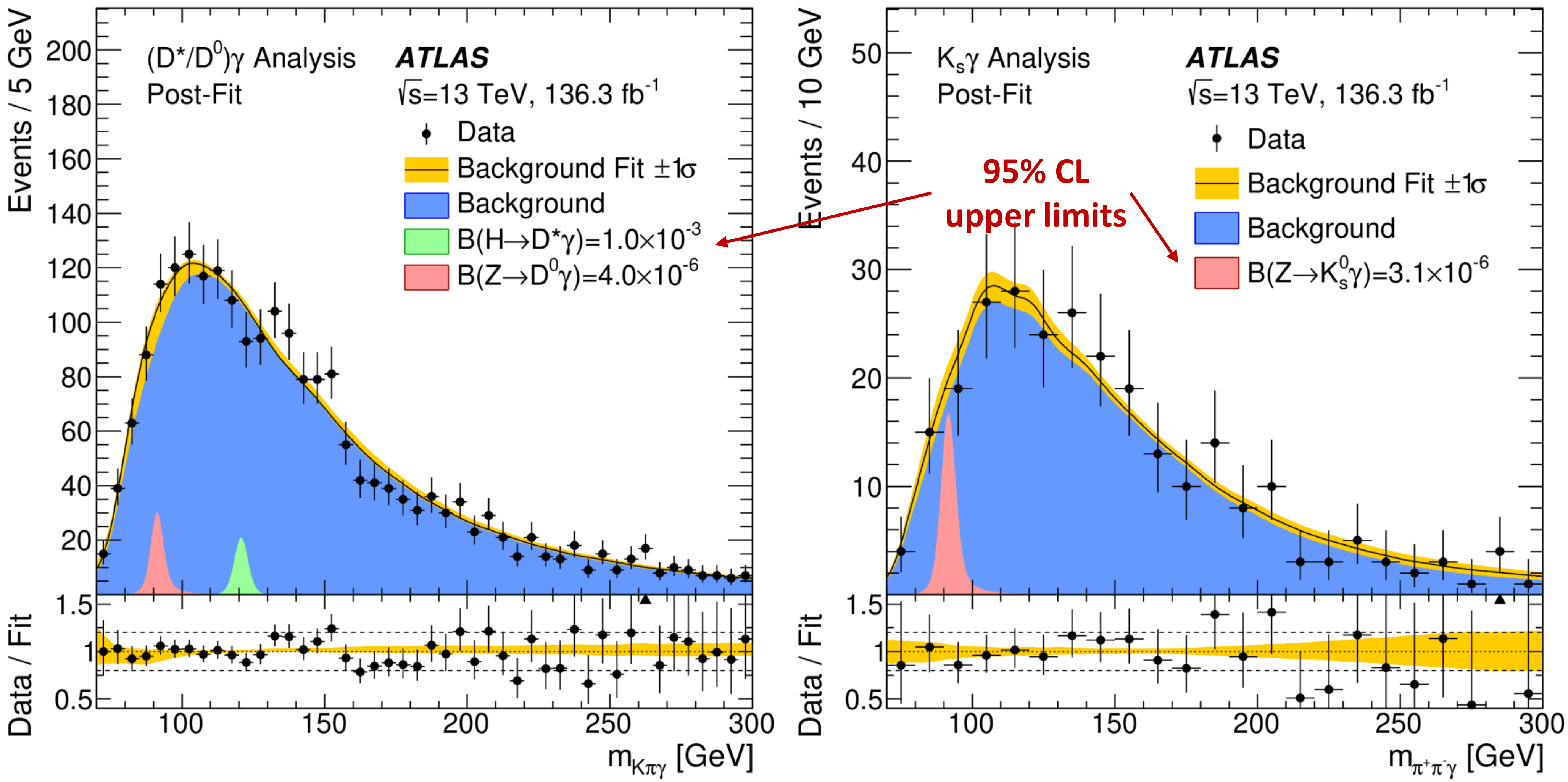

$H(Z) \to Q\gamma$: Overview

- $H \to Q(\mu^+\mu^-)\gamma$: b- & c-quark Yukawa couplings

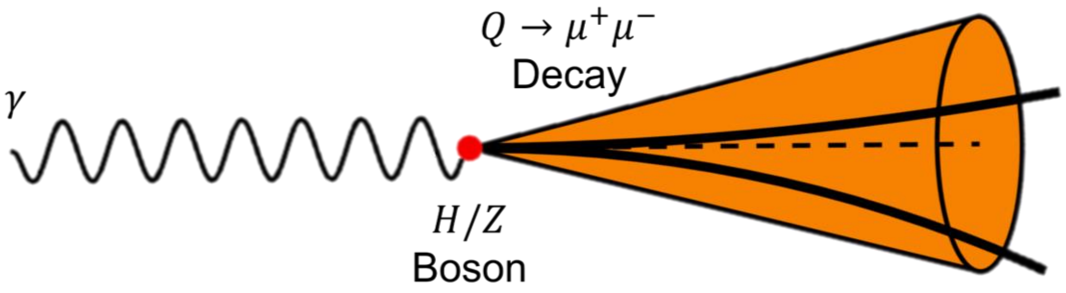

- **Dedicated** single photon + **muon** triggers
  - 97% efficiency w.r.t offline
- Additional resonant $q\bar{q} \to \mu^+\mu^-\gamma$ background
  - Use a **2D** fit in $m_{\mu^+\mu^-\gamma}$ vs $m_{\mu^+\mu^-}$
- Split $\Upsilon(nS)$ into Barrel (B) and Endcap (EC) categories
  - Improved resolution in barrel helps resolve each state
- **Reject** displaced vertices to remove $b \to \psi(nS)$

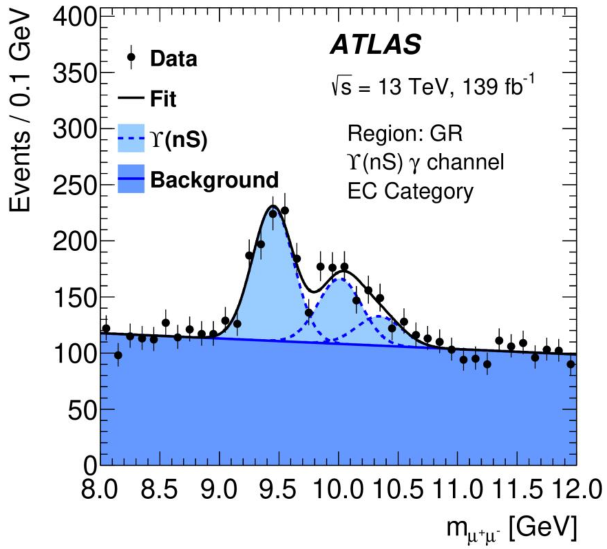

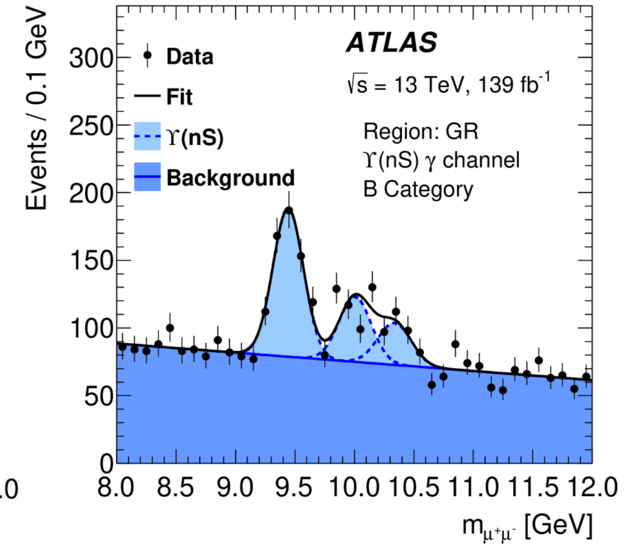

1.6-1.8%
Signal Resolution

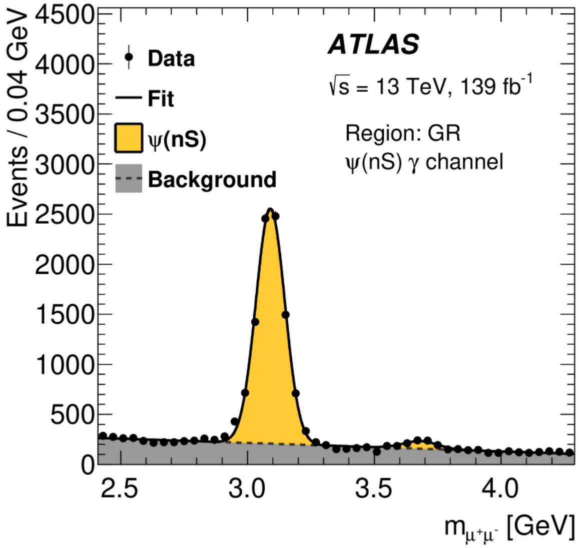

EPJC 83 (2023) 781

$H(Z) \to Q\gamma$: Background Modelling

- **Exclusive background**
  - $q\bar{q} \to \mu^+\mu^-\gamma$ production (Drell-Yan)
  - Analytical fit to simulated events
- **Inclusive background**
  - Multi-jet and γ+jet sources with $Q/\mu^+\mu^-$ production
  - Non-parametric data-driven background model

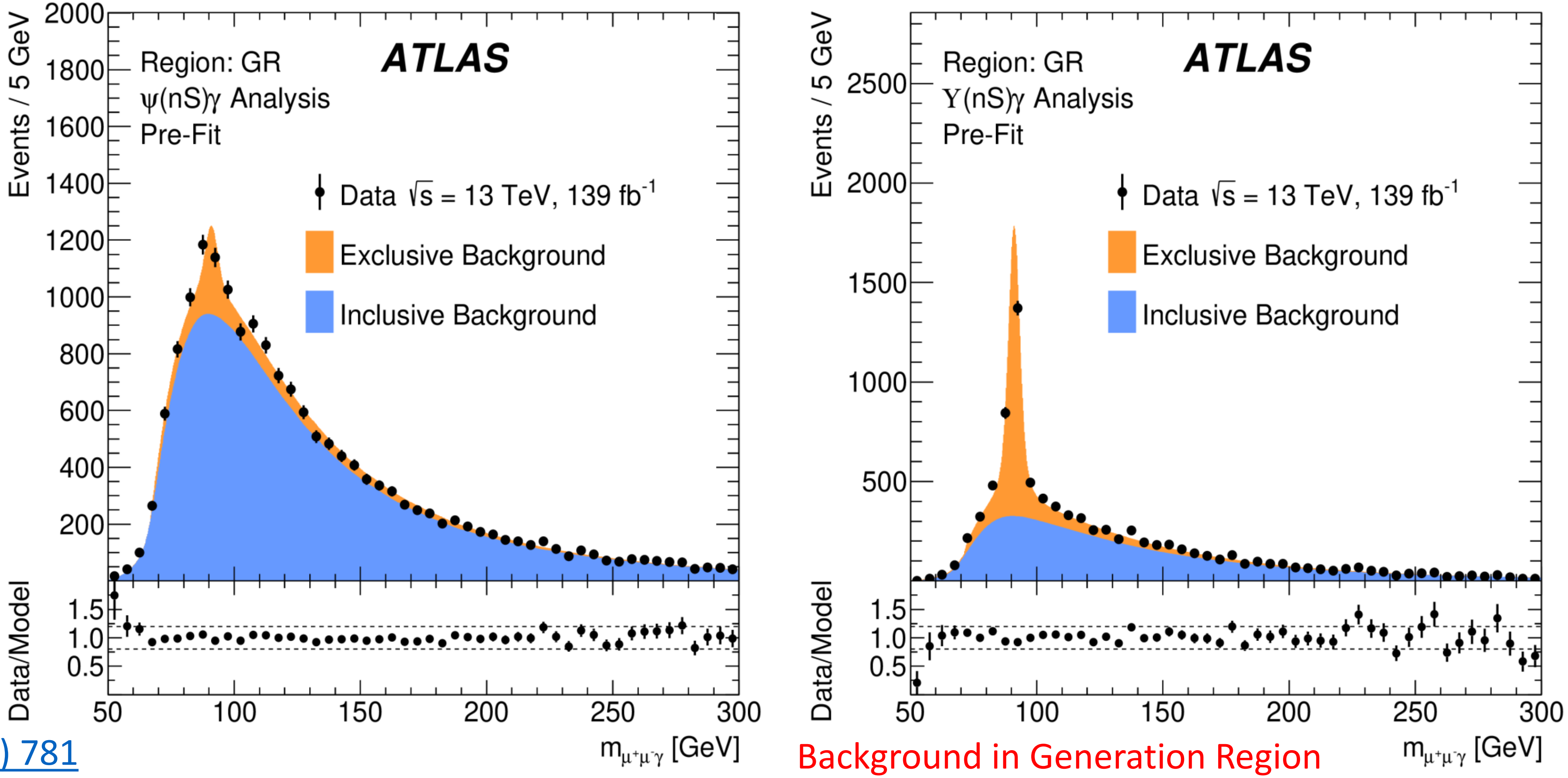

Background in Generation Region

EPJC 83 (2023) 781

$H(Z) \to Q\gamma$: Three-body Mass Versus Dimuon Mass

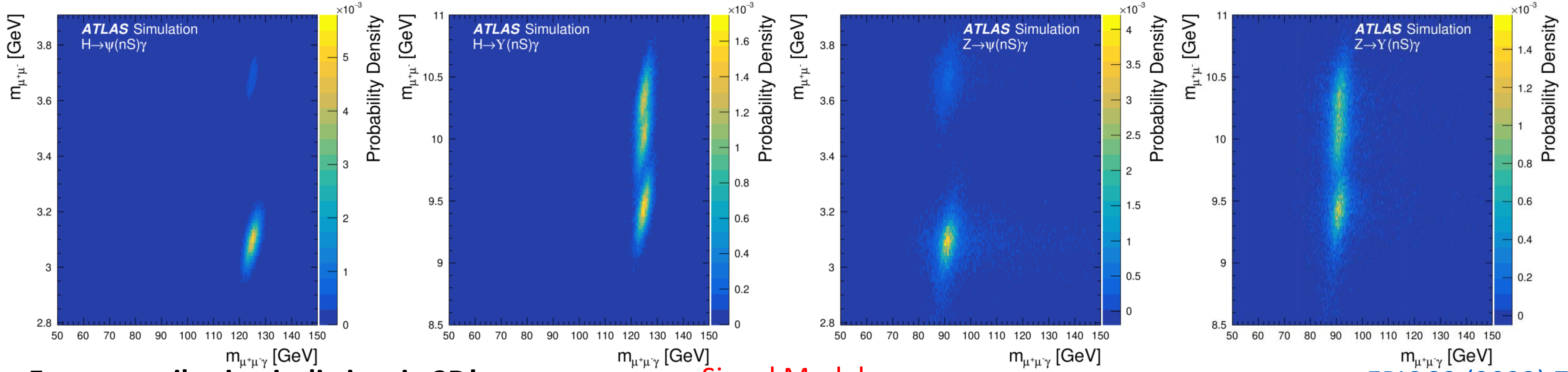

Every contribution is distinct in 2D!

Signal Models

[*EPJC* 83 (2023) 781]

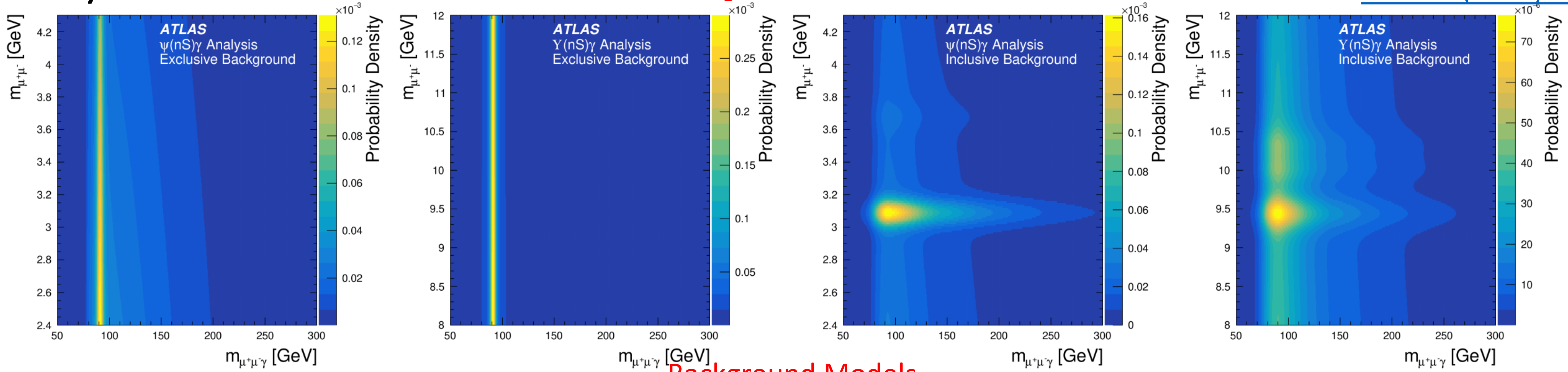

Background Models

$H(Z) \to \psi(nS)\gamma$: Results

- Use **2D** unbinned likelihood fit in $m(\mu^+\mu^-), m(\mu^+\mu^-\gamma)$
  - Discriminates between **all** signal and background contributions
- $\psi(nS)\gamma$ analysis fit is performed in a single category

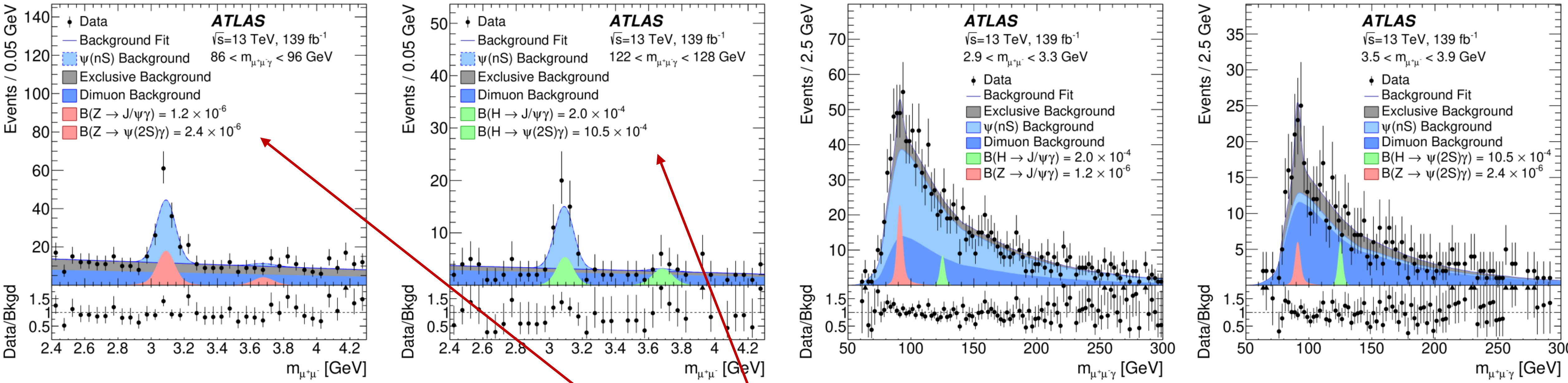

Projections in $m(\mu^+\mu^-)$

Projections in $m(\mu^+\mu^-\gamma)$

95% CL upper limits

EPJC 83 (2023) 781

$H(Z) \to \Upsilon(nS)\gamma$: Results

- $\Upsilon(nS)\gamma$ analysis fit is performed simultaneously in the barrel and endcap categories

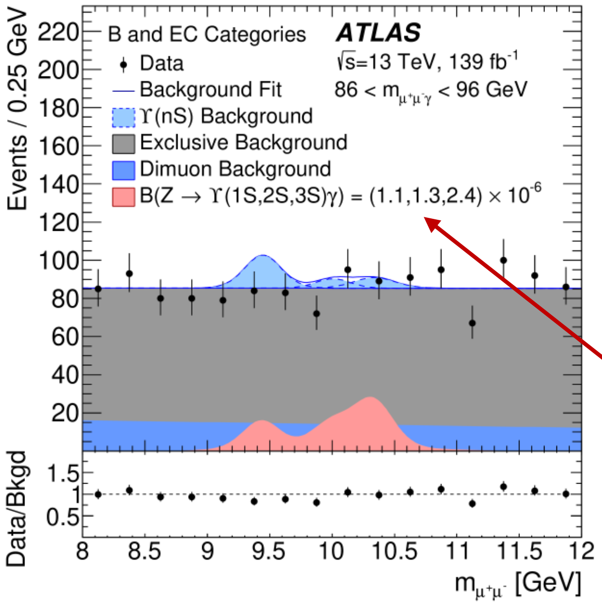

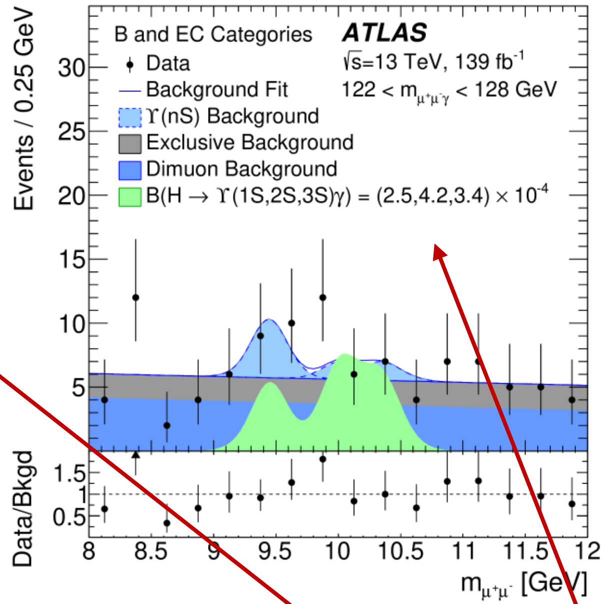

Projections in $m(\mu^+\mu^-)$

95% CL upper limits

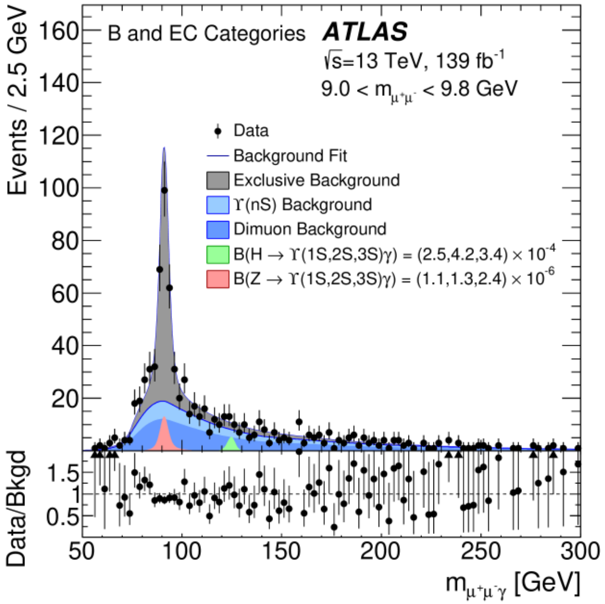

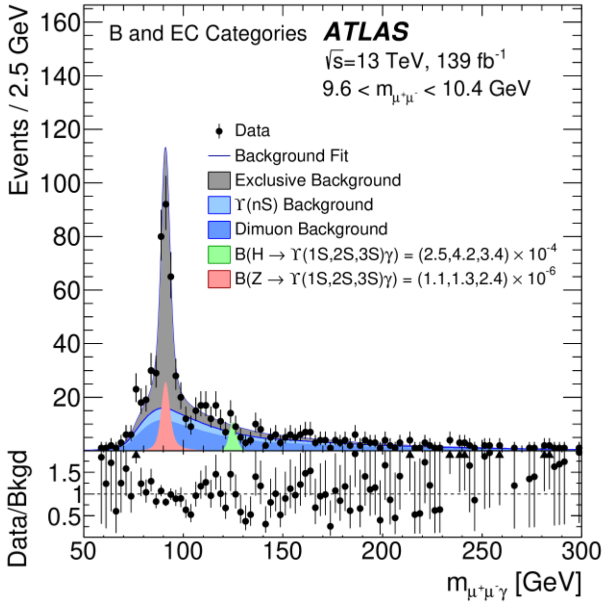

Projections in $m(\mu^+\mu^-\gamma)$

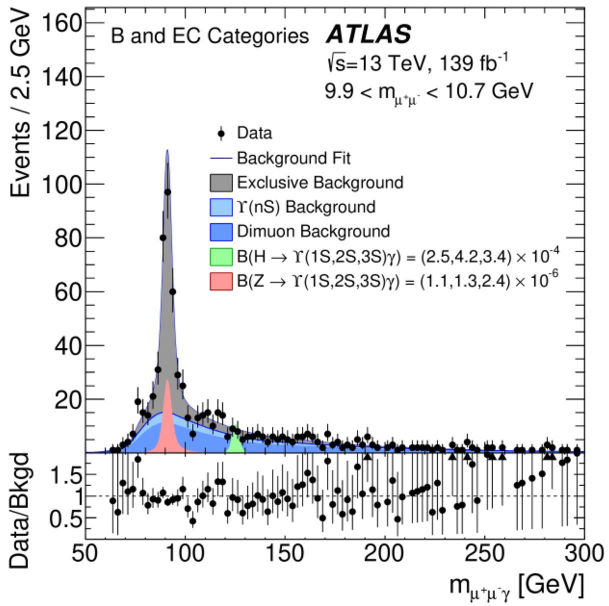

EPJC 83 (2023) 781

$H \to Q\gamma$: κ-Framework Interpretation

- κ_q coupling modifier: ratio of quark coupling g_q over the SM−expectation, $\kappa_q = \frac{g_q}{g_q^{SM}}$
- Combine with $H \to \gamma\gamma$ § to interpret in terms of $\kappa_{c,b}/\kappa_\gamma$:

§ATLAS-CONF-2020-026

$$\frac{\mu_{H\to J/\psi\,\gamma}}{\mu_{H\to\gamma\gamma}} \approx \frac{\left|\mathcal{A}_{\text{ind}} + \frac{\kappa_c}{\kappa_\gamma}\mathcal{A}_{\text{dir}}\right|^2}{\Gamma^{\text{SM}}_{H\to J/\psi\,\gamma}}$$

μ: observed rate normalised to SM rate

Analysis	κ Ratio	Expected Bounds	Observed Bounds
$H \to J/\psi\,\gamma$	κ_c/κ_γ	$(-120, 161)$	$[-133, 175]$
$H \to \Upsilon(nS)\gamma$	κ_b/κ_γ	$(-37, 39)$	$[-37, 40]$

- $BR^{\text{SM}}_{H\to\psi(nS)\gamma} \approx 10^{-6}$
- $|\mathcal{A}_{\text{ind}}| \approx 20 \times |\mathcal{A}_{\text{dir}}|$

- $BR^{\text{SM}}_{H\to\Upsilon(nS)\gamma} \approx 10^{-9} - 10^{-8}$
- $\mathcal{A}_{\text{ind}}, \mathcal{A}_{\text{dir}}$ almost cancel in SM

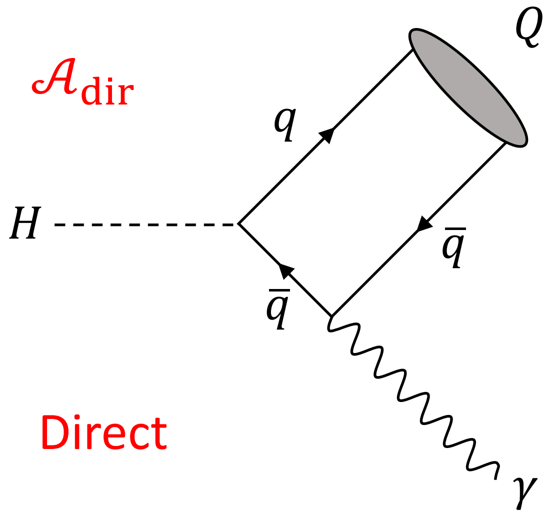

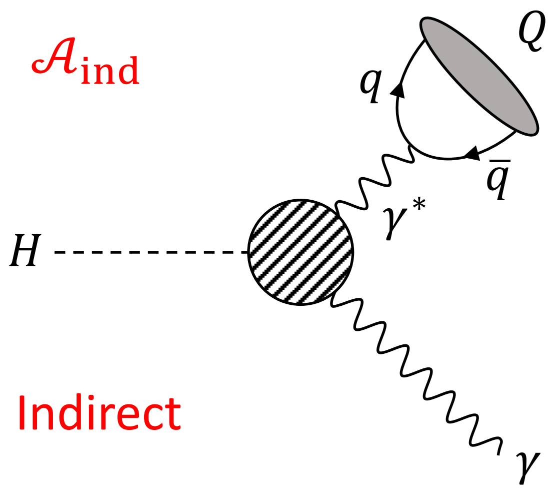

EPJC 83 (2023) 781

Other κ-Framework Results

- κ-interpretation complements results from other searches
  - $H \to b\bar{b}$: EPJC 81 (2021) 178
  - $H \to c\bar{c}$: EPJC 82 (2022) 717
    - $|\kappa_c| < 8.5\ (12.4)$ @ 95% CL
    - $|\kappa_c/\kappa_b| < 4.5\ (5.1)$ @ 95% CL
  - Measurements of p_{T}^{H}: JHEP 05 (2023) 028

Channel	Parameter	Observed 95% confidence interval	Expected 95% confidence interval
$H \to ZZ^* \to 4\ell$	κ_b	$[-1.1,\ 1.2]$	$[-1.2,\ 1.2]$
	κ_c	$[-5.2,\ 5.4]$	$[-5.7,\ 5.6]$
$H \to \gamma\gamma$	κ_b	$[-1.1,\ 1.1]$	$[-1.2,\ 1.2]$
	κ_c	$[-5.2,\ 5.0]$	$[-5.4,\ 5.5]$
Combined	κ_b	$[-1.1,\ 1.1]$	$[-1.2, 1.2]$
	κ_c	$[-5.0,\ 5.1]$	$[-5.2,\ 5.4]$

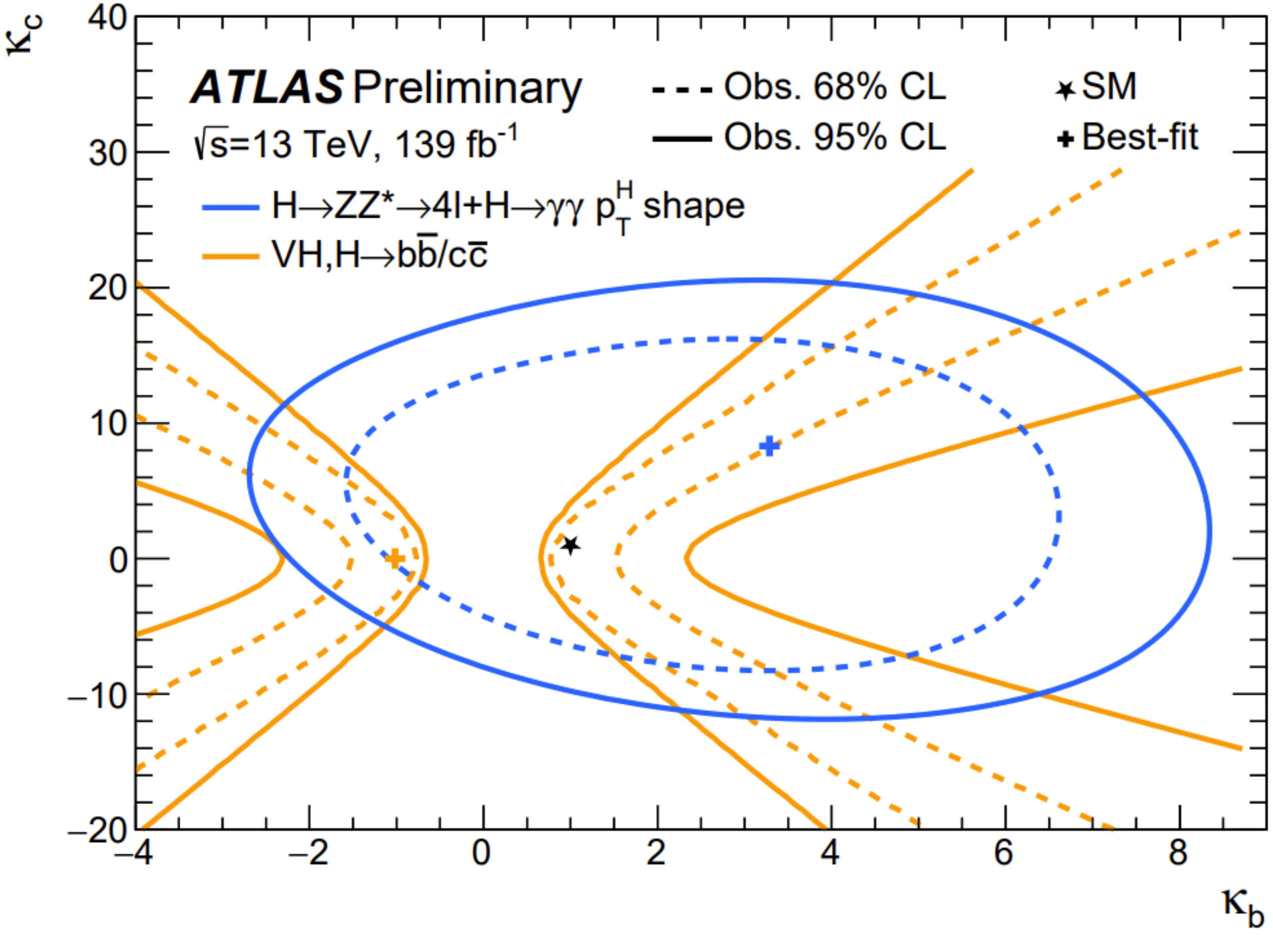

CMS result for κ_c/κ_γ from $H \to J/\psi\,\gamma$: Expected = $(-121{,}161)$; observed = $[-157{,}199]$

CMS-PAS-SMP-22-012

$W^{\pm} \rightarrow (\pi^{\pm}, K^{\pm}, \rho^{\pm})\gamma$: Overview

- $W^{\pm} \rightarrow (\pi^{\pm}, K^{\pm})\gamma$: One category
  - **Dedicated** track + single photon triggers (58% efficiency)

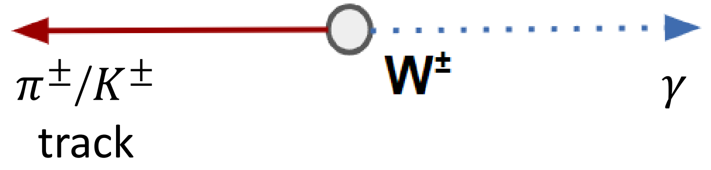

- $W^{\pm} \rightarrow (\rho^{\pm} \rightarrow \pi^{\pm}\pi^{0})\gamma$: Two categories
  - **Di-photon** triggers for τ + photon category (43% efficiency)
    - ρ reconstructed as 1-pronged τ-lepton
  - Some sensitivity with track + photon trigger
    - No π^{0} reconstruction in track + photon category

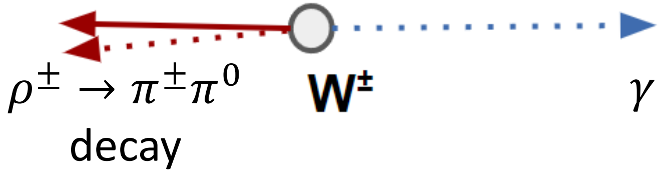

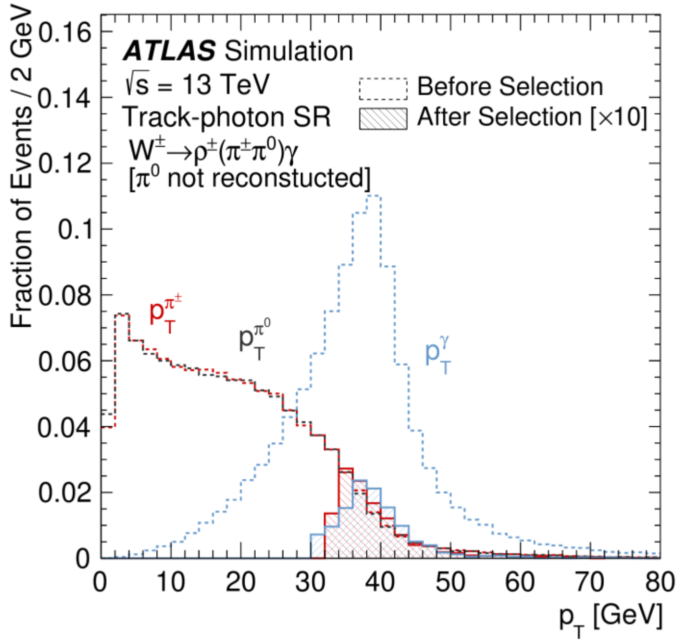

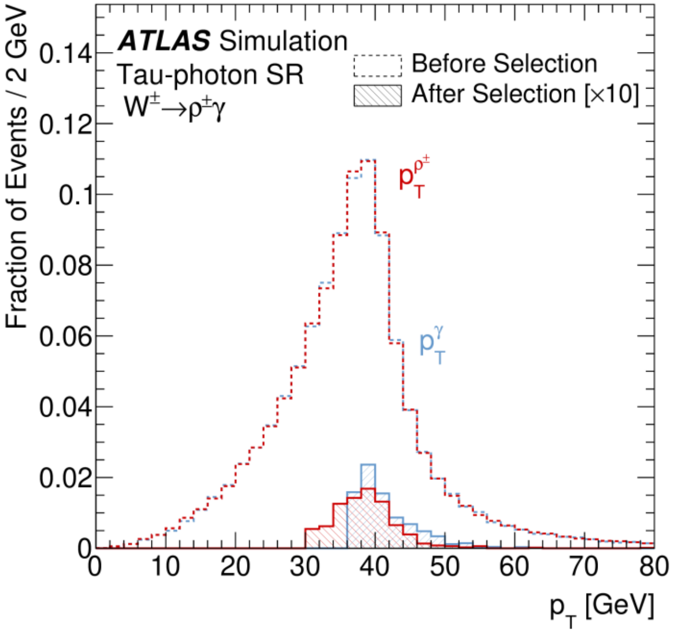

Total Signal Efficiency		
$W^{\pm} \rightarrow \pi^{\pm}\gamma$	$W^{\pm} \rightarrow K^{\pm}\gamma$	$W^{\pm} \rightarrow \rho^{\pm}\gamma$
5.0%	5.5%	0.5% (0.3%)

2.7 – 3.1%
Signal Resolution

arXiv:2309.15887

$W^{\pm} \to (\pi^{\pm}, K^{\pm}, \rho^{\pm})\gamma$: Results

- Binned likelihood fit in $m(\text{track}, \gamma)$ and $m(\tau, \gamma)$
  - Simultaneous fit in two categories: track + photon and τ + photon
- Suppress $Z \to e^{+}e^{-}$ background using TRT to identify $e^{\pm}$
  - Remaining contribution modelled with simulation

	95% CL upper limits	
Branching fraction	Expected $\times 10^{-6}$	Observed $\times 10^{-6}$
$\mathcal{B}(W^{\pm} \to \pi^{\pm}\gamma)$	$1.2^{+0.5}_{-0.3}$	1.9
$\mathcal{B}(W^{\pm} \to K^{\pm}\gamma)$	$1.1^{+0.4}_{-0.3}$	1.7
$\mathcal{B}(W^{\pm} \to \rho^{\pm}\gamma)$	$6.0^{+2.3}_{-1.7}$	5.2

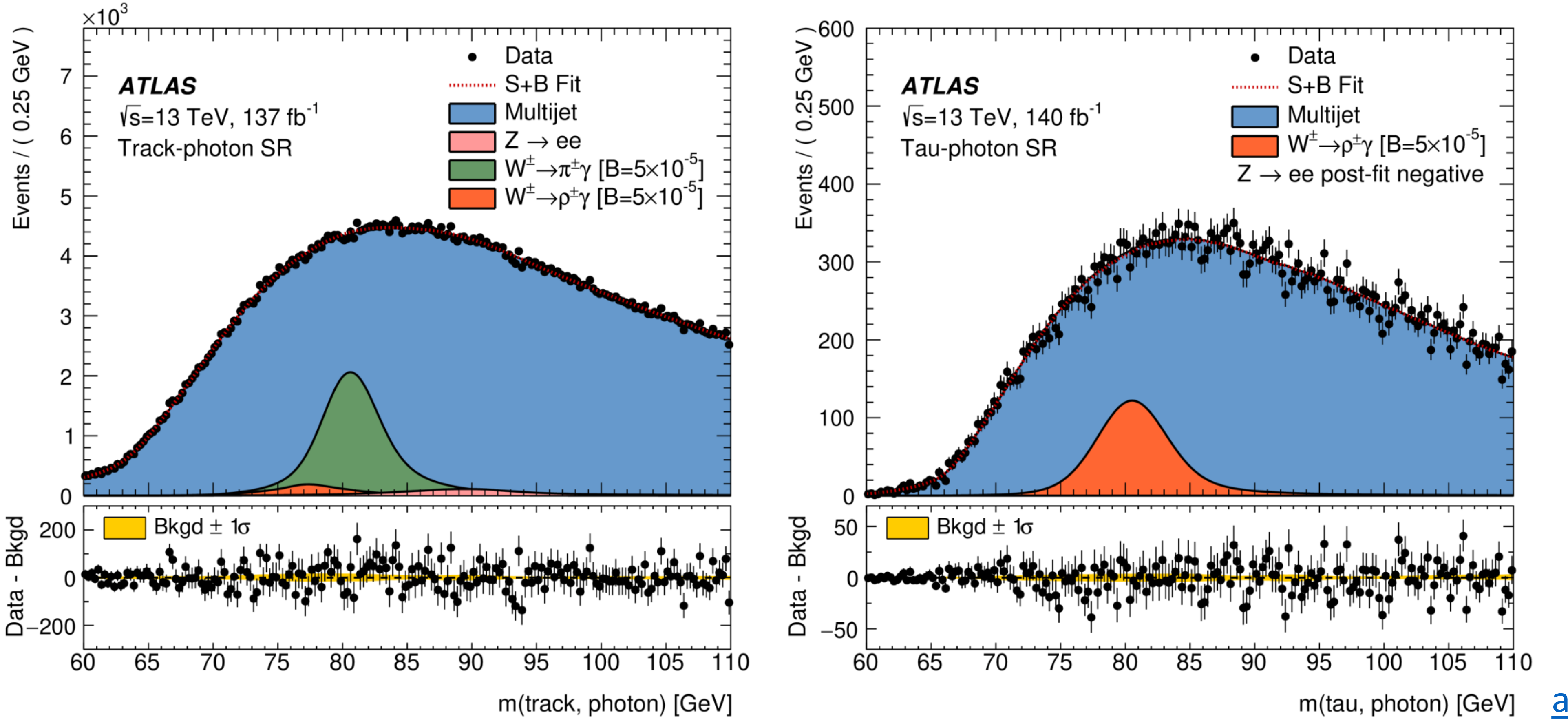

arXiv:2309.15887

Summary of Exclusive $H/W/Z \to \mathcal{M}\gamma$ Search Results

ATL-PHYS-PUB-2023-004

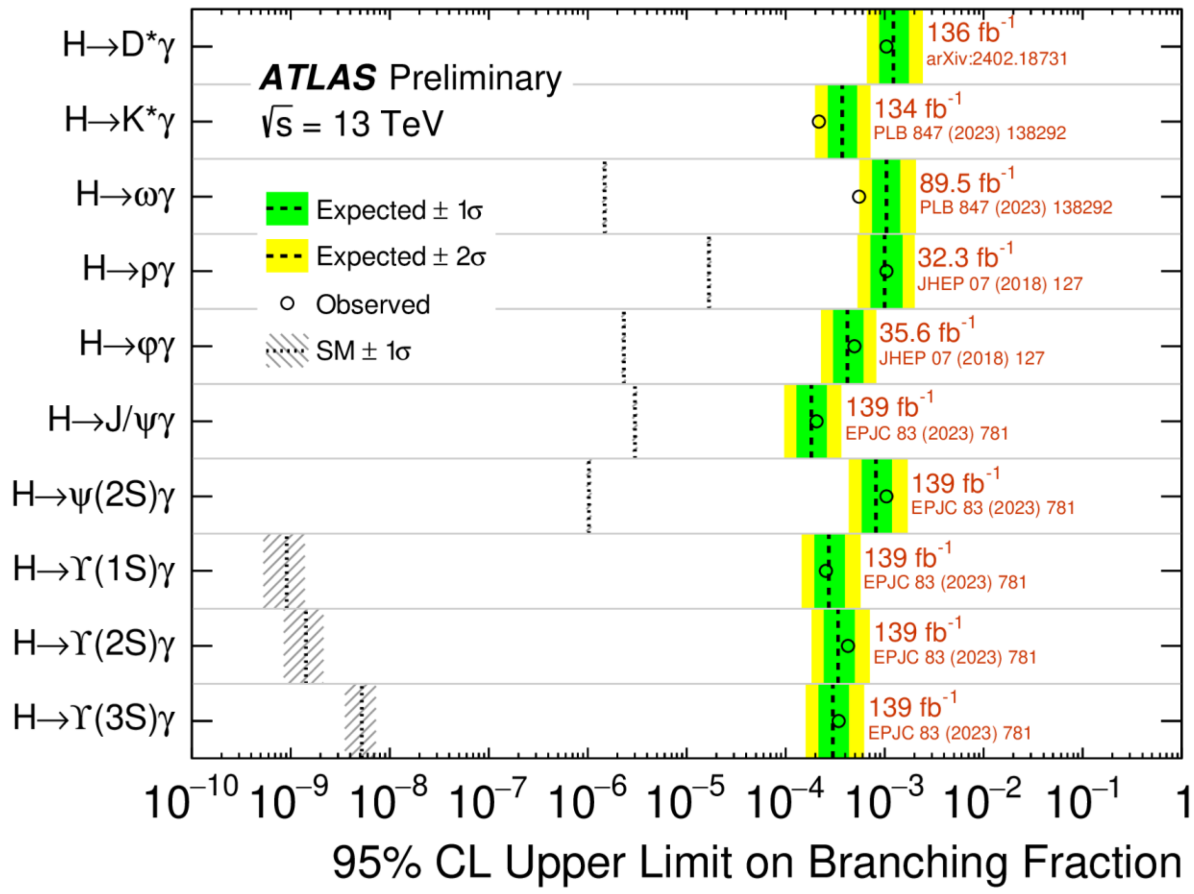

Higgs Boson Decays (with SM Expectations)

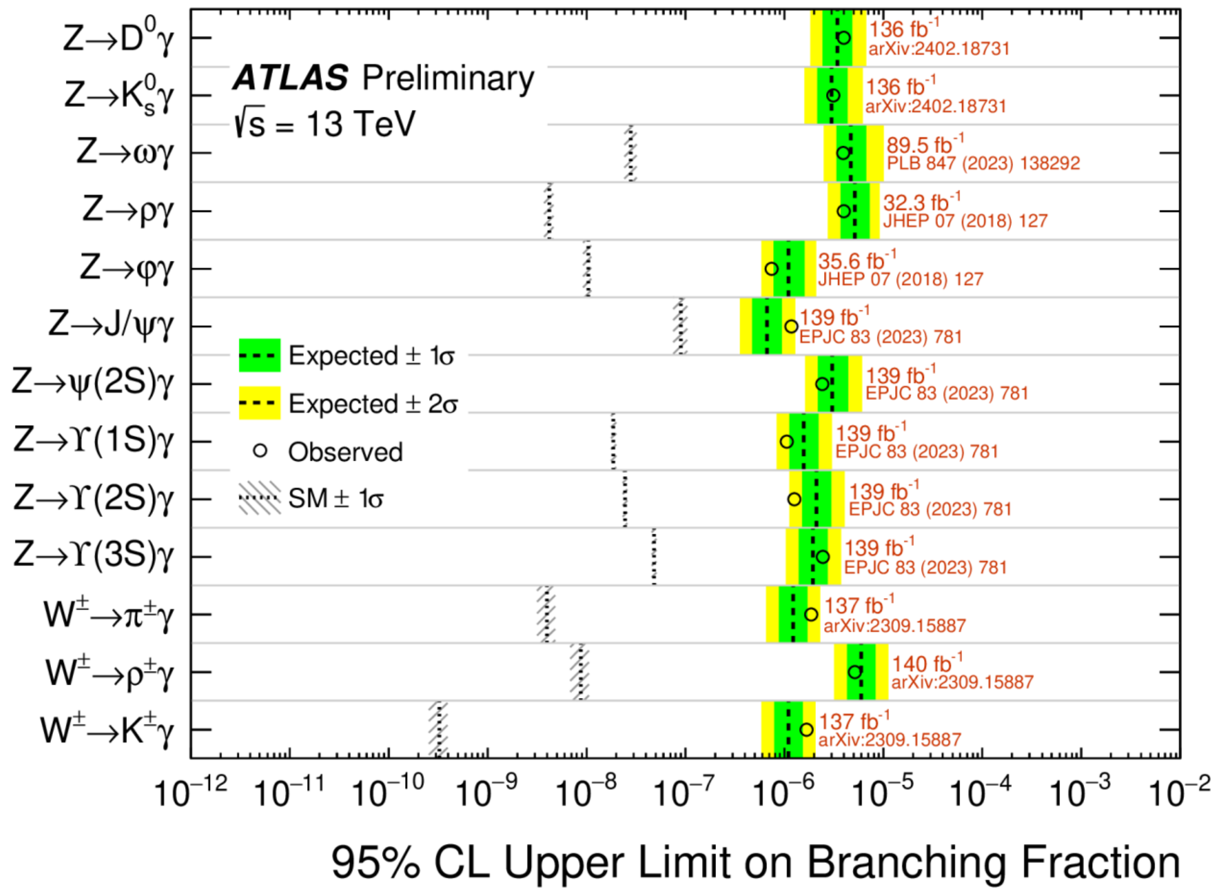

Vector Boson Decays (with SM Expectations)

- ATLAS has the most stringent limits on most of these decay channels

Prospects for Exclusive $H(Z) \rightarrow M\gamma$ Searches

ATL-PHYS-PUB-2015-043

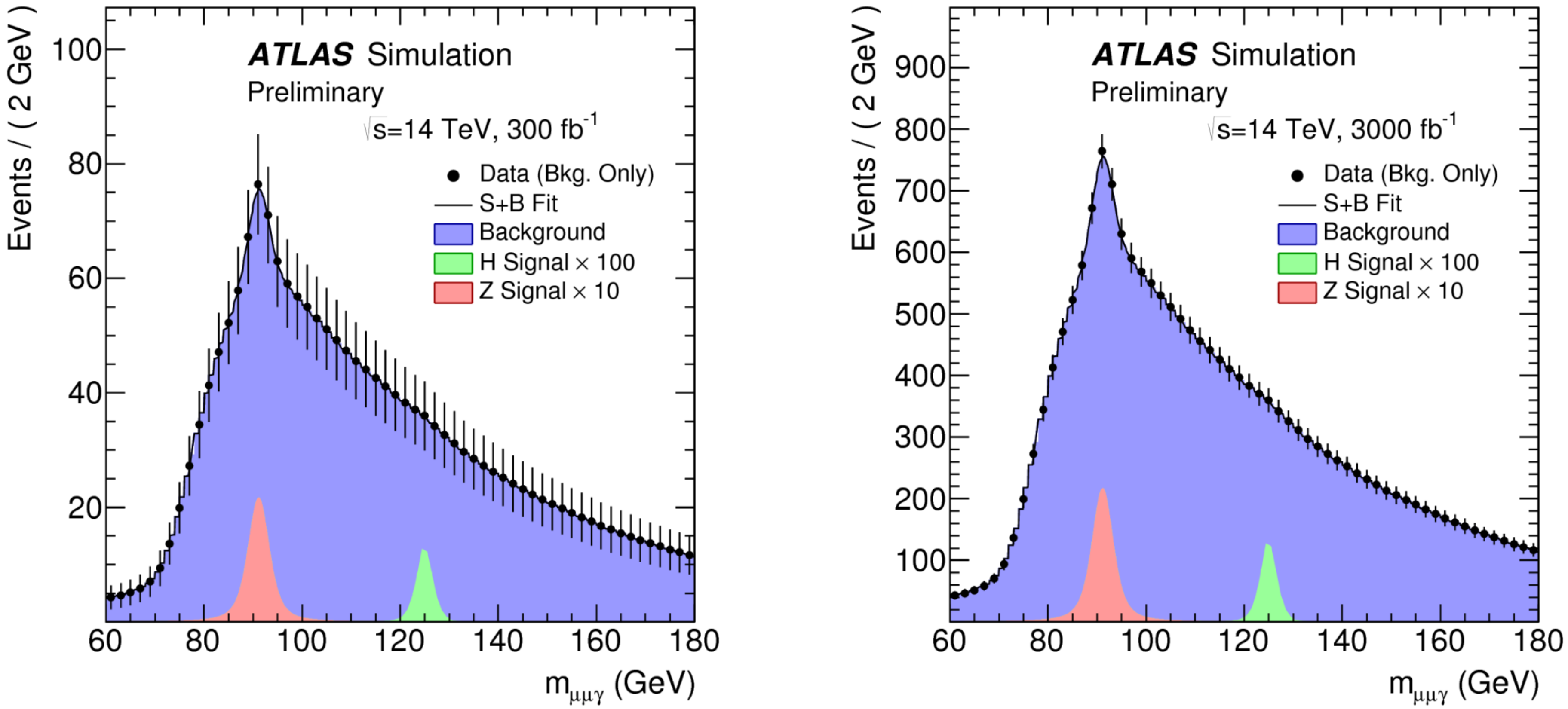

- Performed prospects study for $H(Z) \rightarrow J/\psi\,\gamma$ in 2015 based on Run 1 result
  - Expected to reach $15 \times \mathrm{SM}$ and $4 \times \mathrm{SM}$ sensitivity respectively with HL-LHC (simple assumptions)
  - Room for improvement – but not far off!

Summary

- **ATLAS Searches for exclusive $H/W/Z \to \mathcal{M}\gamma$ decays**
  - H decays: magnitude and sign of quark couplings
  - Z decays: reference channels + tests of QCD factorisation
  - W decays: QCD factorisation + W mass measurements
  - Dedicated triggers capture decays
  - Non-parametric data-driven model for the backgrounds
    - Procedure: [JHEP 10 (2022) 001]
- New $H(Z) \to Q\gamma$ and $H(Z) \to \omega\gamma + H \to K^*\gamma$ results published last year
- $W^\pm \to (\pi^\pm, K^\pm, \rho^\pm)\gamma$ recently public
  - Submitted to PRL
- $H \to D^*\gamma + Z \to (D^0, K_s^0)\gamma$ public this month!
  - Submitted to PLB
- Summary of results: [ATL-PHYS-PUB-2023-004]

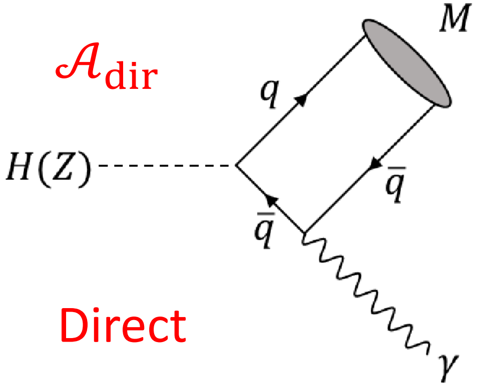

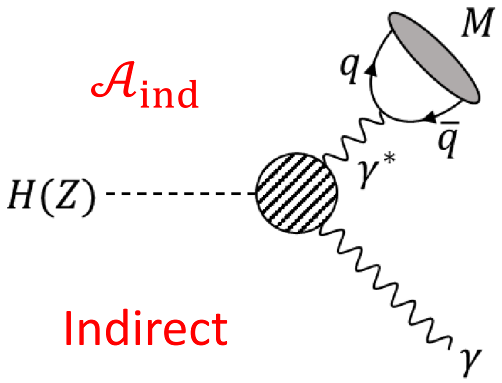

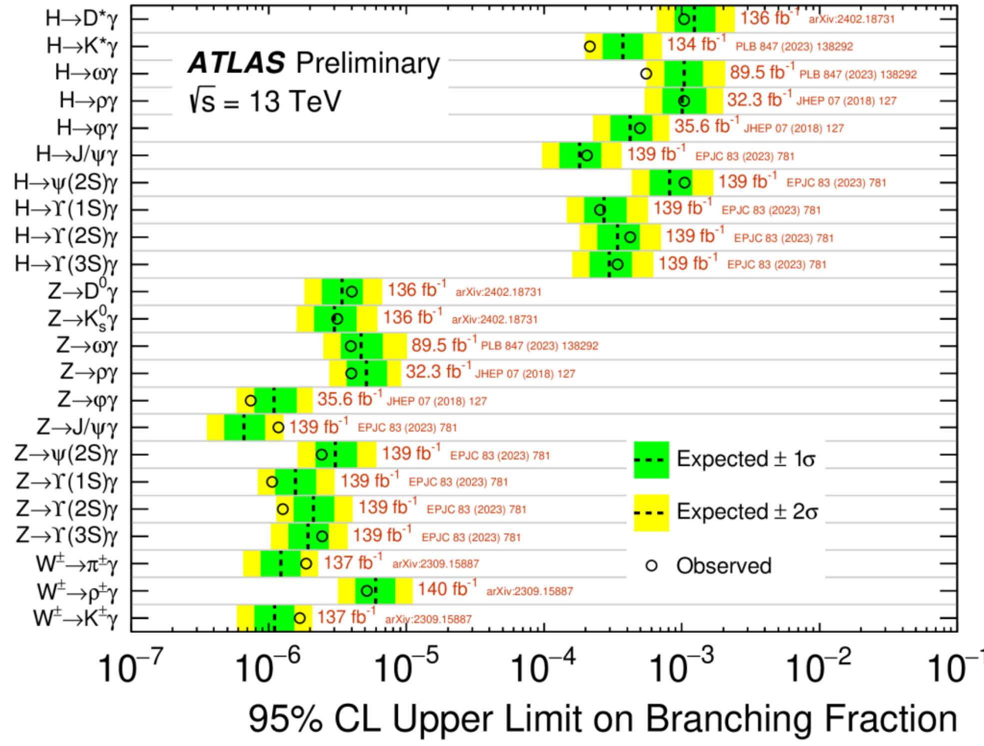

ADDITIONAL SLIDES

$H(Z) \rightarrow (\phi, \rho)\gamma$: Signal Efficiency

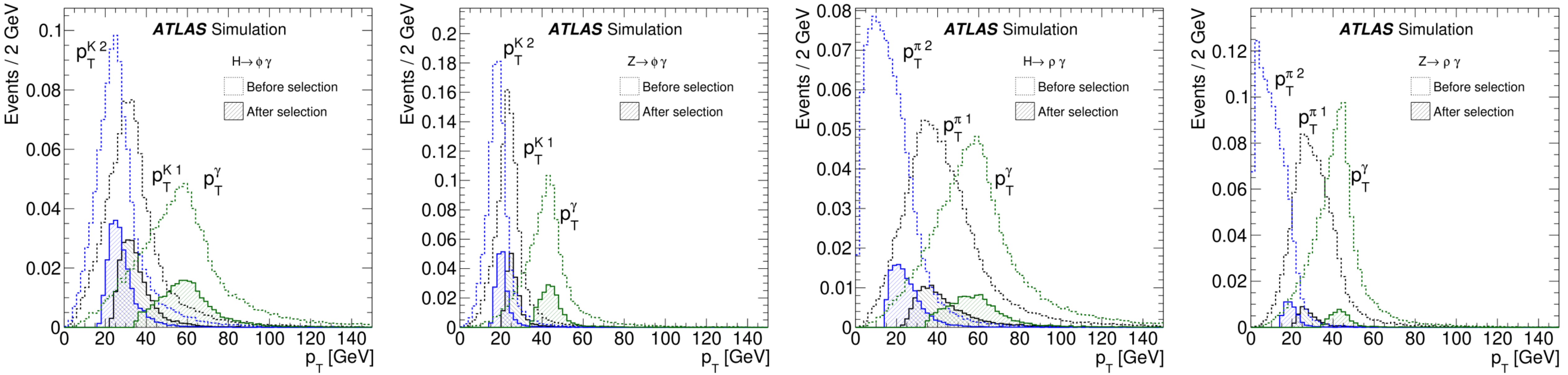

Total Signal Efficiency		
Decay Channel	Z Signal	H Signal
$\phi\gamma$	10%	17%
$\rho\gamma$	2.4%	8%

- Larger photon and track p_{T} in H decays leads to larger signal efficiencies than for Z decays

JHEP 07 (2018) 127

$H(Z) \to (\phi, \rho)\gamma$: Opening Angles

JHEP 07 (2018) 127

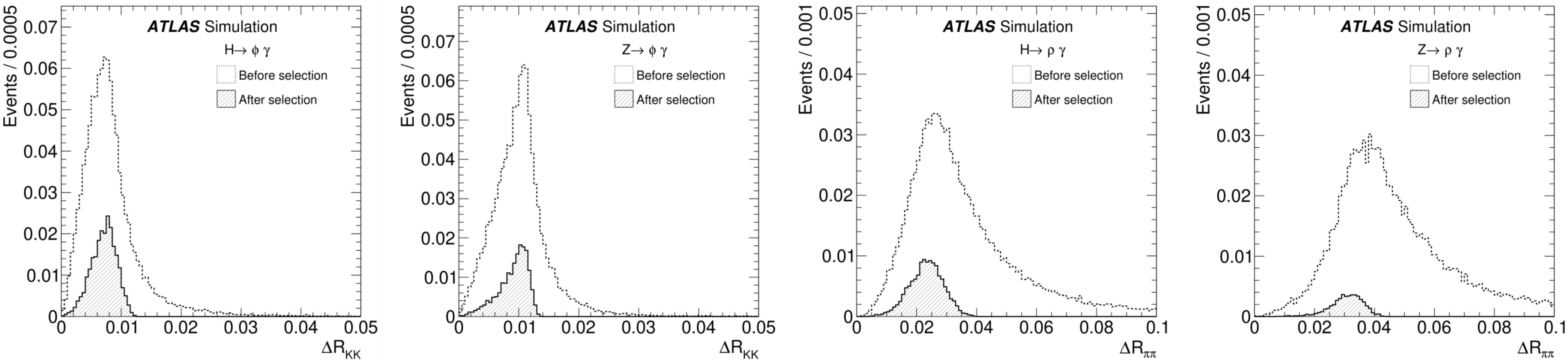

- ➢Small opening angles between decay products
  - ○ Particularly for $\phi \to K^+K^-$: tracking in dense environments

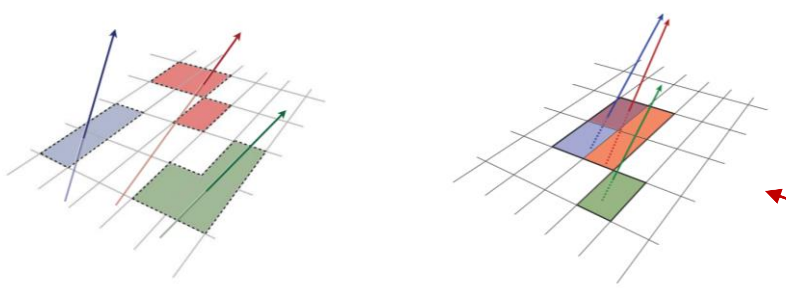

Single-Particle Clusters   Merged Clusters

EPJC 77 (2017) 673

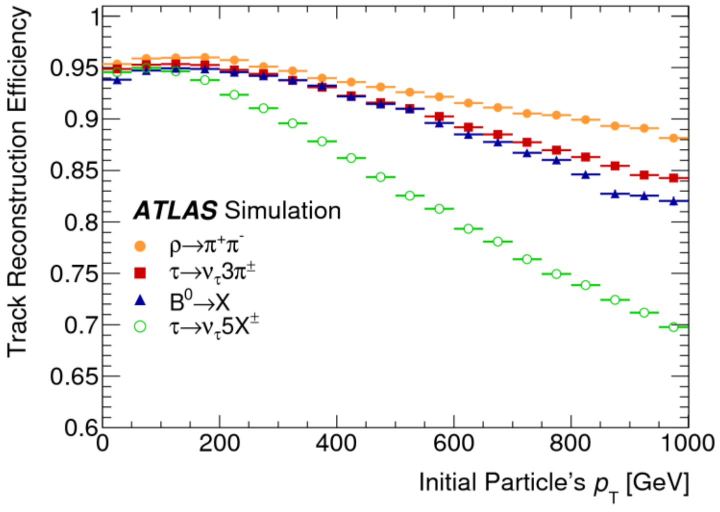

$H(Z) \to (\phi, \rho)\gamma$: Signal Acceptance

- Meson p_{T} distributions for each signal decay

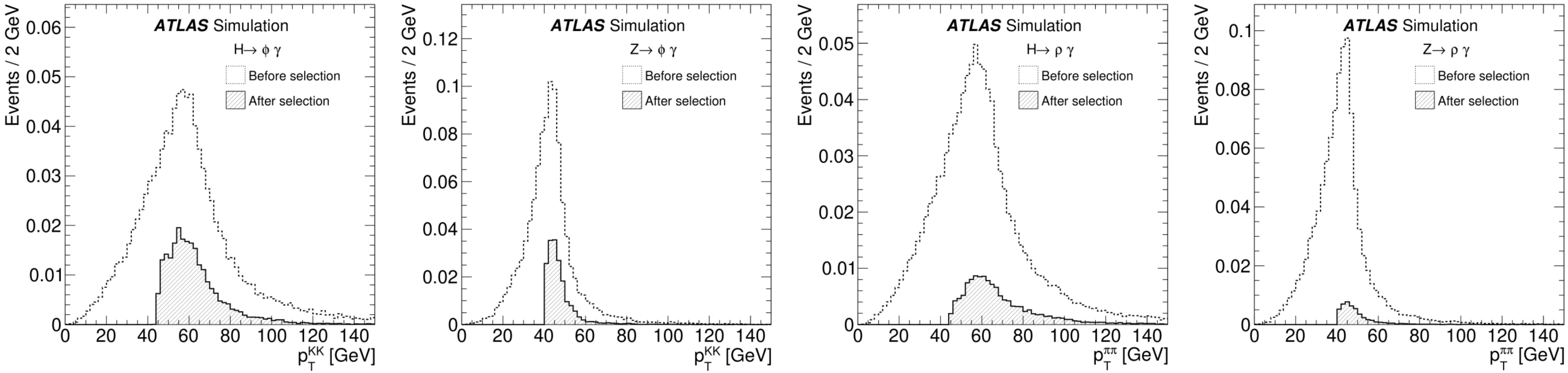

JHEP 07 (2018) 127

$H(Z) \rightarrow (\phi, \rho)\gamma$: Signal Modelling

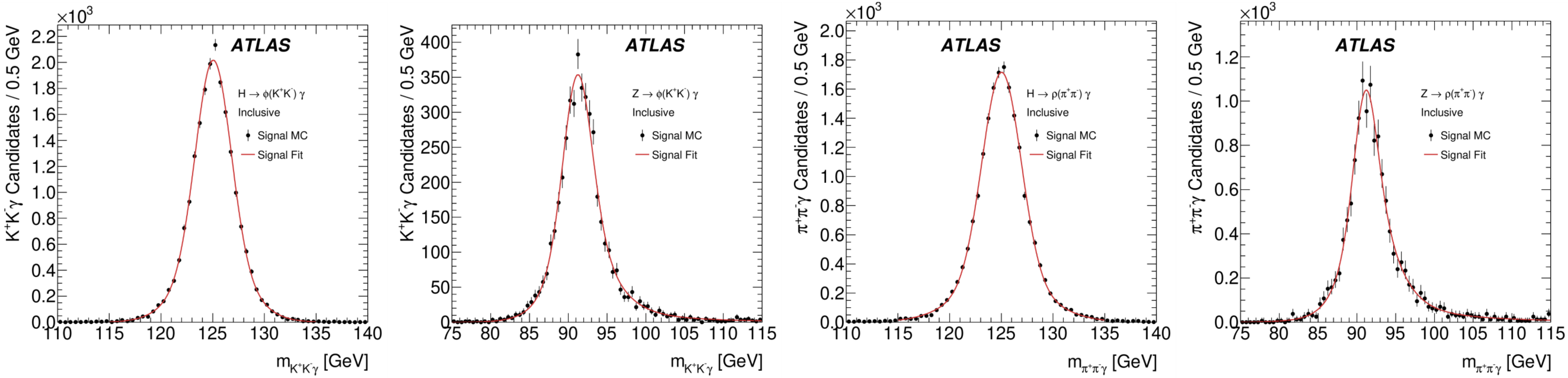

1.8% Resolution

- Model boson mass distributions with analytical fits to simulated events
  - Higgs decays - sum of two Gaussian distributions with a common mean
  - Z decays - (sum of two Voigtian distributions) $\times$ efficiency factor
    - Voigtian: convolution of Gaussian (detector resolution) and Lorentz (Z width) distributions
    - Efficiency factor: accounts for turn-on in signal efficiency with Z mass
- Same approach is applied across all exclusive $\mathcal{M}\gamma$ searches

JHEP 07 (2018) 127

Non-Parametric Data Driven Model: Sampling Scheme 1

- Specific sampling scheme is based on studies of correlations between variables

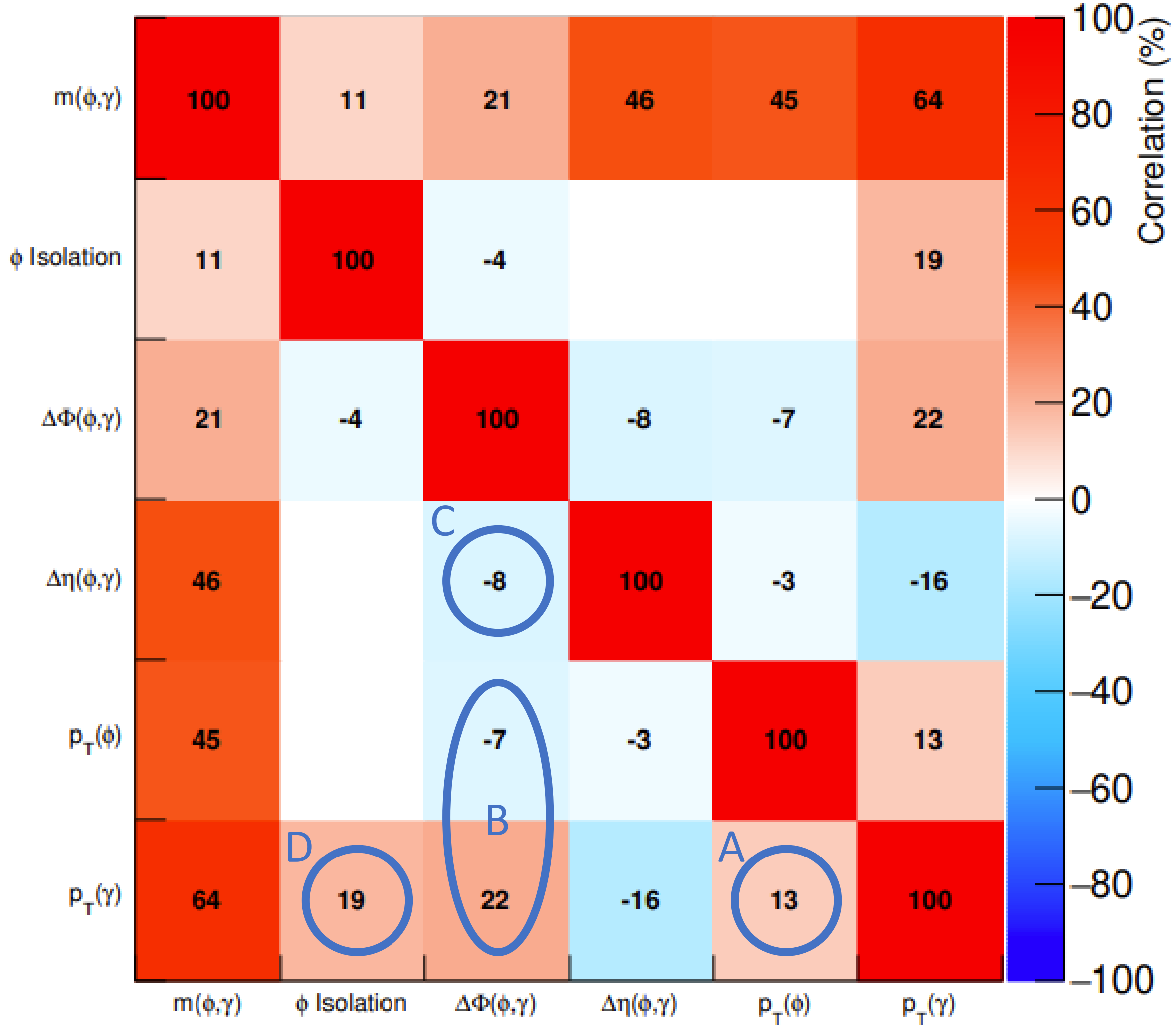

Correlations in "Data"

- Populate series of PDFs (histograms) using data in GR
  - Use these to sample pseudo-events

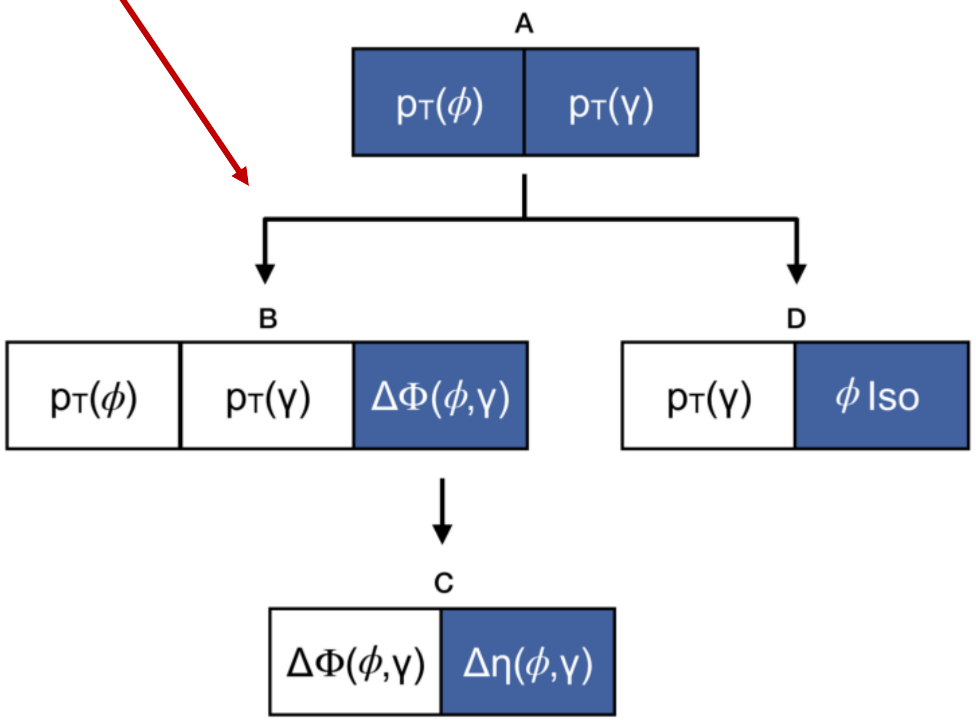

Sampling Scheme

JHEP 10 (2022) 001

Non-Parametric Data Driven Model: Sampling Scheme 2

➢ Important correlations are reproduced in pseudo-events generated with model

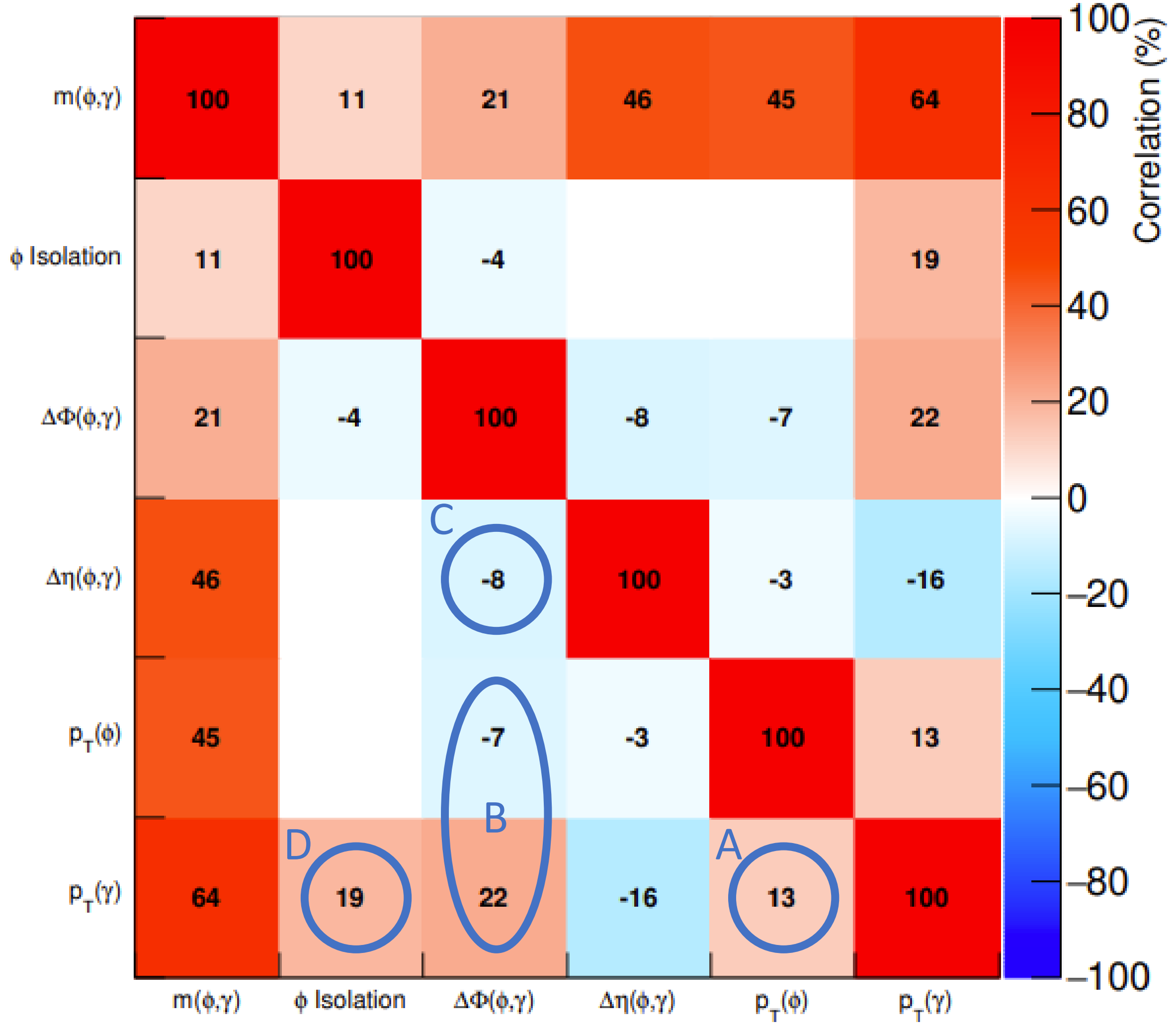

Correlations in “Data”

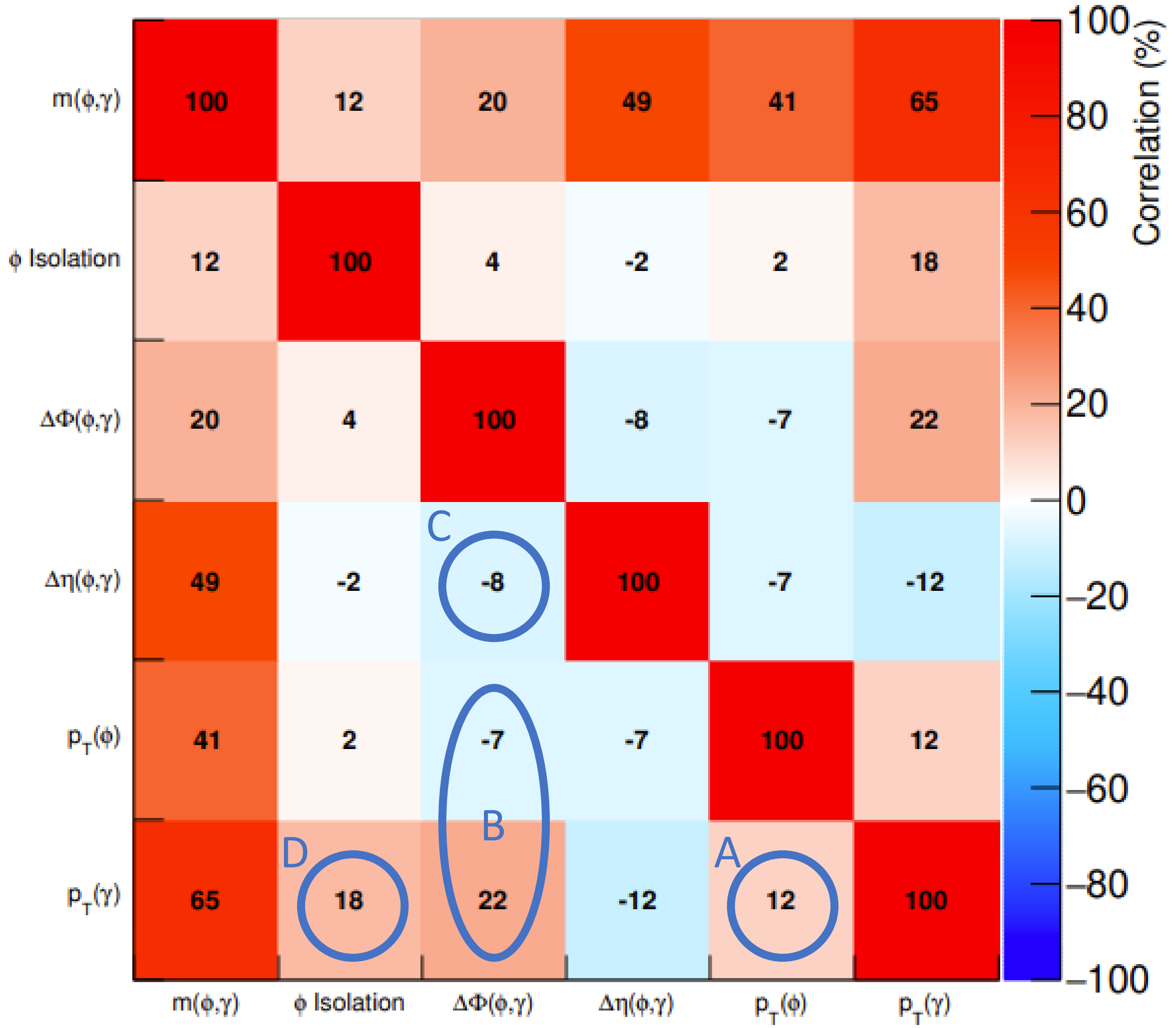

Correlations in Model

JHEP 10 (2022) 001

Non-Parametric Data Driven Model: Demonstration

- Ultimately, only the modelling of the discriminant variable in the SR is important
  - VRs help with troubleshooting

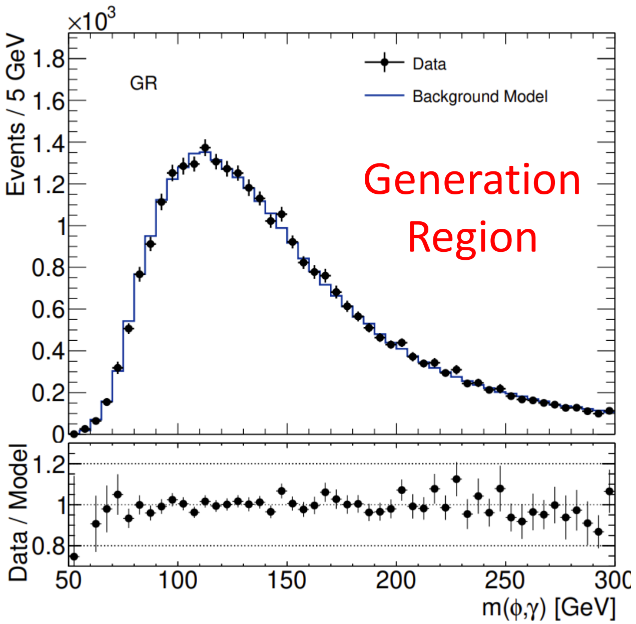

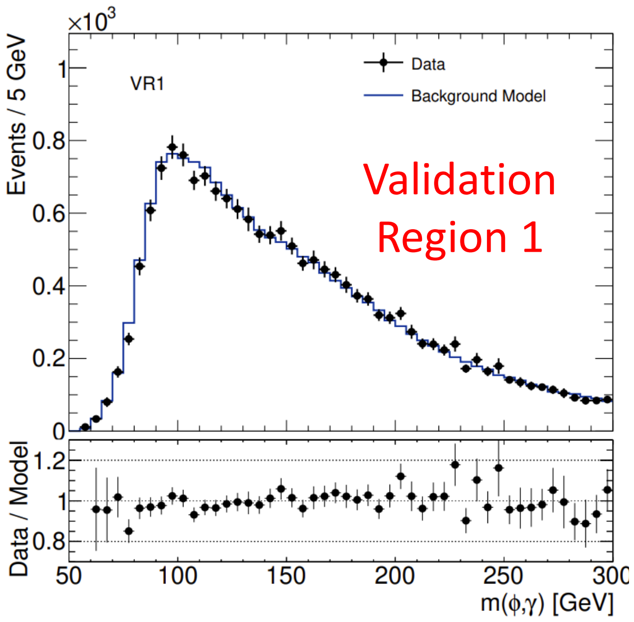

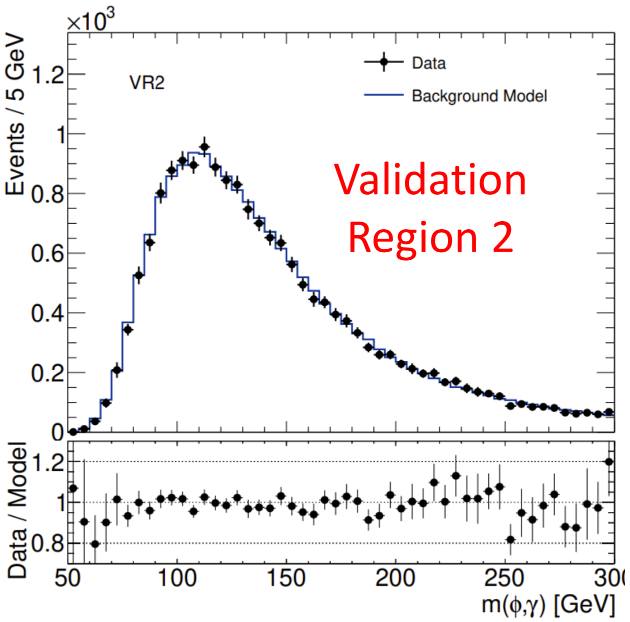

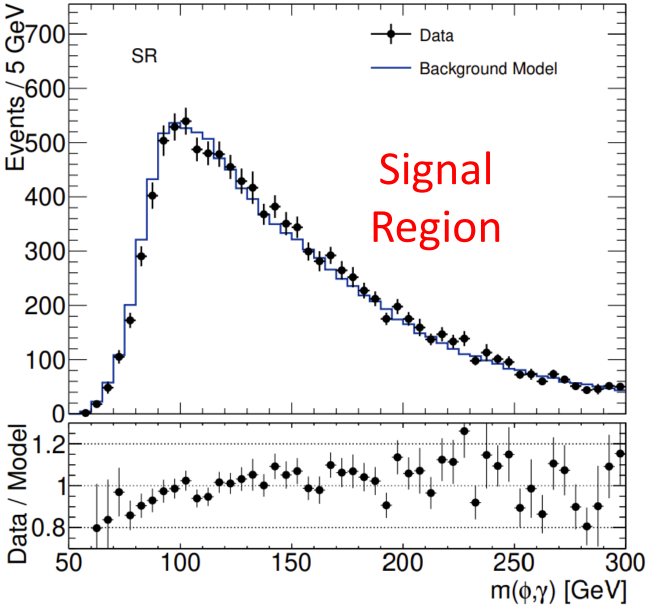

(Plots are Pre-Fit)

	Minimum $p_T(\phi)$ requirement	Maximum $I(\phi)$ requirement
GR	35 GeV	Not applied
VR1	Varying from 40 to 47.2 GeV	Not applied
VR2	35 GeV	0.5
SR	Varying from 40 to 47.2 GeV	0.5

JHEP 10 (2022) 001

Non-Parametric Data Driven Model: Shape Systematics

- Typically define several shape uncertainties to allow model to adapt to data
  - Generate alternate templates by modifying generation procedure

- Mass tilt: reweight mass distribution with a linear function
  - Distribution can adapt to tilts in ratio
- p_{T} shift: shift generated photon p_{T} in GR
  - Distribution can shift higher/lower
- $\Delta\phi$ distortion: reweight generated $\Delta\phi$ in GR
  - Width of distribution can increase/decrease

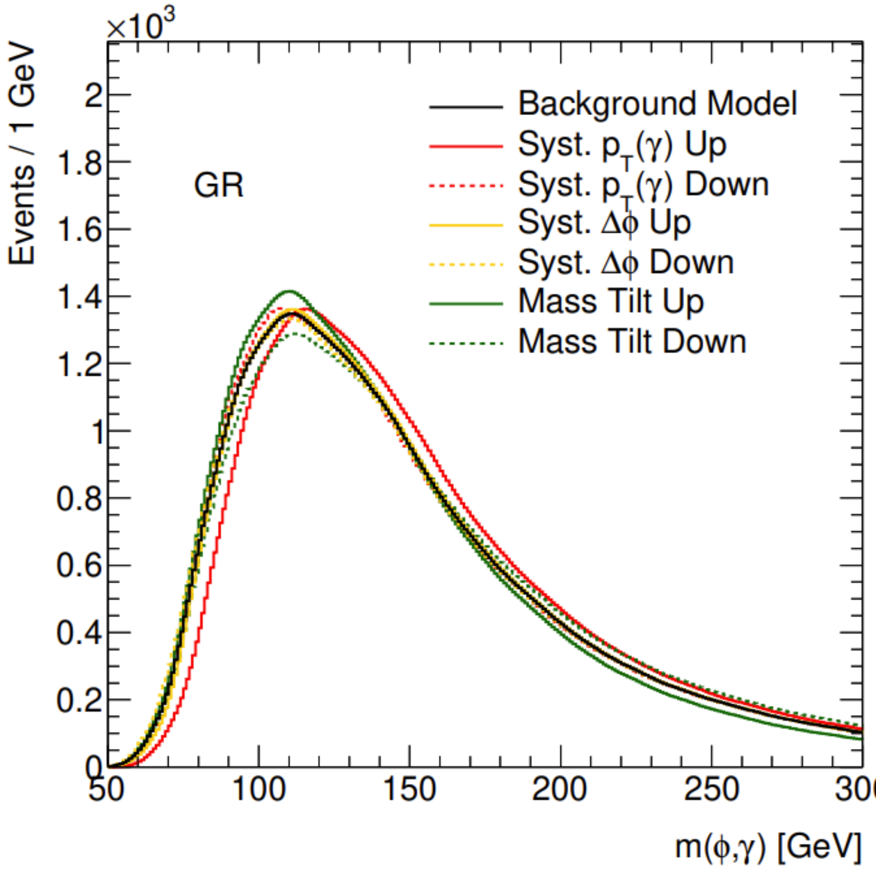

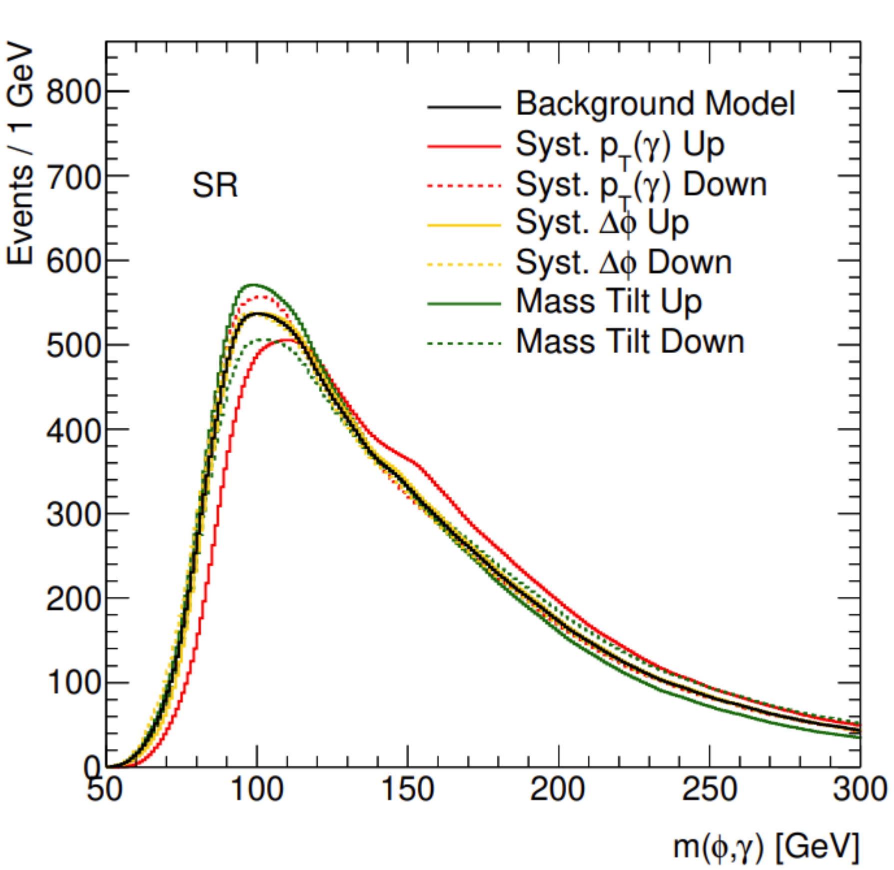

JHEP 10 (2022) 001

Non-Parametric Data Driven Model: Additional Variables 1

- Non-discriminant variables can also be used in model validation
  - Less important as not used in fit – but can help troubleshoot issues

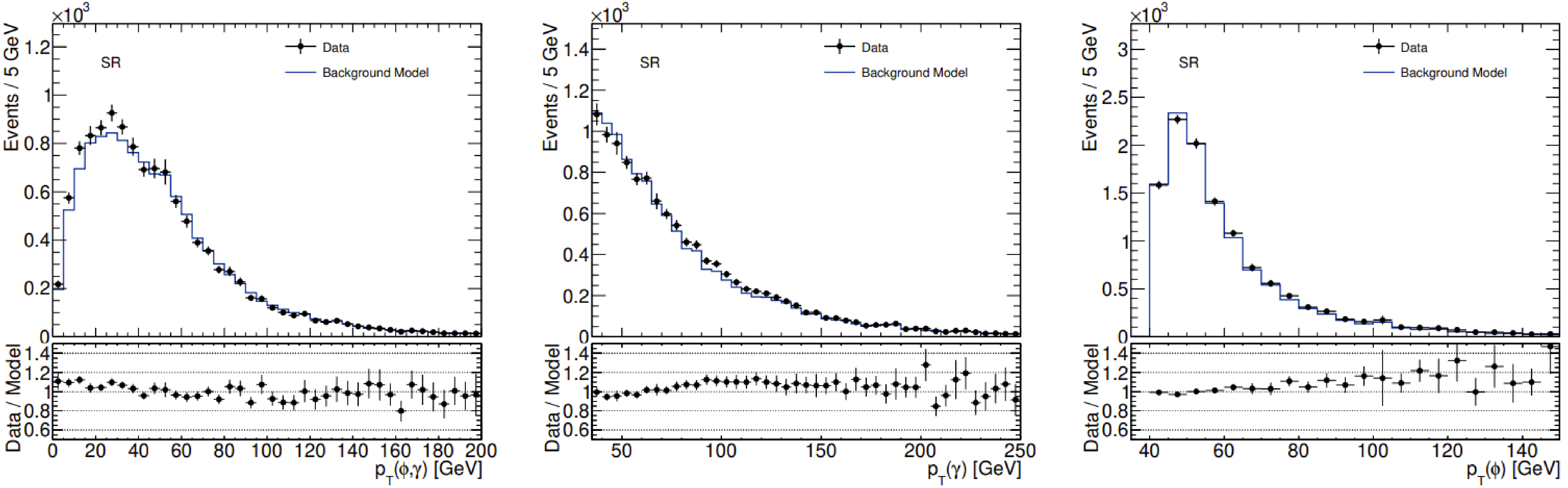

JHEP 10 (2022) 001

Non-Parametric Data Driven Model: Additional Variables 2

- Non-discriminant variables can also be used in model validation
  - Less important as not used in fit – but can help troubleshoot issues

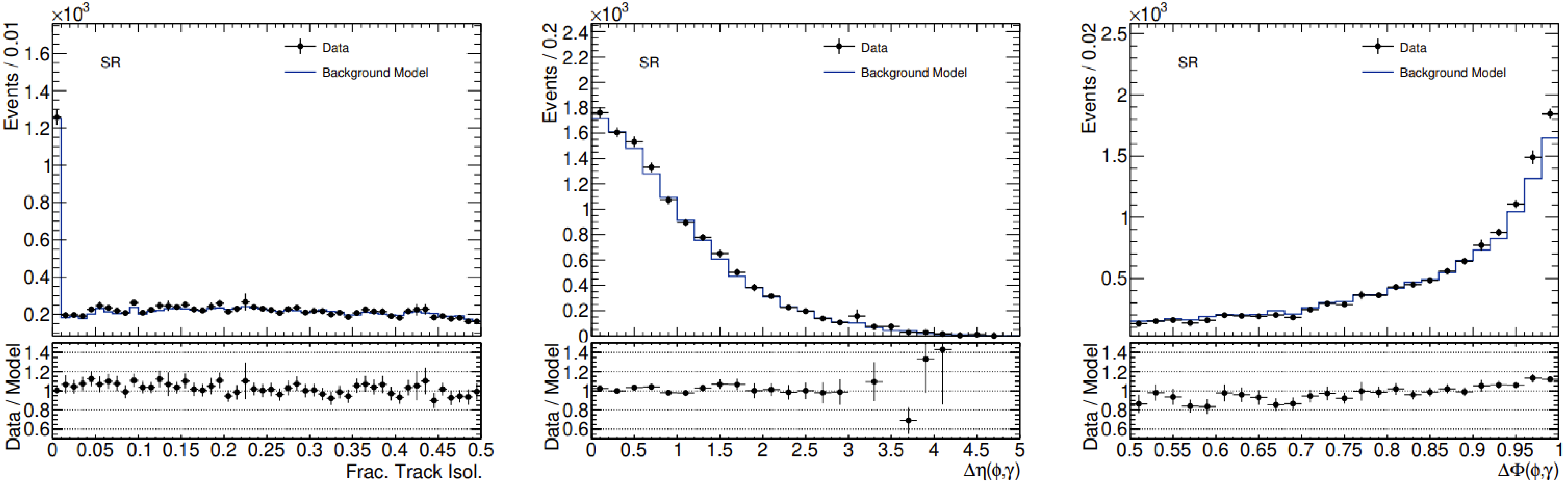

JHEP 10 (2022) 001

$H(Z) \to (\phi, \rho)\gamma$: Background Modelling

- Background is multi-jet and γ+jet sources – treat inclusively
  - Use non-parametric data-driven background model
  - Define sideband regions for further validation

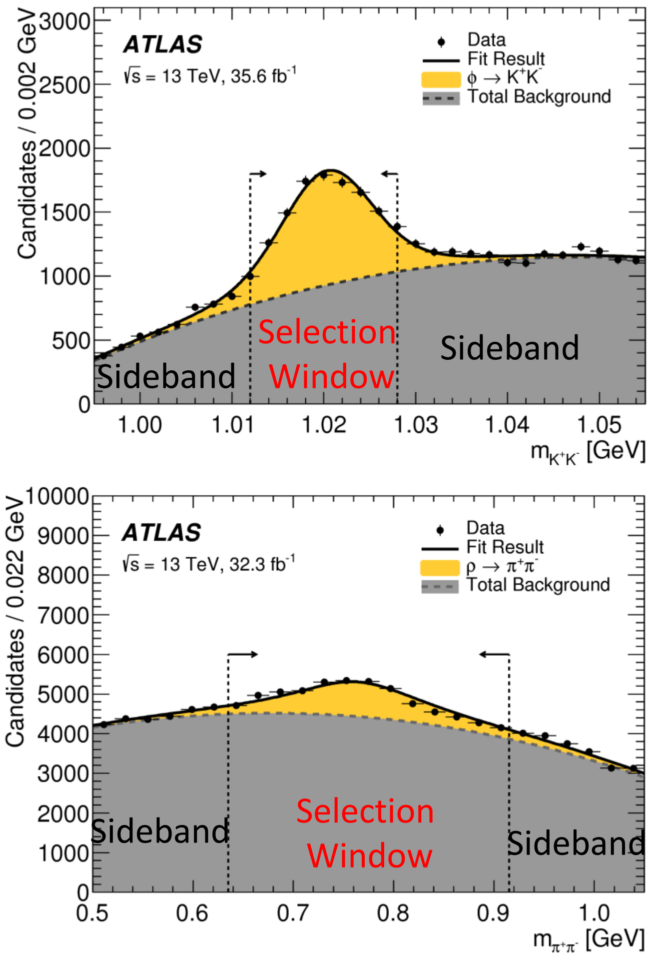

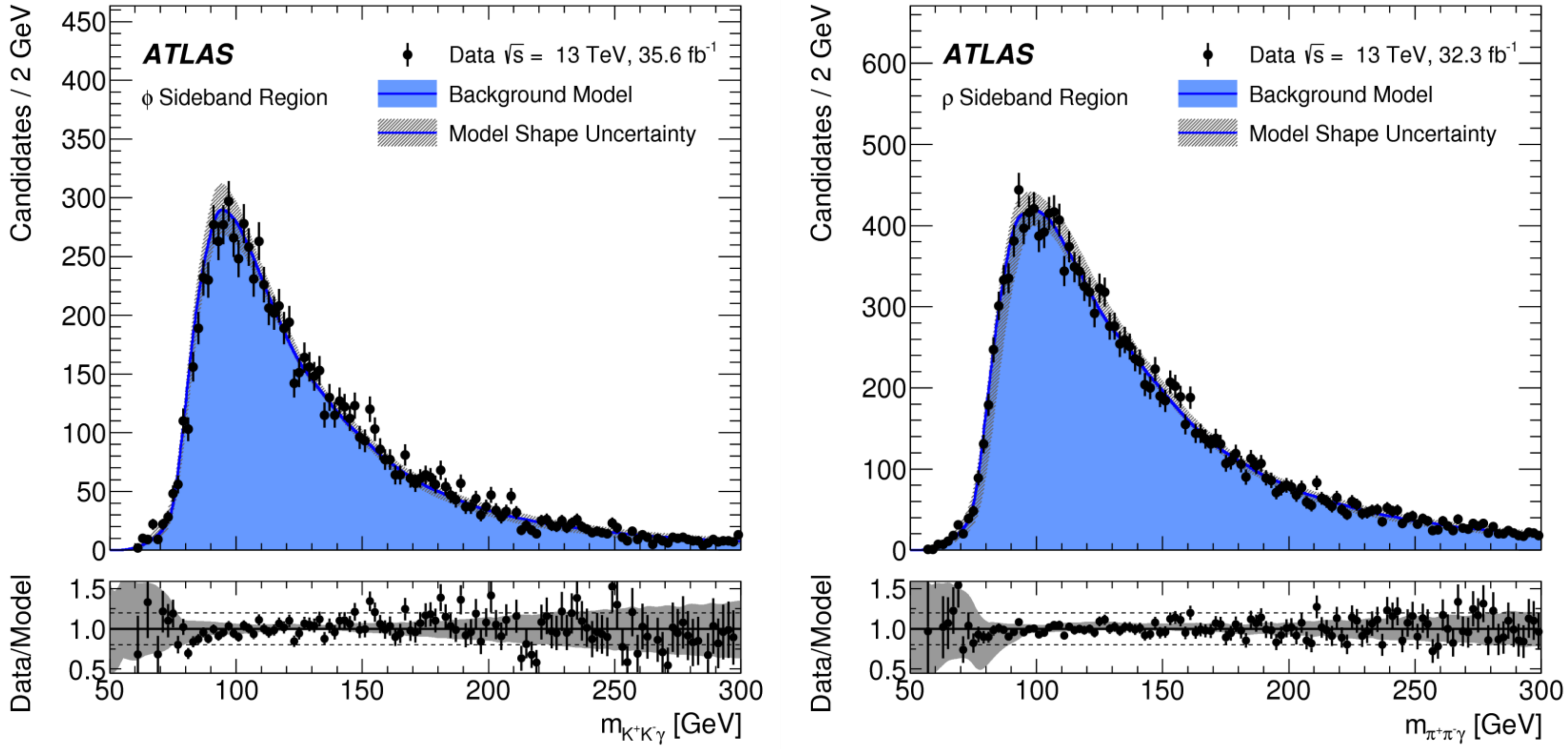

Background in ϕ/ρ-mass Sidebands (Pre-Fit)

JHEP 07 (2018) 127

$H(Z) \to (\phi, \rho)\gamma$: Background Validation

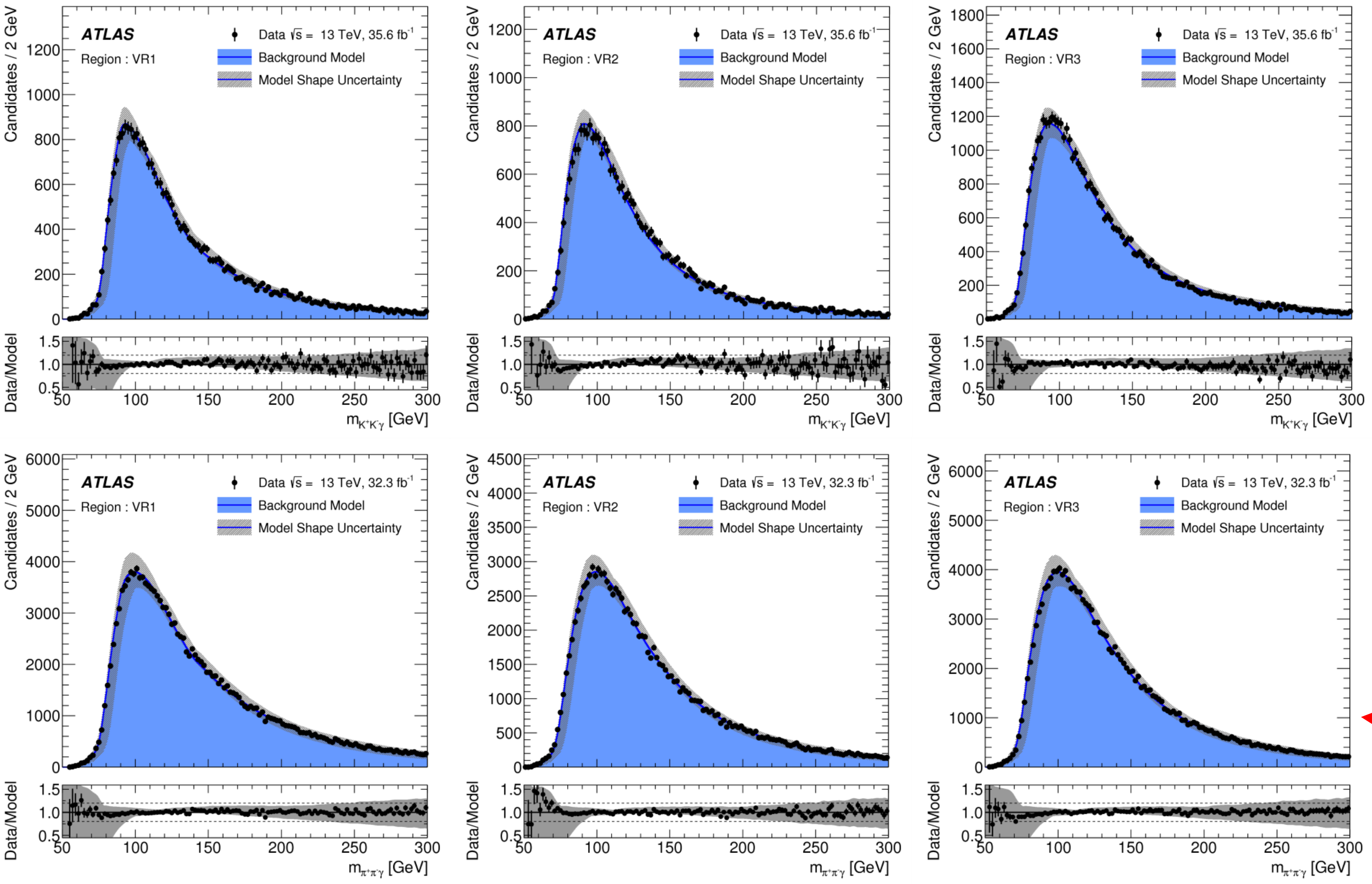

- Freedom via shape systematics: mass-tilt, $\Delta\phi$-distortion, p_{T}-shift

$\phi\gamma$ Background Validation

$\rho\gamma$ Background Validation

JHEP 07 (2018) 127

$H(Z) \to (\phi, \rho)\gamma$: Sideband Background Validation

- Validation plots in $\phi\gamma$ sideband regions

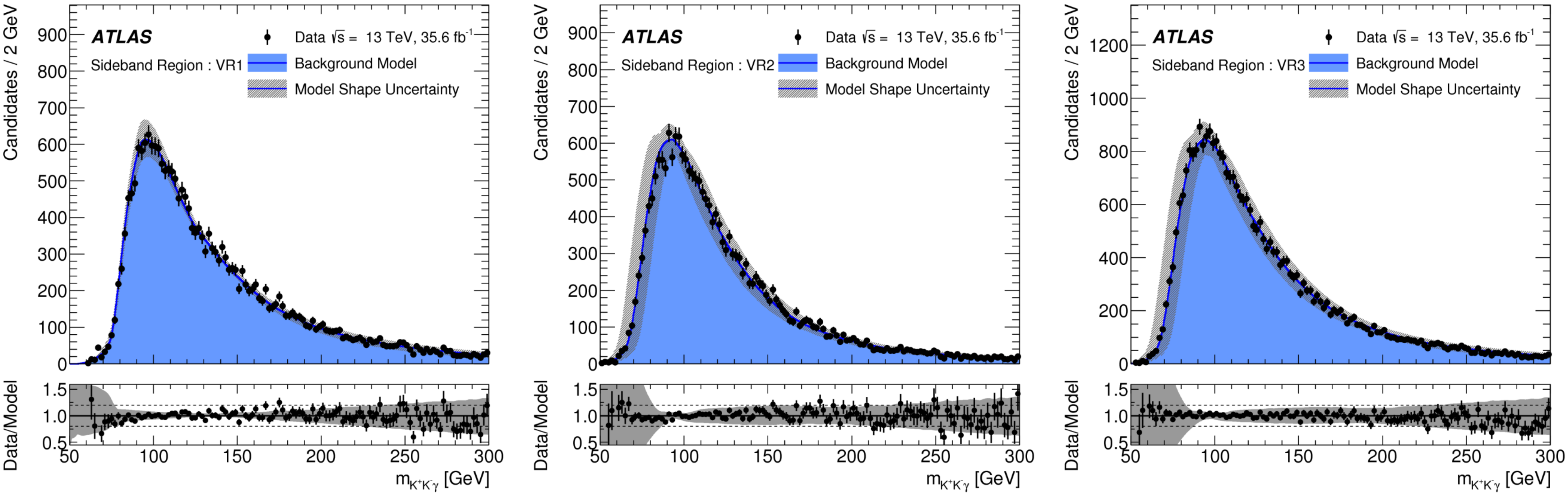

JHEP 07 (2018) 127

$H(Z) \to (\phi, \rho)\gamma$: Sideband Background Validation

- Validation plots in $\rho\gamma$ sideband regions

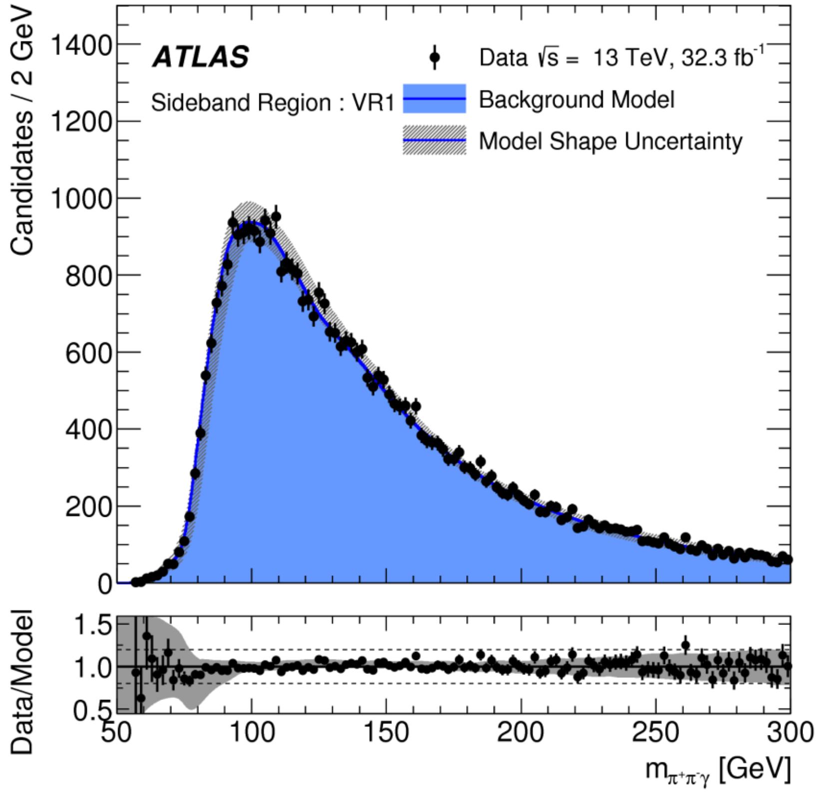

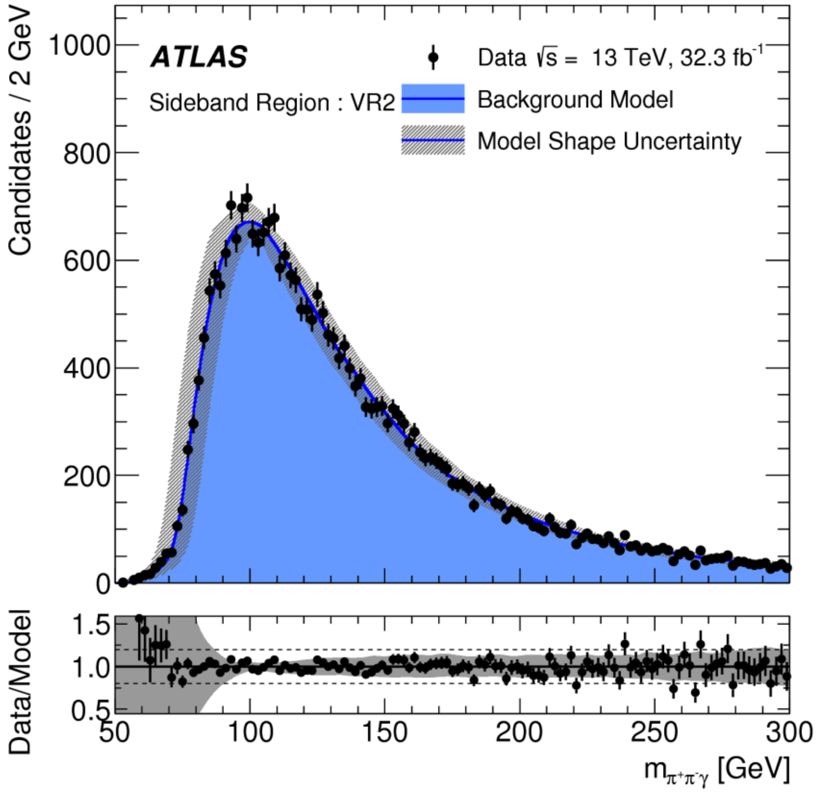

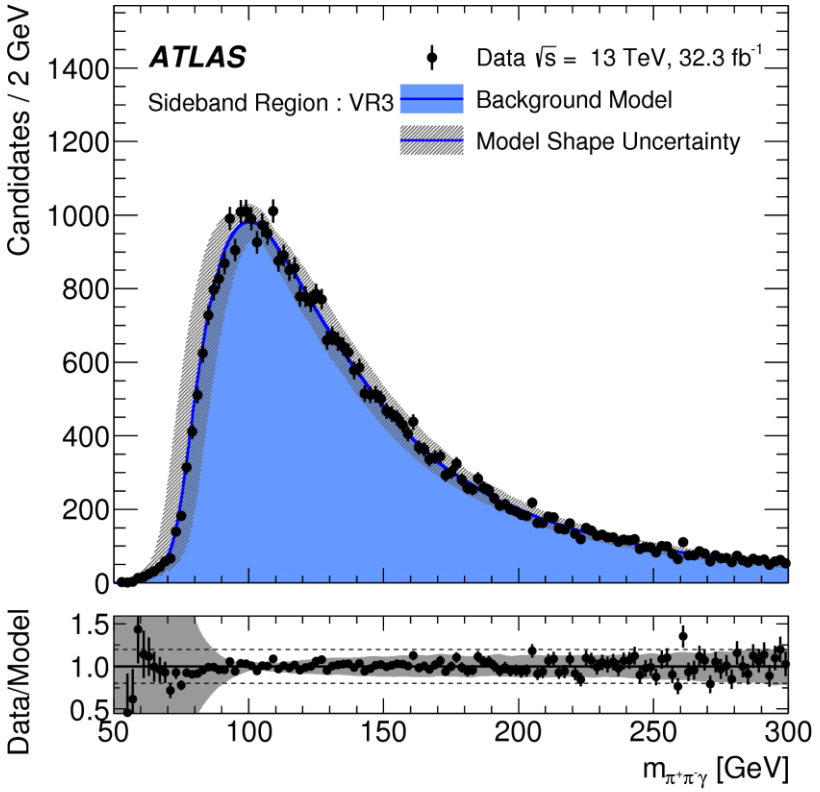

JHEP 07 (2018) 127

$H(Z) \rightarrow (\phi, \rho)\gamma$: Results (Full Mass Range)

- Unbinned likelihood fit in $m(K^+K^-\gamma)$ and $m(\pi^+\pi^-\gamma)$

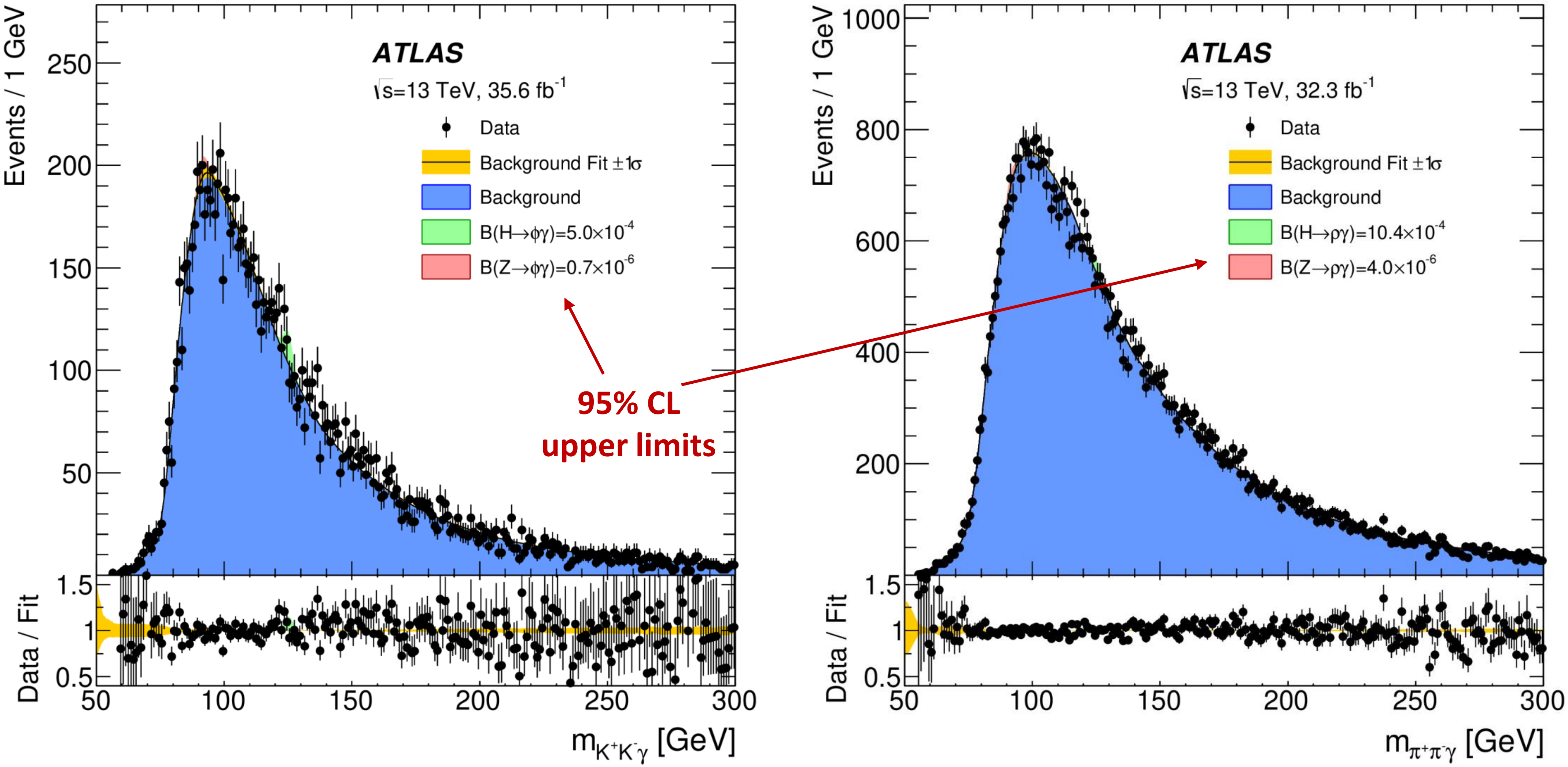

JHEP 07 (2018) 127

$H(Z) \rightarrow (\phi, \rho)\gamma$: Limits and Observed Events

- Unbinned likelihood fit in $m(K^+K^-\gamma)$ and $m(\pi^+\pi^-\gamma)$

	Observed yields (Mean expected background)					Expected signal yields	
	Mass range [GeV]					H	Z
	All	81–101		120–130		$[\mathcal{B} = 10^{-4}]$	$[\mathcal{B} = 10^{-6}]$
$\phi\gamma$	12051	3364	(3500 ± 30)	1076	(1038 ± 9)	15.1 ± 1.5	98 ± 8
$\rho\gamma$	58702	12583	(12660 ± 60)	5473	(5450 ± 30)	14.3 ± 1.4	47 ± 4

Observed and Expected Events

Branching Fraction Limit (95% CL)	Expected	Observed
$\mathcal{B}(H \rightarrow \phi\gamma)$ [10^{-4}]	$4.2^{+1.8}_{-1.2}$	5.0
$\mathcal{B}(Z \rightarrow \phi\gamma)$ [10^{-6}]	$1.1^{+0.5}_{-0.3}$	0.7
$\mathcal{B}(H \rightarrow \rho\gamma)$ [10^{-4}]	$10.0^{+4.9}_{-2.8}$	10.4
$\mathcal{B}(Z \rightarrow \rho\gamma)$ [10^{-6}]	$5.1^{+2.1}_{-1.4}$	4.0

Observed and Expected Limits

JHEP 07 (2018) 127

$H \to K^*\gamma$ and $H(Z) \to \omega\gamma$: Ancestral Sampling Scheme

- Important correlations differ compared to $H(Z) \to (\phi, \rho)\gamma$ searches: adapt sampling scheme

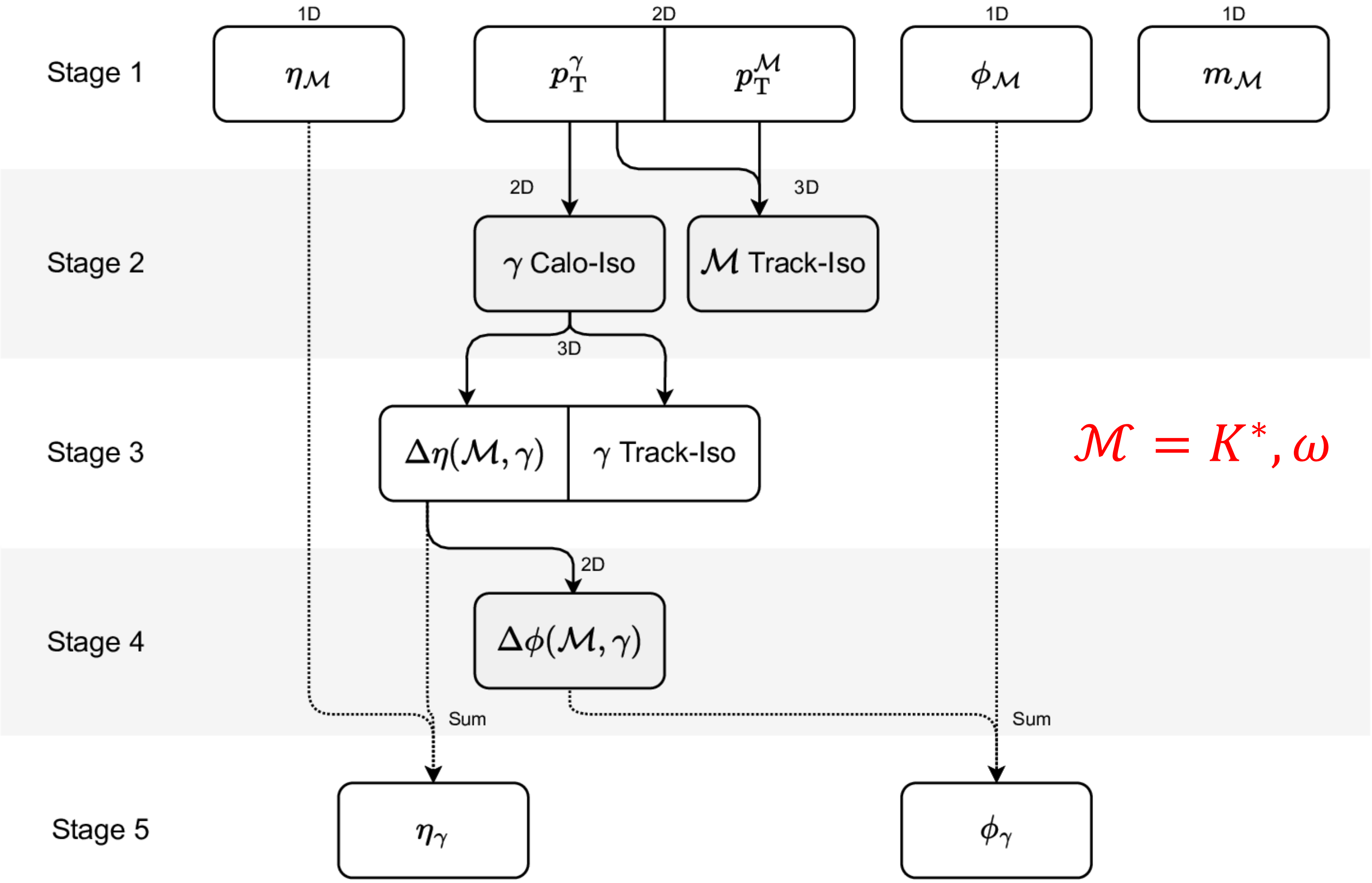

$\mathcal{M} = K^*, \omega$

PLB 847 (2023) 138292

$H \to K^*\gamma$ and $H(Z) \to \omega\gamma$: Strategy

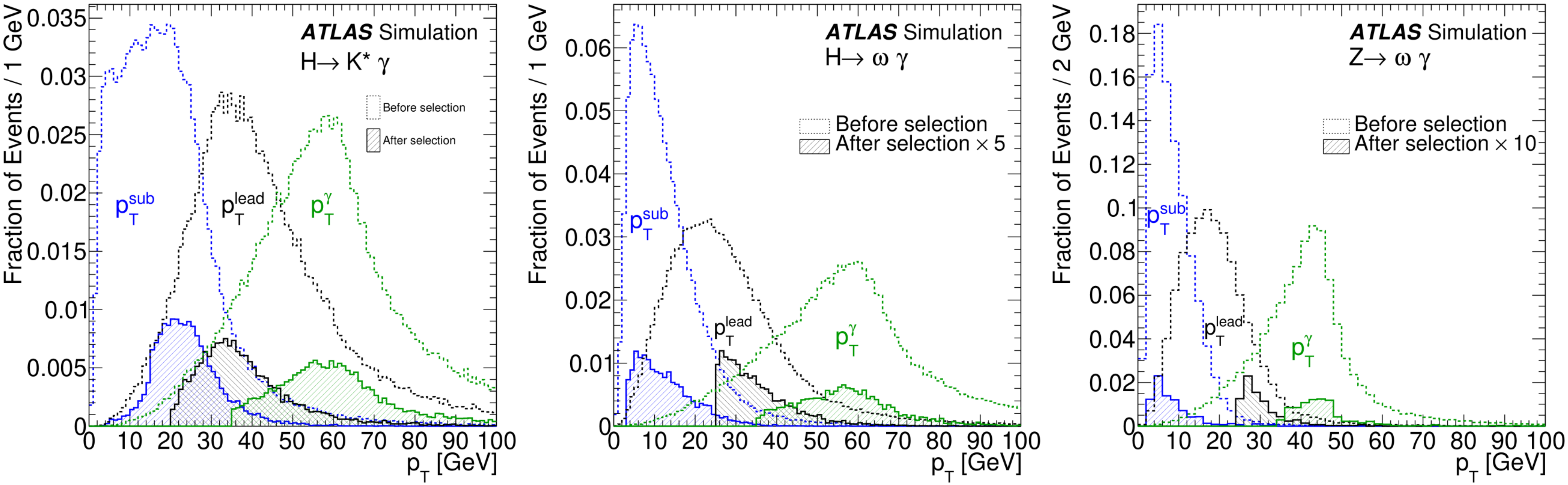

- Shapes for $H \to K^*\gamma$ and $Z \to \omega\gamma$ same form as in $(\phi, \rho)\gamma$
  - $H \to \omega\gamma$ modelled with Gaussian + crystal-ball distribution
- Background is multi-jet and γ+jet sources
  - Use non-parametric data-driven background model

Total Signal Efficiency		
$H \to K^*\gamma$	$H \to \omega\gamma$	$Z \to \omega\gamma$
12.1%	2.2%	0.4%

PLB 847 (2023) 138292

$H \to K^*\gamma$ and $H(Z) \to \omega\gamma$: Background Model

- Background is multi-jet and γ+jet sources – treat inclusively
  - Use non-parametric data-driven background model

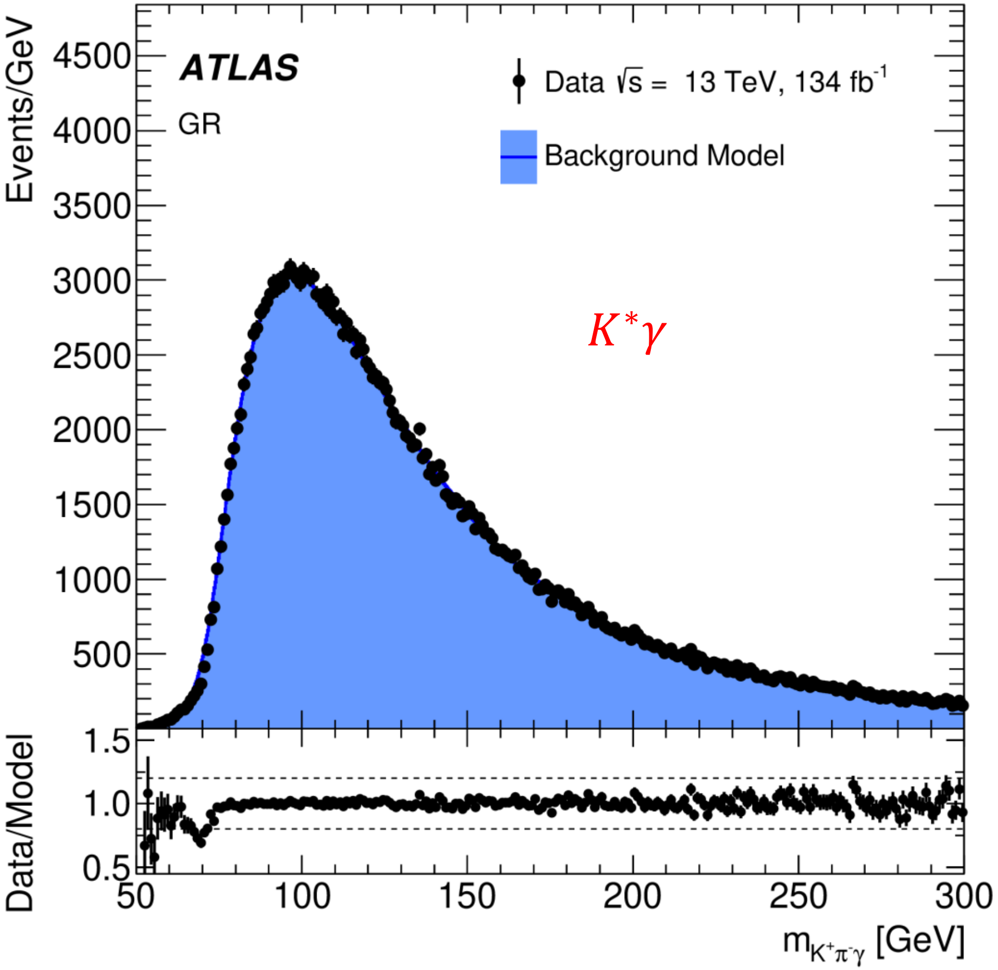

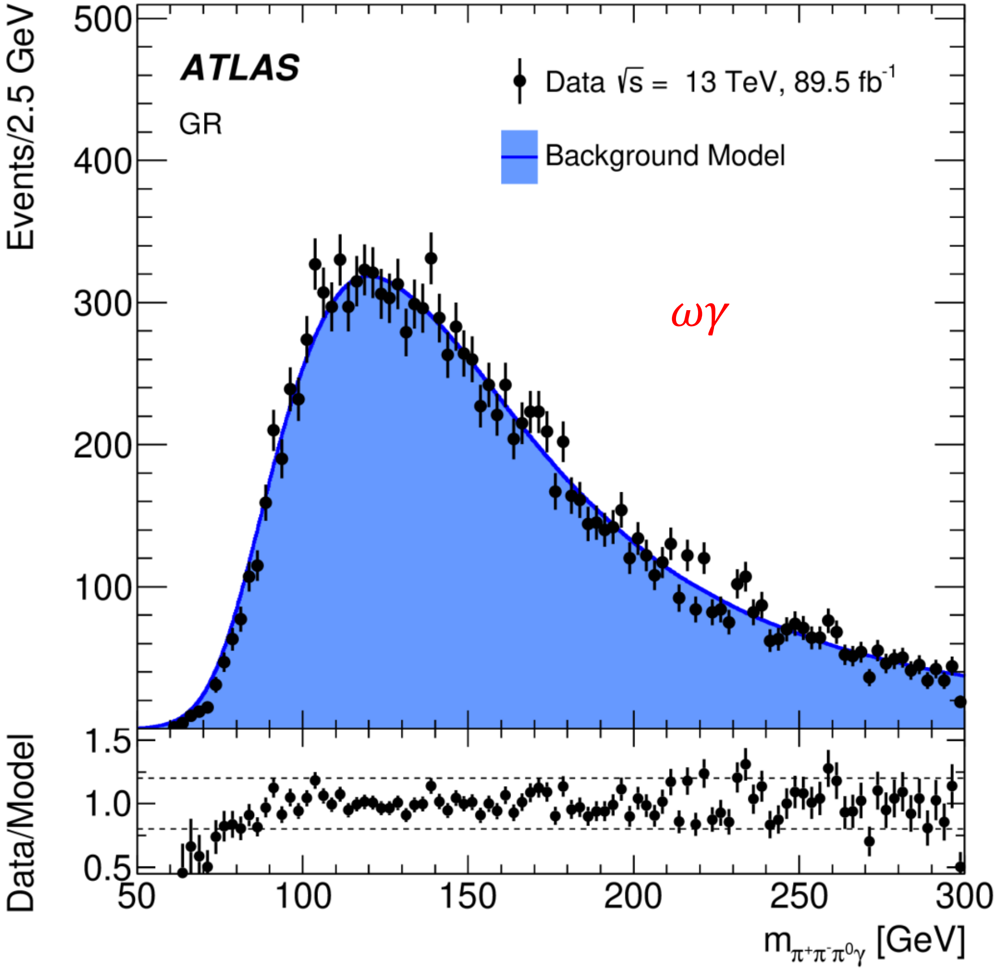

Background in Generation Region

PLB 847 (2023) 138292

$H \to K^*\gamma$ and $H(Z) \to \omega\gamma$: Background Validation

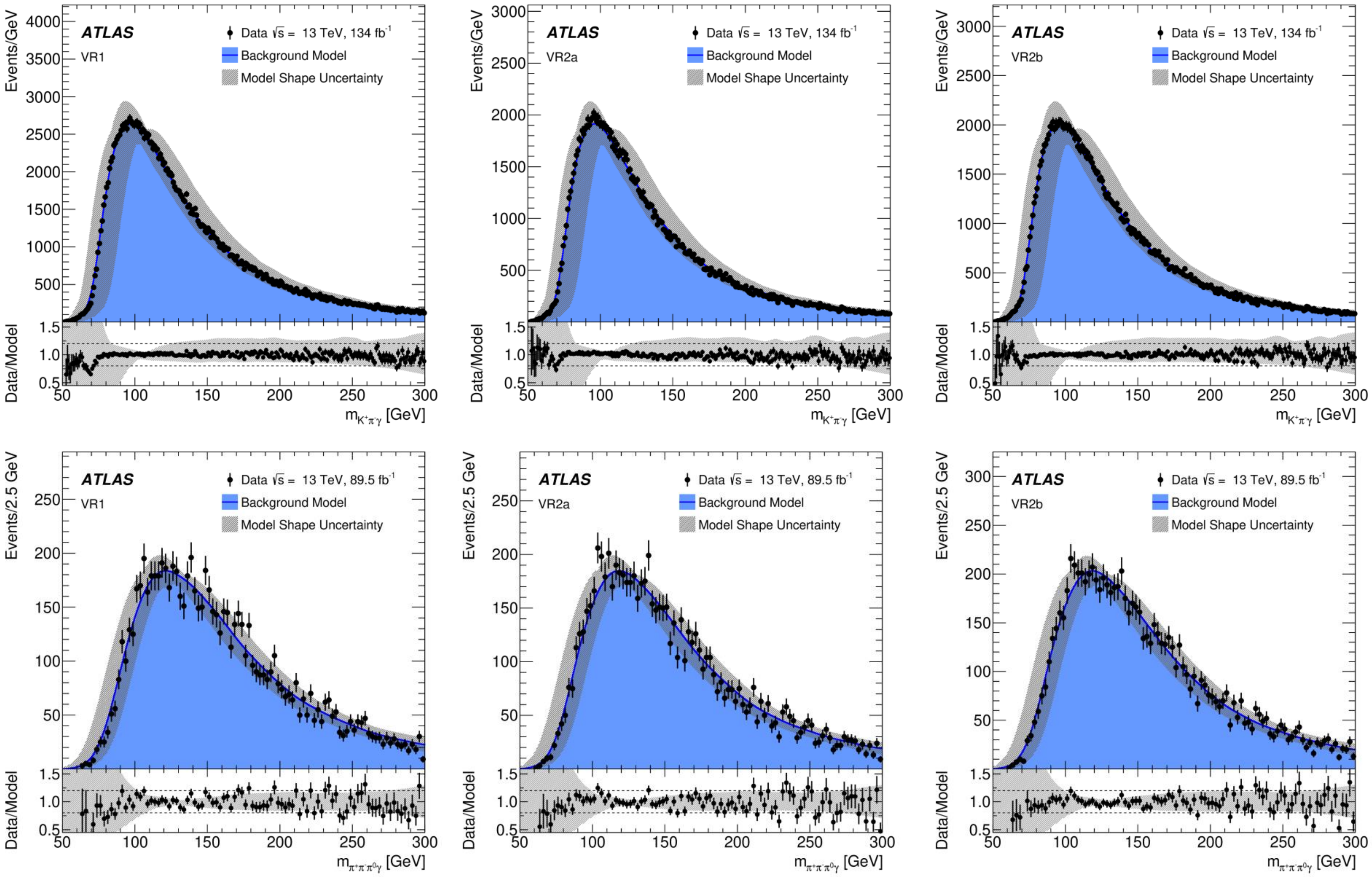

- Freedom via shape systematics: mass-tilt, $\Delta\phi$-distortion, p_{T}-shift

$K^*\gamma$ Background Validation

$\omega\gamma$ Background Validation

PLB 847 (2023) 138292

$H \to K^* \gamma$ and $H(Z) \to \omega\gamma$: Sideband Validation

- Unbinned likelihood fit in $m(K^{\pm}\pi^{\mp}\gamma)$ and $m(\pi^+\pi^-\pi^0\gamma)$

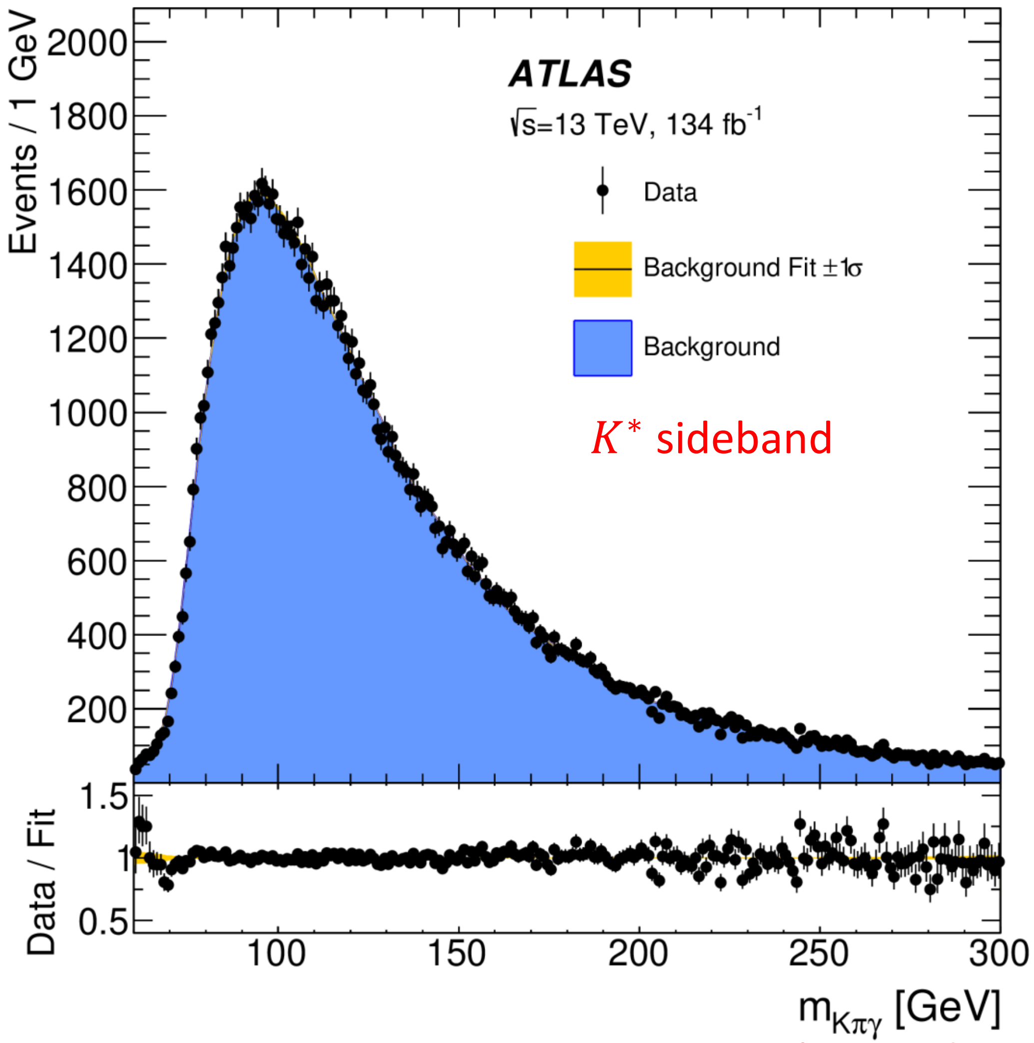

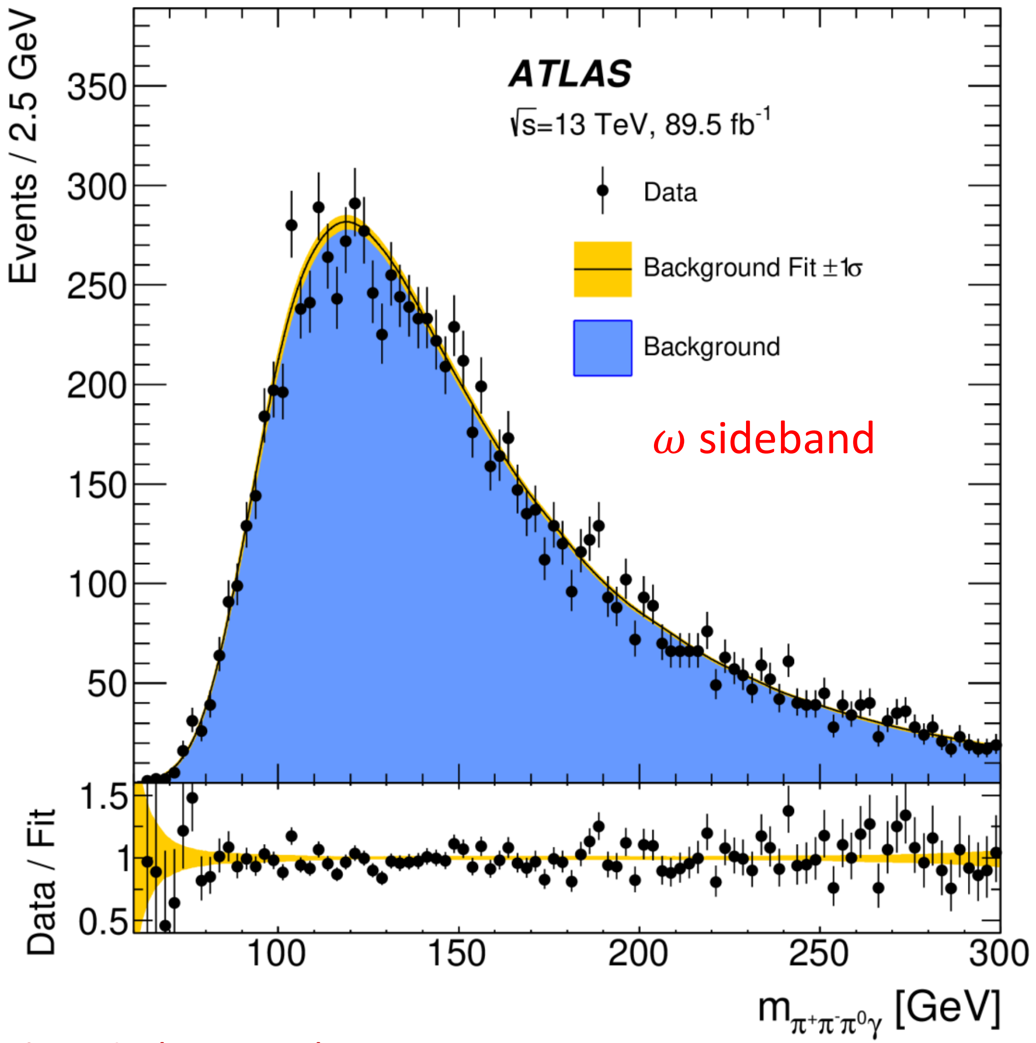

Background in Sidebands (Post-Fit)

PLB 847 (2023) 138292

$H \to K^*\gamma$ and $H(Z) \to \omega\gamma$: Limits and Observed Events

- Unbinned likelihood fit in $m(K^{\pm}\pi^{\mp}\gamma)$ and $m(\pi^+\pi^-\pi^0\gamma)$

Channel	Mass range [GeV]	Observed (Expected) background	H signal $\mathcal{B} = 10^{-4}$	Z signal $\mathcal{B} = 10^{-6}$
$H \to \omega\gamma$	115–135	686 (730 ± 17)	9 ± 1	–
$Z \to \omega\gamma$	80–100	388 (386 ± 16)	–	18 ± 2
$H \to K^*\gamma$	120–130	9526 (9630 ± 50)	53 ± 4	–

Observed and Expected Events

Channel	95% CL upper limit	
	Expected	Observed
$H \to \omega\gamma$ $[10^{-4}]$	$10.4^{+3.8}_{-2.9}$	5.5
$Z \to \omega\gamma$ $[10^{-6}]$	$4.7^{+2.0}_{-1.3}$	3.9
$H \to K^*\gamma$ $[10^{-4}]$	$3.7^{+1.5}_{-1.0}$	2.2

Observed and Expected Limits

PLB 847 (2023) 138292

$H \to D^*\gamma$ & $Z \to (D^0, K_s^0)\gamma$: Signal Efficiency

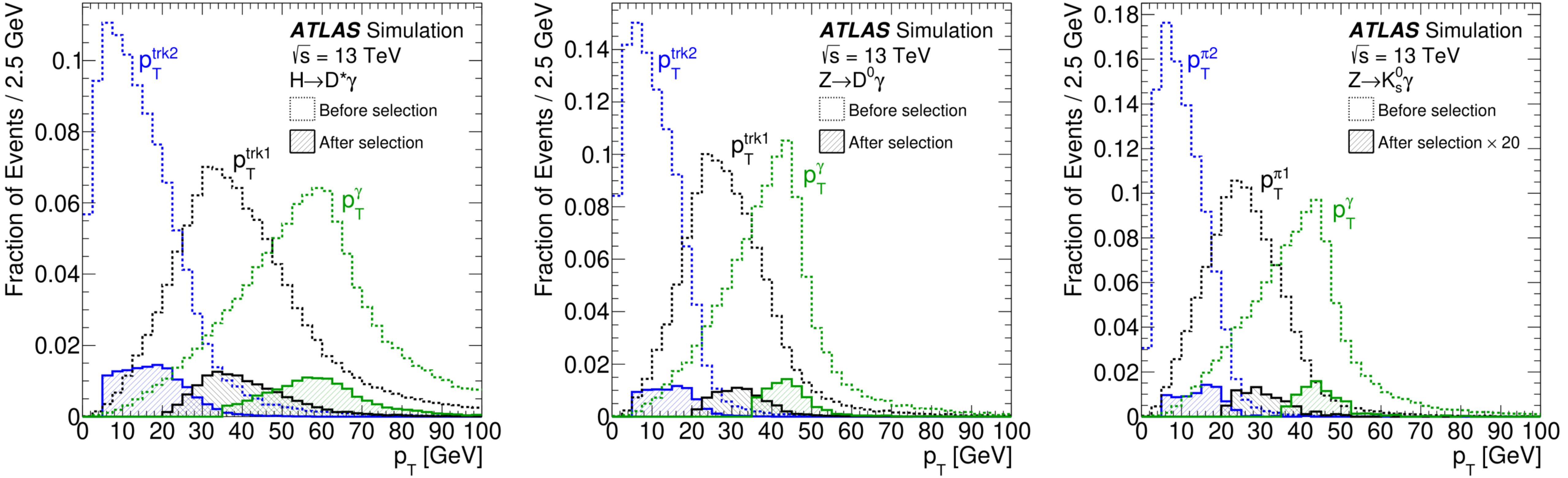

Total Signal Efficiency		
$H \to D^*\gamma$	$Z \to D^0\gamma$	$Z \to K_s^0\gamma$
9%	3%	0.2%

- Larger photon and track p_T in H decays leads to larger signal efficiencies than for Z decays
- Particularly small efficiency for $Z \to K_s^0\gamma$ as many K_s^0 decays occur beyond innermost ID layers

arXiv:2402.18731

$H \to D^*\gamma$ & $Z \to (D^0, K_s^0)\gamma$: Signal Modelling

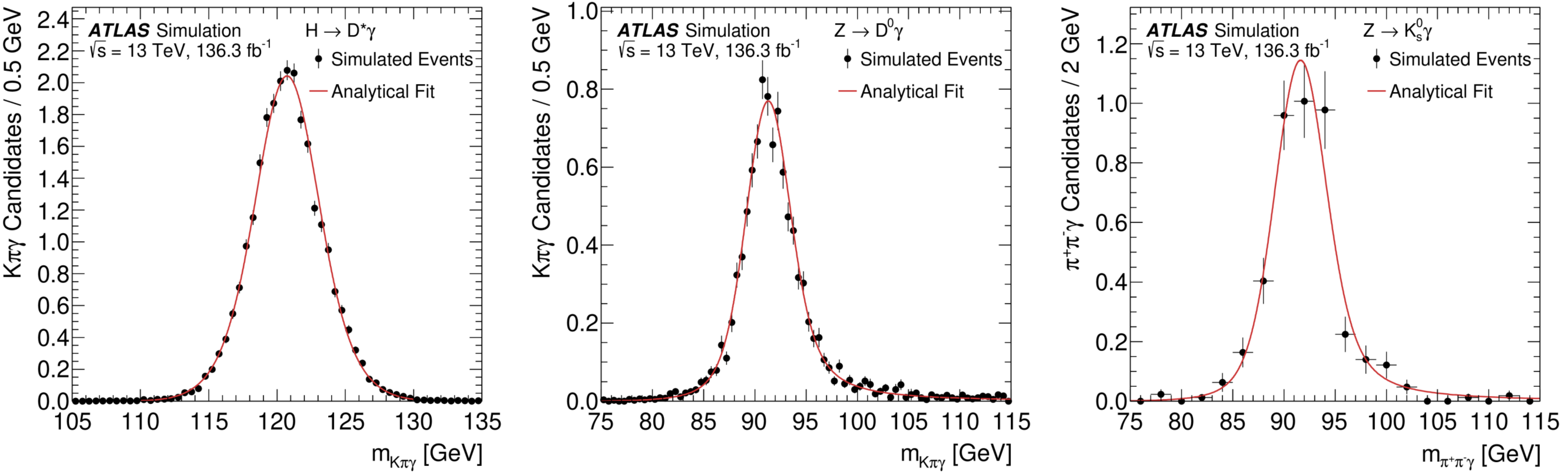

- Model with analytical fits to simulated events
  - Higgs mass - sum of two Gaussian distributions with a common mean
  - Z mass - Voigtian distribution × efficiency factor
    - Voigtian: convolution of Gaussian (detector resolution) and Lorentz (Z width) distributions
    - Efficiency factor: accounts for turn-on in signal efficiency with Z mass

1.9 – 2.3%
Resolution

arXiv:2402.18731

$H \to D^*\gamma$ & $Z \to (D^0, K_s^0)\gamma$: Sampling Scheme

- Ancestral sampling scheme used to produce pseudo-events

arXiv:2402.18731

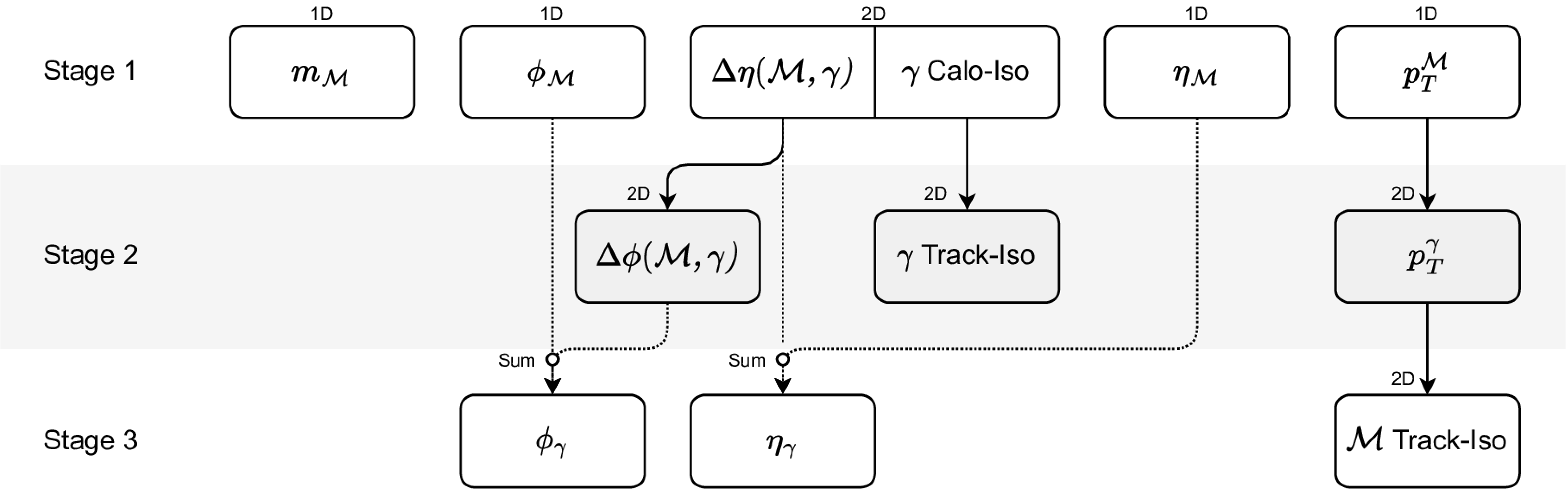

$H \rightarrow D^*\gamma$ & $Z \rightarrow (D^0, K^0_s)\gamma$: Background Generation

- Data in generation region is used to produce model

arXiv:2402.18731

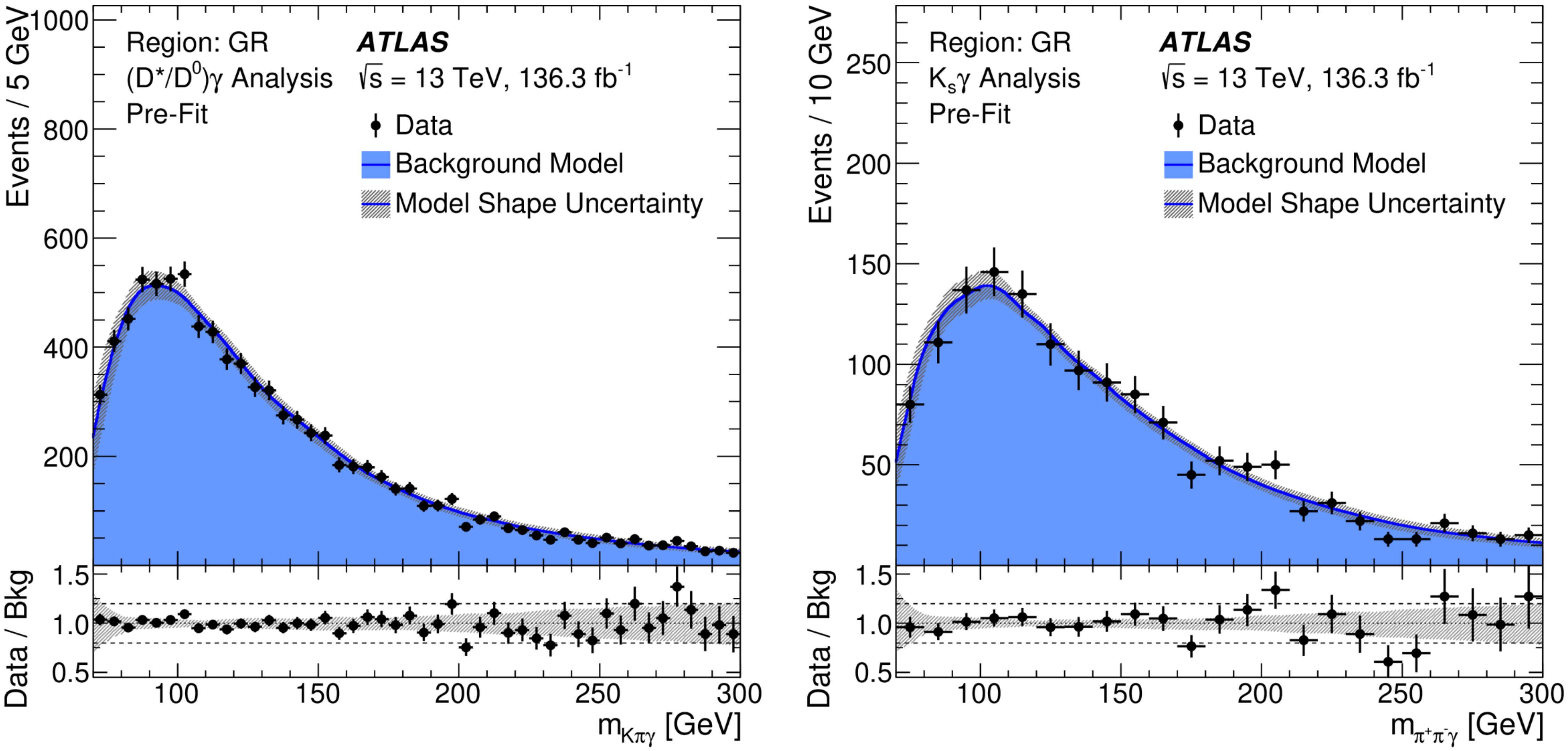

$H \to D^*\gamma$ & $Z \to (D^0, K_s^0)\gamma$: Background Validation

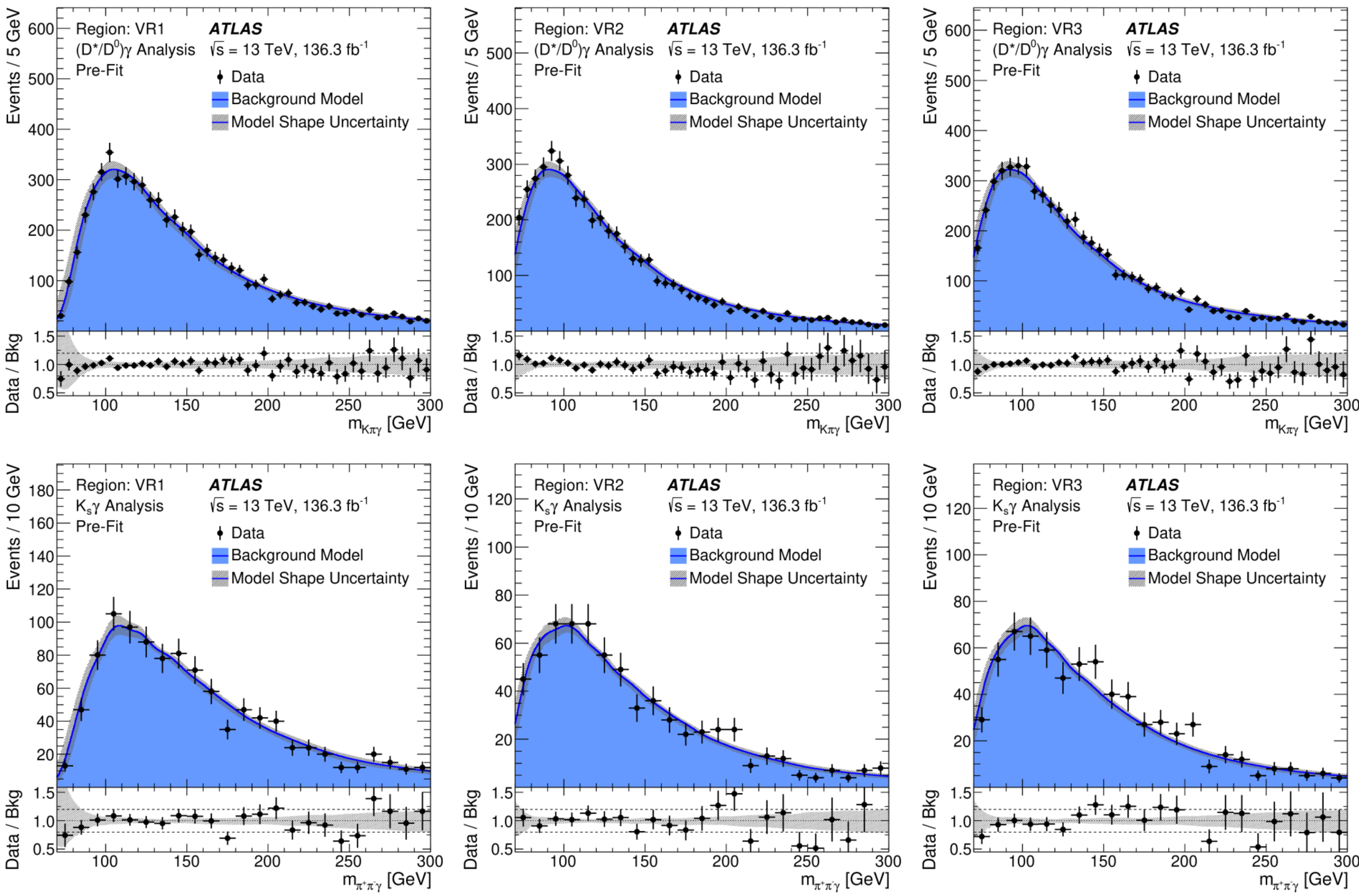

- Plots are pre-fit

Selection	Meson p_T	Meson Isolation	Photon Isolation
GR	> 25 GeV	None	None
VR1	> 39(38) GeV	None	None
VR2	> 25 GeV	Tight	None
VR3	> 25 GeV	None	Tight
SR	> 39(38) GeV	Tight	Tight

$(D^*/D^0)\gamma$ Background Validation

$K_s^0\gamma$ Background Validation

arXiv:2402.18731

$H \to D^*\gamma$ & $Z \to (D^0, K_s^0)\gamma$: Background Systematics

- Freedom via shape systematics: mass-tilt, $\Delta\phi$-distortion, p_T-shift

arXiv:2402.18731

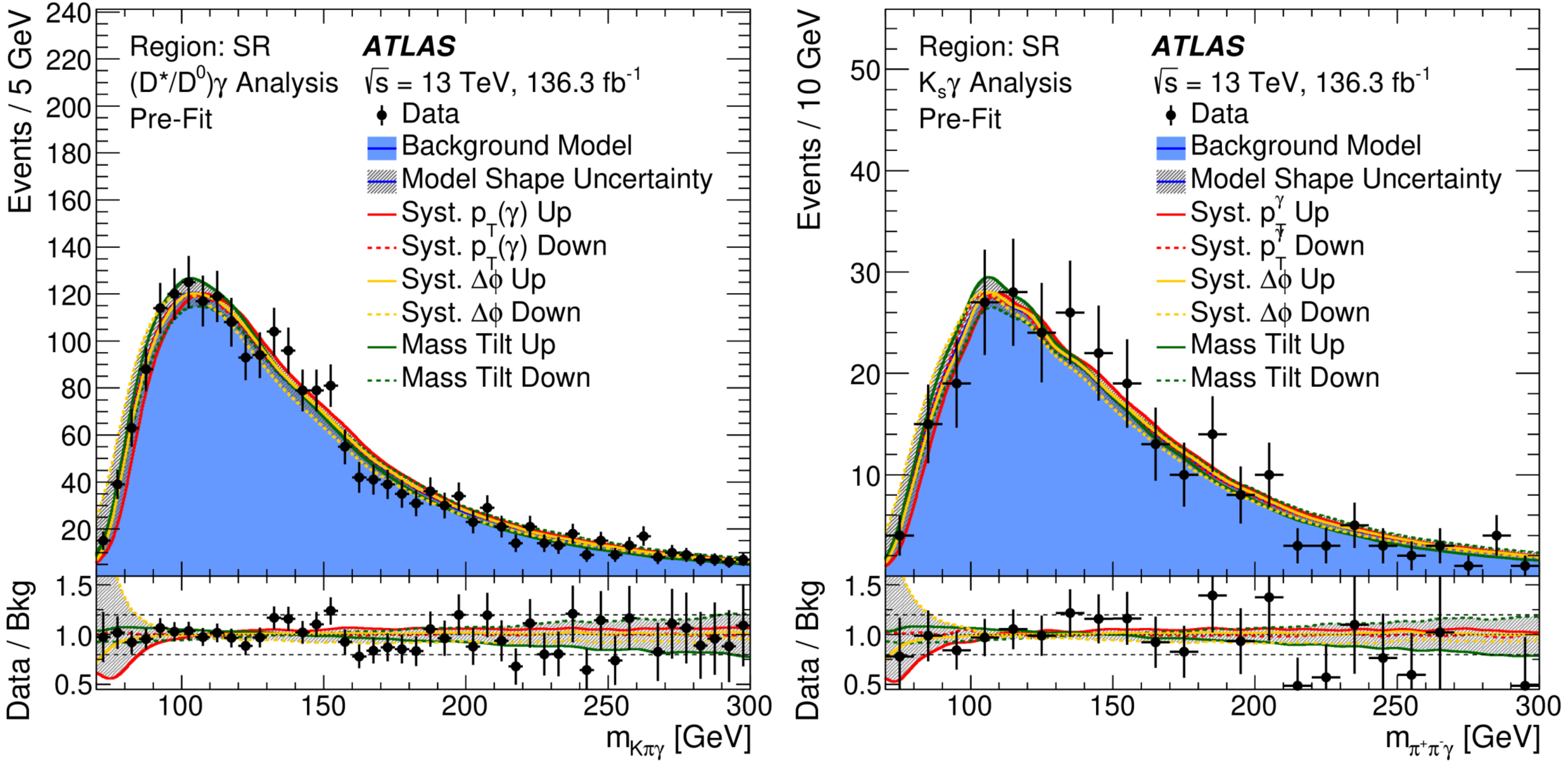

$H \to D^{*}\gamma$ & $Z \to (D^0, K_s^0)\gamma$: Background Control Regions

- Define orthogonal selections (with analogous backgrounds) to validate model procedure

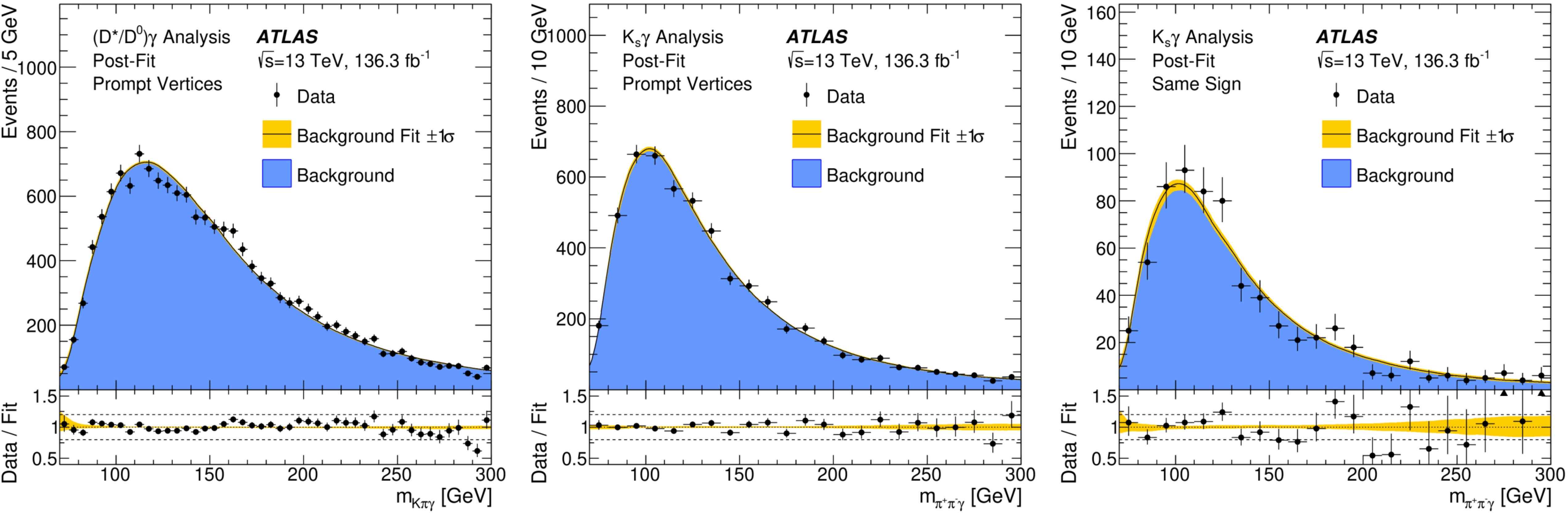

arXiv:2402.18731

$H \to D^*\gamma$ & $Z \to (D^0, K_s^0)\gamma$: Results Tables

Channel	Mass range [GeV]	Observed (Expected) background	H signal $\mathcal{B} = 10^{-3}$	Z signal $\mathcal{B} = 10^{-6}$
$H \to D^*\gamma$	116–126	203 (214.8 ± 5.5)	25.4 ± 2.0	–
$Z \to D^0\gamma$	86–96	215 (206 ± 14)	–	10.3 ± 0.7
$Z \to K_s^0\gamma$	86–96	21 (19.5 ± 2.0)	–	4.2 ± 0.4

Observed and expected events

	95% CL upper limits			
	Branching Fraction		$\sigma \times \mathcal{B}$ [fb]	
Channel	Observed	Expected	Observed	Expected
$H \to D^*\gamma$	1.0×10^{-3}	$1.2^{+0.5}_{-0.3} \times 10^{-3}$	58	68^{+28}_{-19}
$Z \to D^0\gamma$	4.0×10^{-6}	$3.4^{+1.4}_{-1.0} \times 10^{-6}$	235	200^{+82}_{-56}
$Z \to K_s^0\gamma$	3.1×10^{-6}	$3.0^{+1.3}_{-0.8} \times 10^{-6}$	185	176^{+77}_{-49}

Observed and expected limits

arXiv:2402.18731

$Z \rightarrow K_s^0\gamma$: Trigger Efficiency

- Potential to improve K_s^0 trigger by triggering on displaced vertices

arXiv:2402.18731

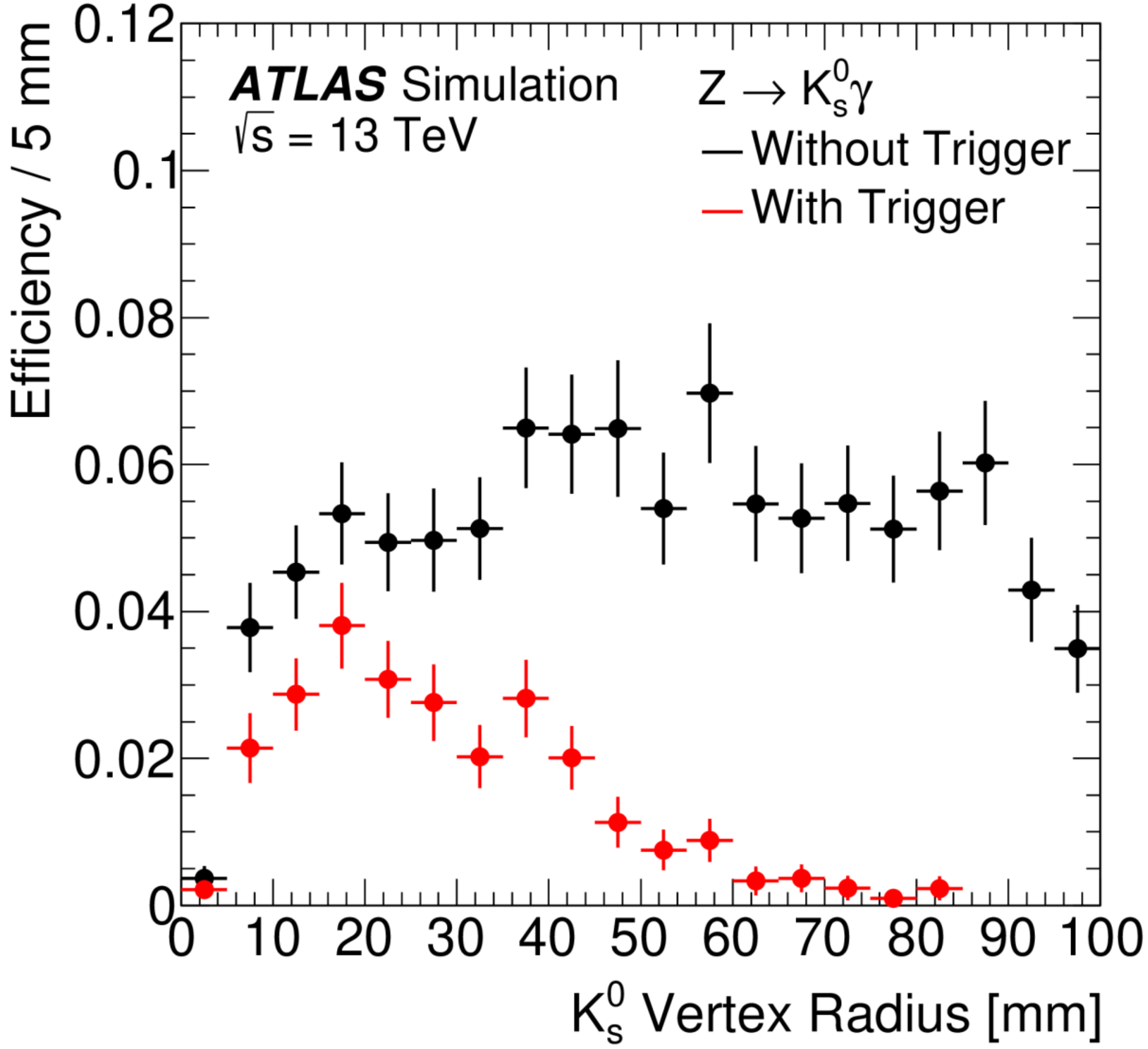

$H(Z) \to Q\gamma$: Selection

- Selection defined largely by trigger thresholds, geometry constraints, and recommended working points
  - Variable $p_{\mathrm{T}}^{\mu^+\mu^-}$ threshold optimised based on $S/\sqrt{B}$ near H and Z signal peaks

Photon Selection:

- $p_{\mathrm{T}}^{\gamma} > 35$ GeV
- $|\eta^{\gamma}| < 2.37$ and outside transition region $1.37 < |\eta^{\gamma}| < 1.52$
- Tight quality
- $\Delta\phi(Q,\gamma) > \pi/2$
- Photon isolation

Meson Selection:

- $p_{\mathrm{T}}^{\mathrm{lead}} > 18$ GeV; $p_{\mathrm{T}}^{\mathrm{sublead}} > 3$ GeV
- $|\eta^{\mu}| < 2.5$
- Oppositely charged muons
- Medium quality
- $m(\mu^+\mu^-)$ near meson mass
- Transverse decay length significance $|L_{xy}/\sigma_{L_{xy}}| < 3$
- $p_{\mathrm{T}}(\mu^+\mu^-)$ cut varies with $m(\mu^+\mu^-\gamma)$
- Muon isolation

Red: Not applied in GR

Quarkonium	Composition	Mass [GeV]	Width [keV]	$\mathcal{B}(Q \to \mu^+\mu^-)$
J/ψ	$c\bar{c}$	3.10	92.9 ± 2.8	$(5.96 \pm 0.03)\%$
$\psi(2S)$	$c\bar{c}$	3.69	294.0 ± 8.0	$(0.80 \pm 0.06)\%$
$\Upsilon(1S)$	$b\bar{b}$	9.46	54.0 ± 1.3	$(2.48 \pm 0.05)\%$
$\Upsilon(2S)$	$b\bar{b}$	10.02	32.0 ± 2.6	$(1.93 \pm 0.17)\%$
$\Upsilon(3S)$	$b\bar{b}$	10.36	20.3 ± 1.9	$(2.18 \pm 0.21)\%$

EPJC 83 (2023) 781

$H(Z) \rightarrow Q\gamma$: Signal Modelling

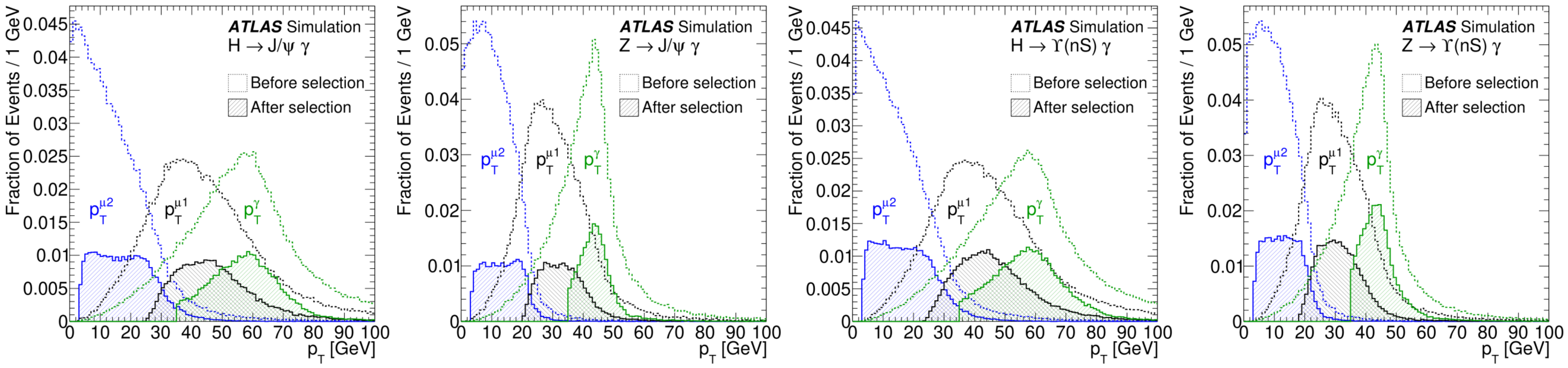

- Higgs decays – sum of two bivariate Gaussians $(m_{\mu^+\mu^-\gamma}; m_{\mu^+\mu^-})$
- Z decays – double Voigtian × efficiency factor $(m_{\mu^+\mu^-\gamma})$
  × double Gaussian $(m_{\mu^+\mu^-})$

1.6-1.8%
Resolution

Total Signal Efficiency		
Decay Channel	Z Signal	H Signal
$\psi(nS)\gamma$	10%	19%
$\Upsilon(nS)\gamma$	13%	21%

EPJC 83 (2023) 781

$H(Z) \rightarrow Q\gamma$: Signal Efficiency

- Generator p_{T} plots for $\psi(2S)$ channels

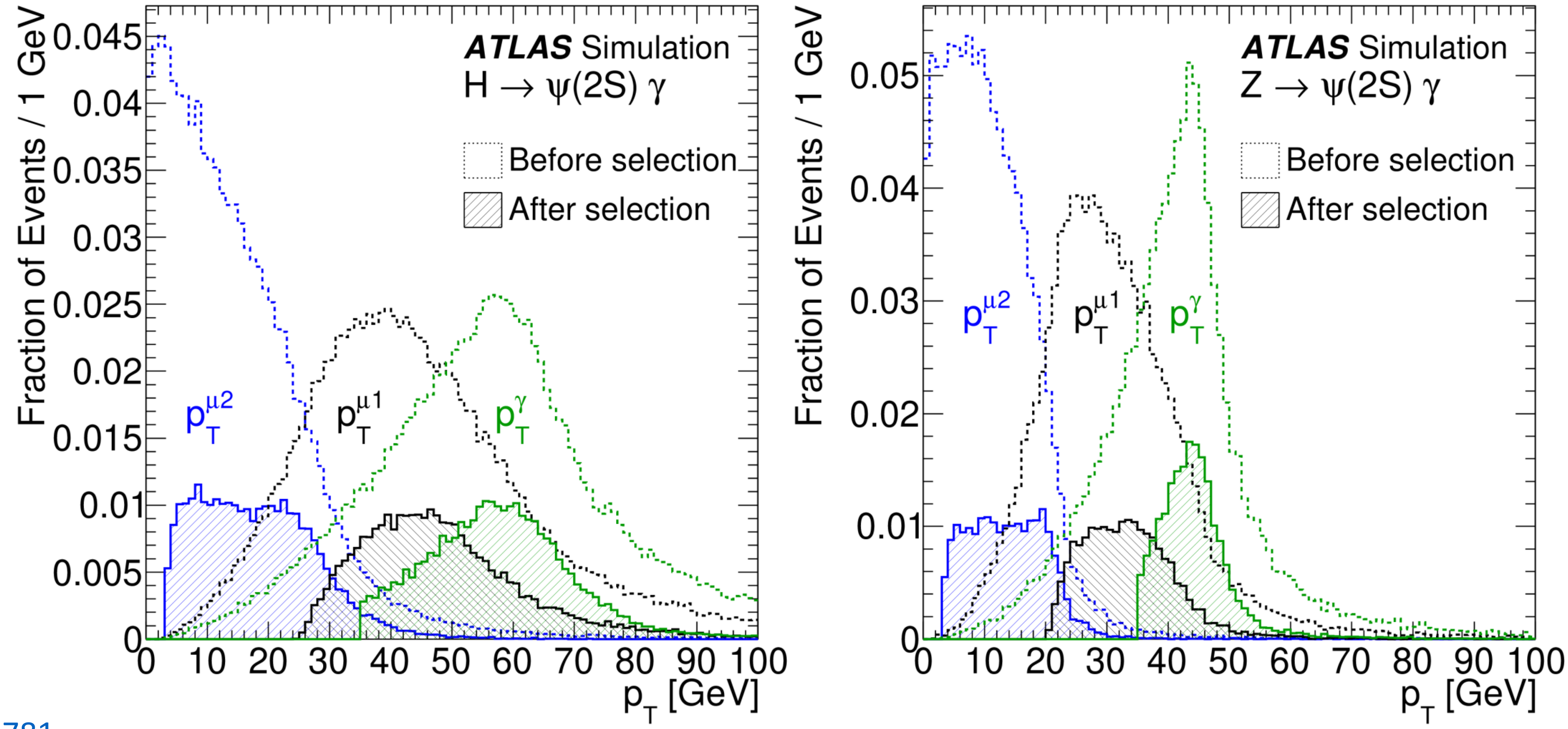

[EPJC 83 (2023) 781](https://doi.org/)

$H(Z) \rightarrow Q\gamma$: Quarkonium Reconstruction

- Split $\Upsilon(nS)$ into Barrel (B) and Endcap (EC) categories
  - Improved resolution in barrel helps resolve each state
- Reject displaced vertices to avoid $b \rightarrow \psi(nS)$

Meson Reconstruction in GR

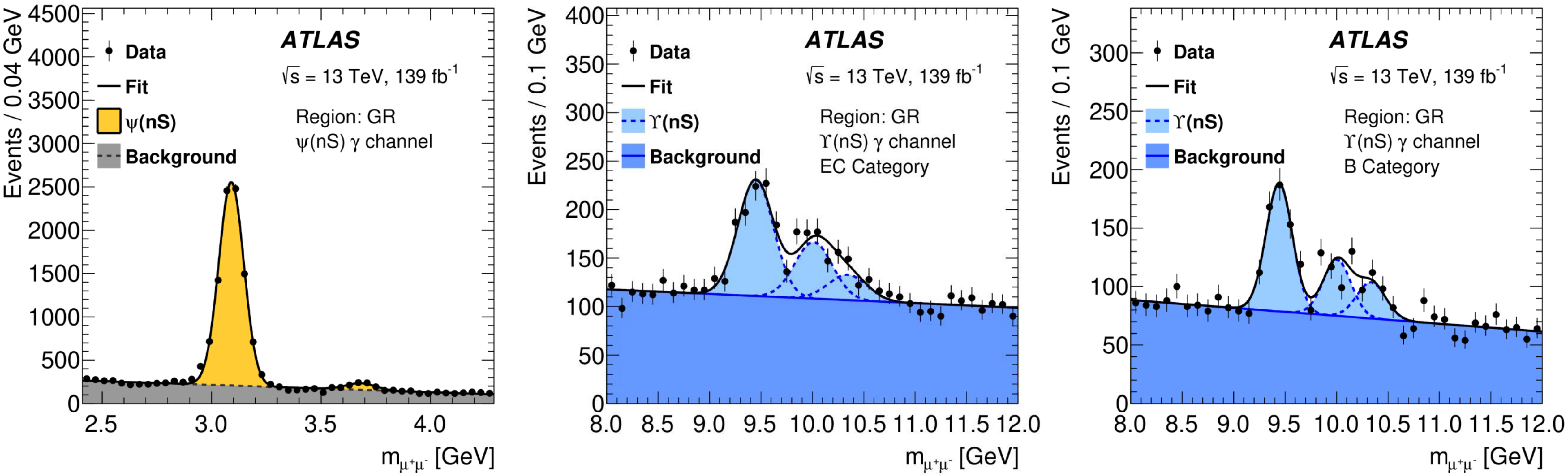

- Extract $m_{\mu^+\mu^-}$ shapes for final fit
  - Quarkonium states – Gaussian; combinatoric – straight line

EPJC 83 (2023) 781

$H(Z) \rightarrow Q\gamma$: Signal Modelling and Resolution

➢Signal resolution for $Q\gamma$ searches

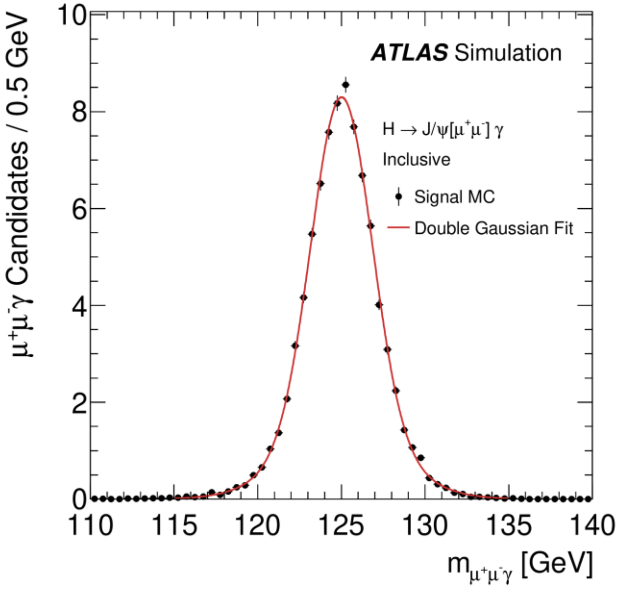

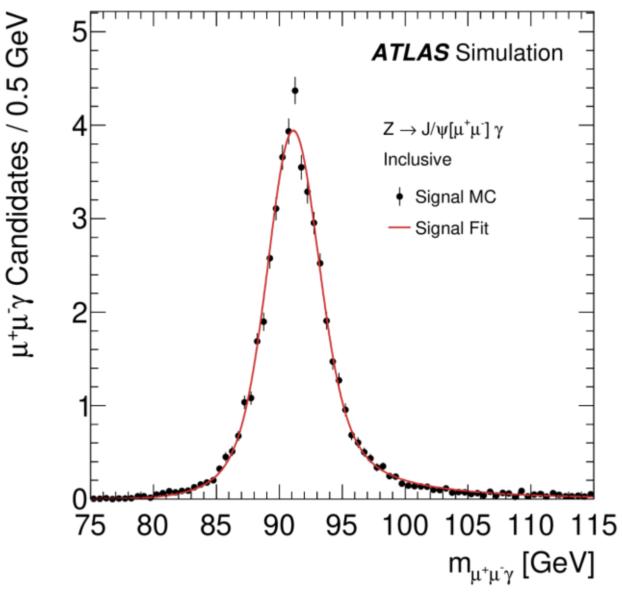

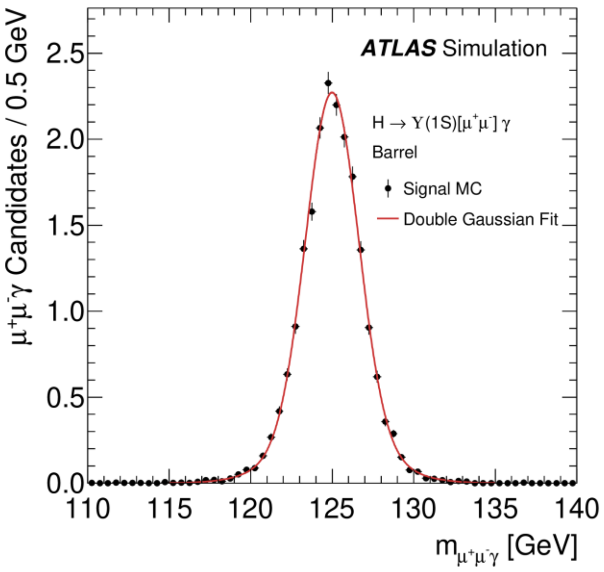

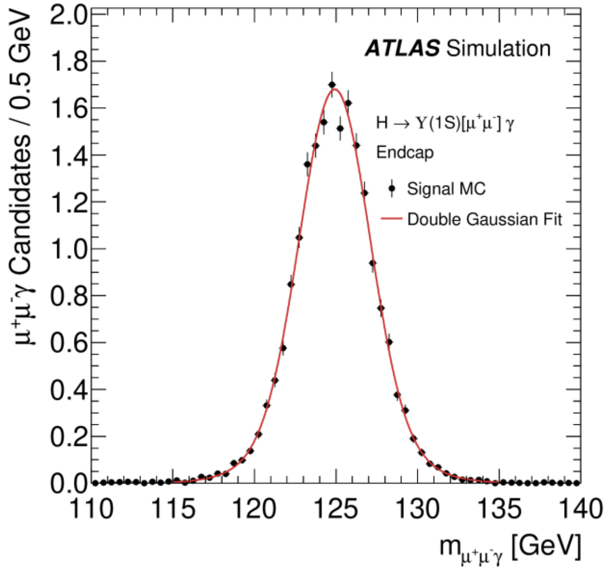

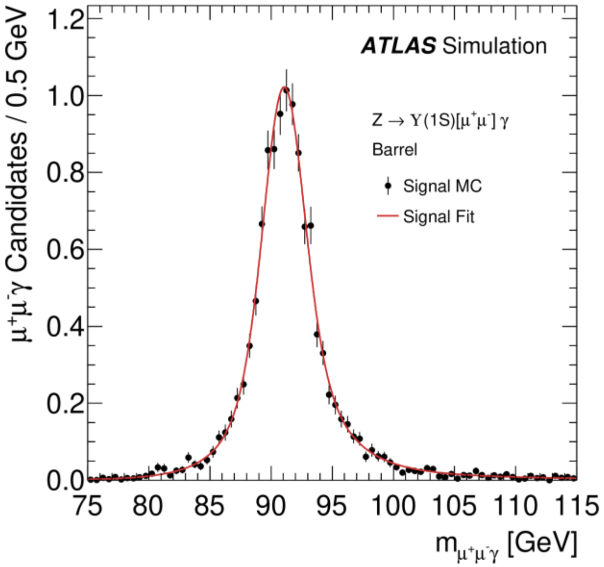

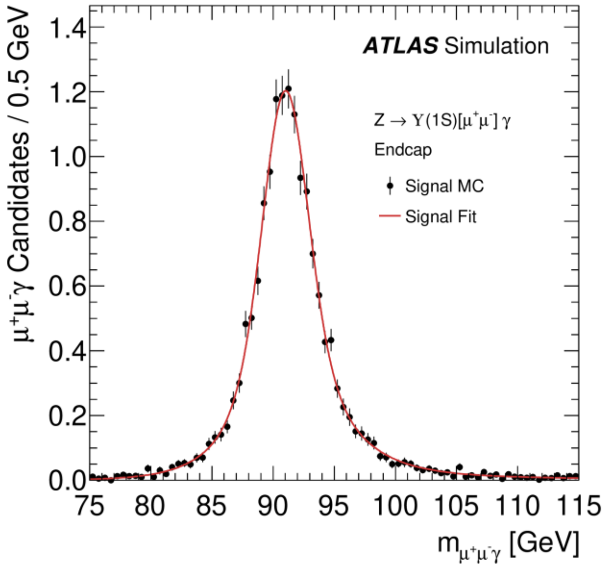

EPJC 83 (2023) 781

$H(Z) \rightarrow Q\gamma$: Signal Systematic Uncertainties

- Consider relevant uncertainties on the total signal yield
  - Nuisance parameters with standard Gaussian constraints in maximum likelihood fit

Source of systematic uncertainty	Signal yield uncertainty			
	$H \rightarrow \psi(nS)\,\gamma$	$H \rightarrow \Upsilon(nS)\,\gamma$	$Z \rightarrow \psi(nS)\,\gamma$	$Z \rightarrow \Upsilon(nS)\,\gamma$
Total cross section	5.8%	5.8%	2.9%	2.9%
Integrated luminosity	1.7%	1.7%	1.7%	1.7%
Signal acceptance	1.8%	1.8%	1.0%	1.0%
Muon reconstruction	2.3%	2.2%	2.4%	2.4%
Photon identification	1.7%	1.7%	1.9%	1.9%
Pile-up uncertainty	0.8%	0.7%	1.1%	1.1%
Trigger efficiency	0.7%	0.7%	0.8%	0.8%
Photon energy scale	0.1%	0.1%	0.2%	0.2%
Muon momentum scale	0.1%	0.1%	0.5%	0.2%
Muon momentum resolution (ID)	<0.01%	0.01%	0.06%	0.02%
Muon momentum resolution (MS)	0.02%	0.01%	0.04%	0.01%

EPJC 83 (2023) 781

$H(Z) \to Q\gamma$: Ancestral Sampling Scheme

- Subtract exclusive background events from data in GR before generating inclusive model

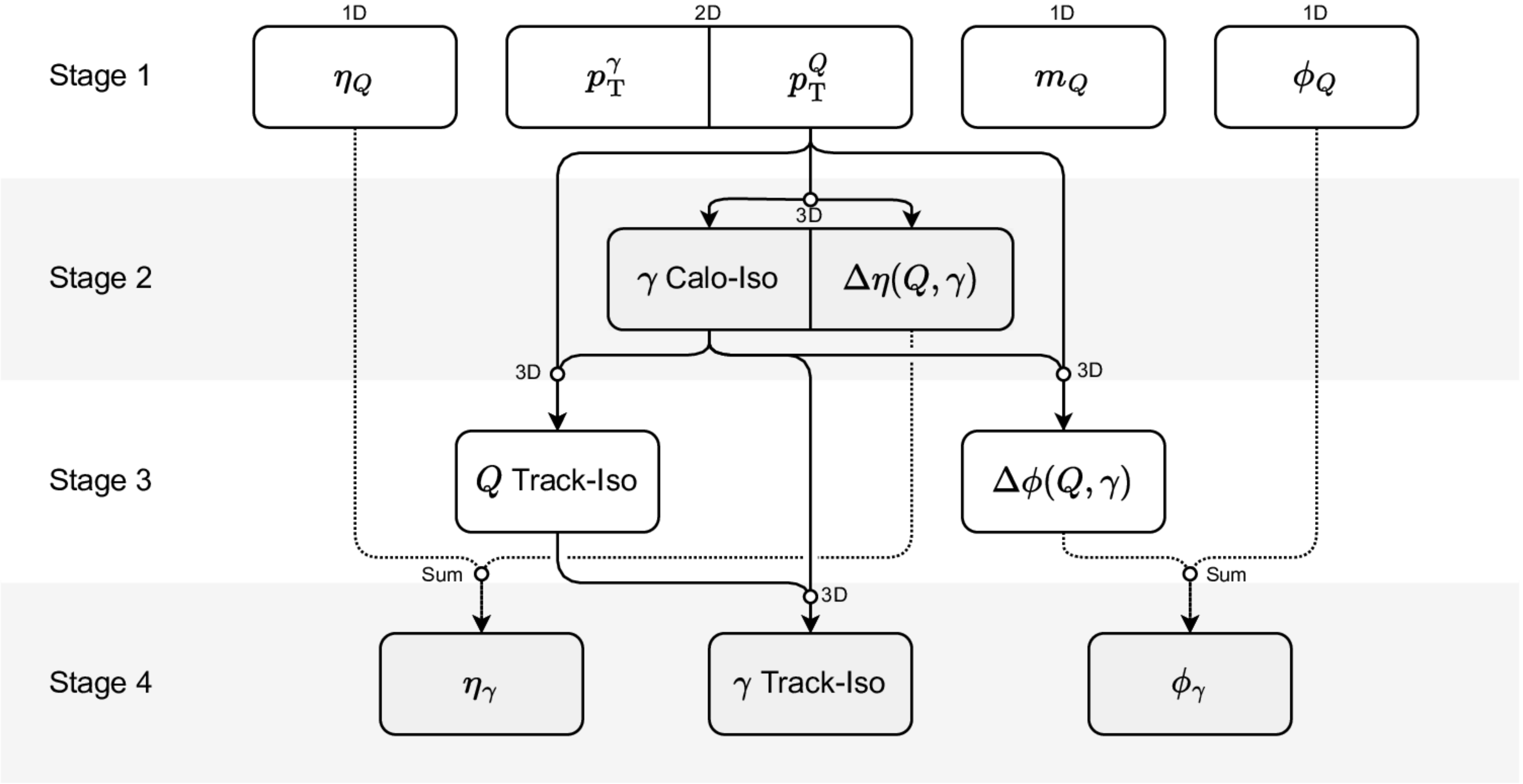

[EPJC 83 (2023) 781](#)

$H(Z) \rightarrow Q\gamma$: Background Validation Regions

- Define three VRs for $Q\gamma$

Region		$p_T^{\mu\mu}$	Photon Isolation	Q Isolation
Generation Region	(GR)	> 30 GeV	Relaxed	Relaxed
Validation Region 1	(VR1)	Full	Relaxed	Relaxed
Validation Region 2	(VR2)	> 30 GeV	Relaxed	Full
Validation Region 3	(VR3)	> 30 GeV	Full	Relaxed
Signal Region	(SR)	Full	Full	Full

Region Definitions

EPJC 83 (2023) 781

$H(Z) \to Q\gamma$: Background Validation and Systematic Uncertainties

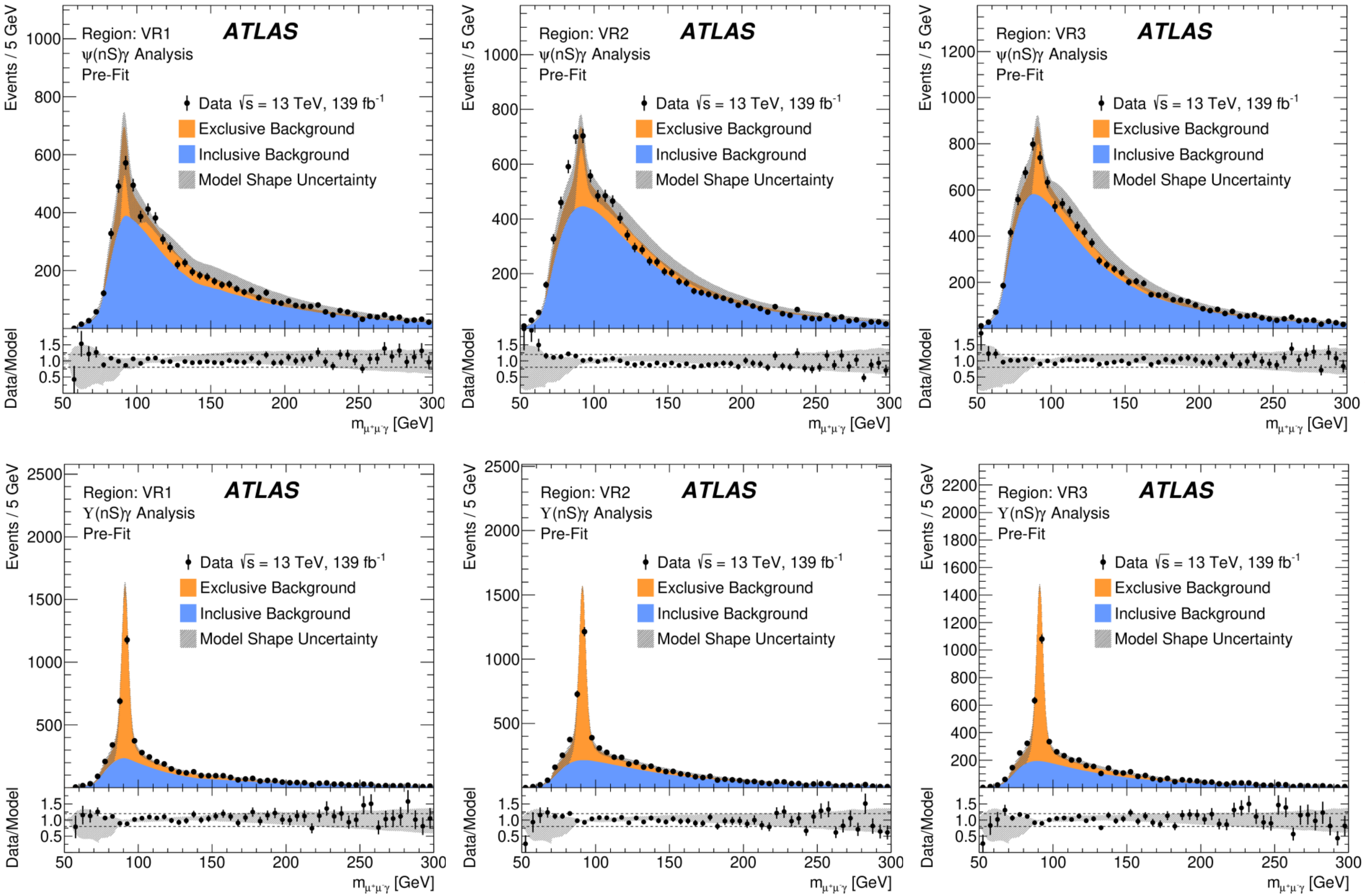

- Subtract exclusive contribution from data in GR to prepare for inclusive model
- Freedom via shape systematics: mass-tilt, $\Delta\phi$-distortion, p_{T}-shift

$\psi(nS)\gamma$ Background Validation

$\Upsilon(nS)\gamma$ Background Validation

EPJC 83 (2023) 781

$H(Z) \to \psi(nS)\gamma$: Inclusive Fit

- Use **2D** unbinned likelihood fit in $m(\mu^+\mu^-), m(\mu^+\mu^-\gamma)$
  - Discriminates between **all** signal and background contributions

EPJC 83 (2023) 781

- $\psi(nS)\gamma$ analysis fit is performed in a single category

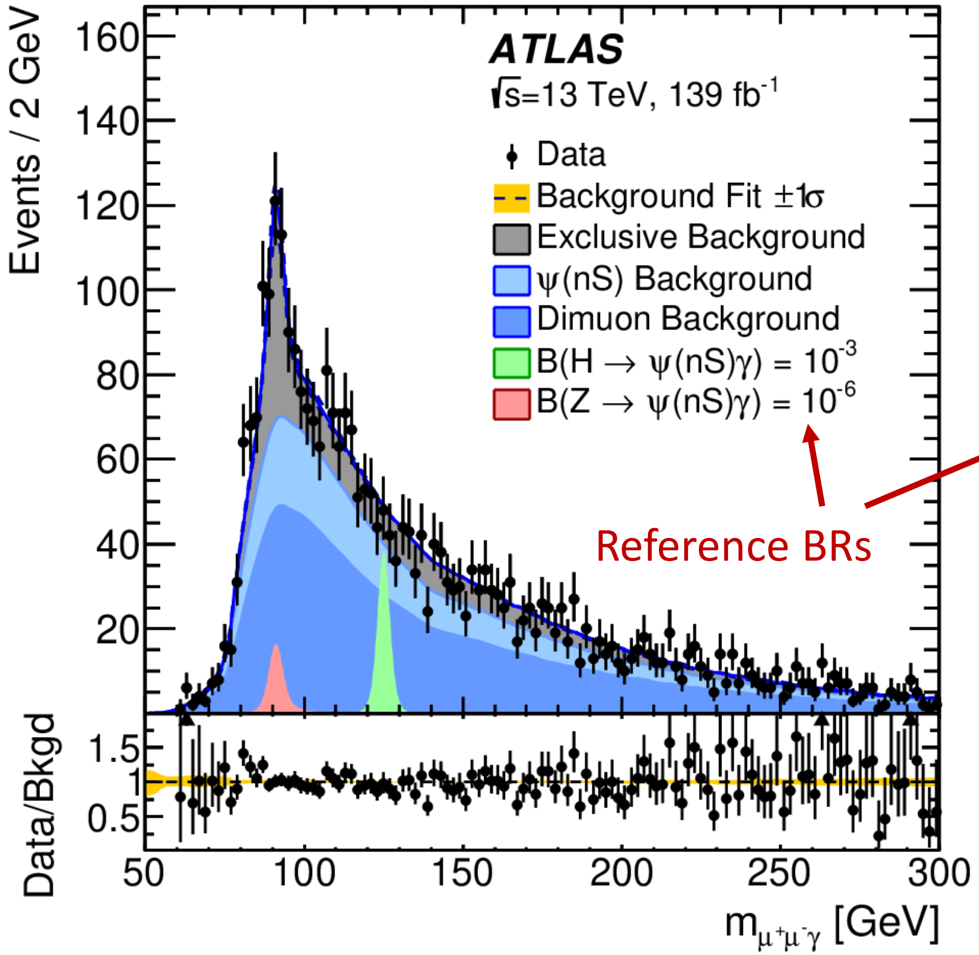

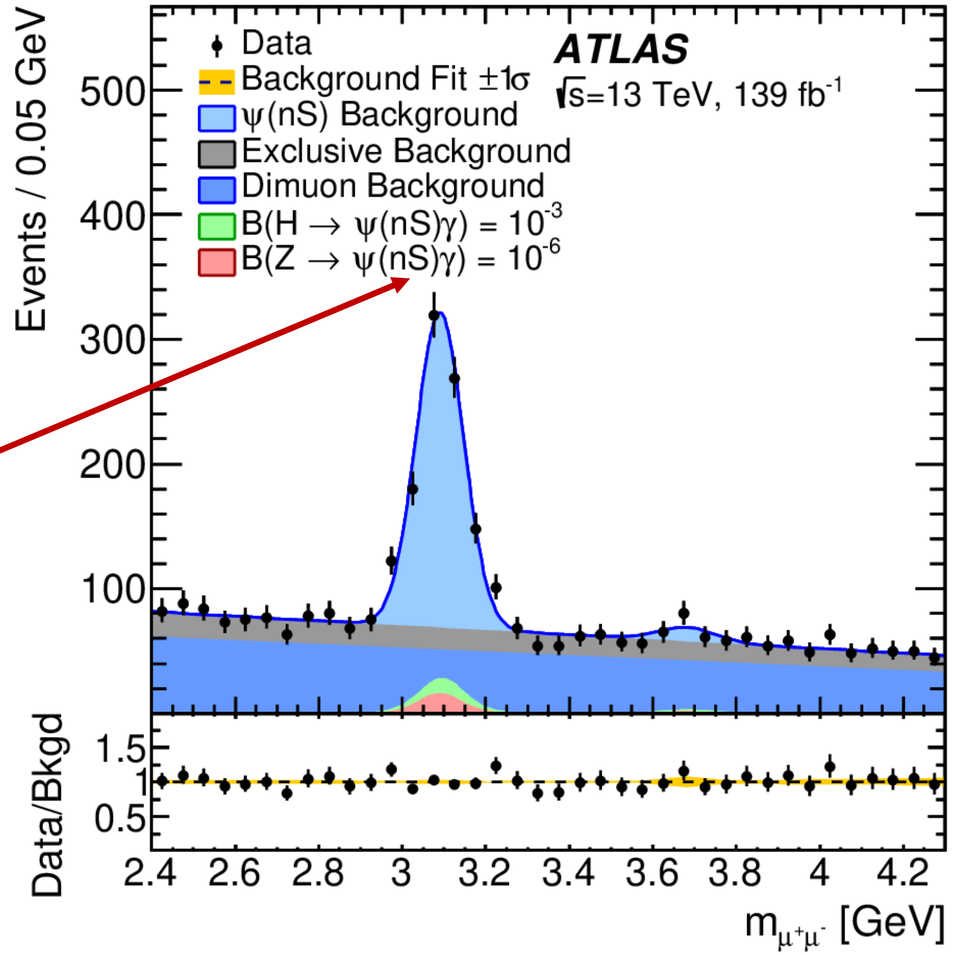

$H(Z) \to \Upsilon(nS)\gamma$: Inclusive Fit

- Use **2D** unbinned likelihood fit in $m(\mu^+\mu^-), m(\mu^+\mu^-\gamma)$
  - Discriminates between **all** signal and background contributions

EPJC 83 (2023) 781

- $\Upsilon(nS)\gamma$ analysis fit is performed simultaneously in the barrel and endcap categories

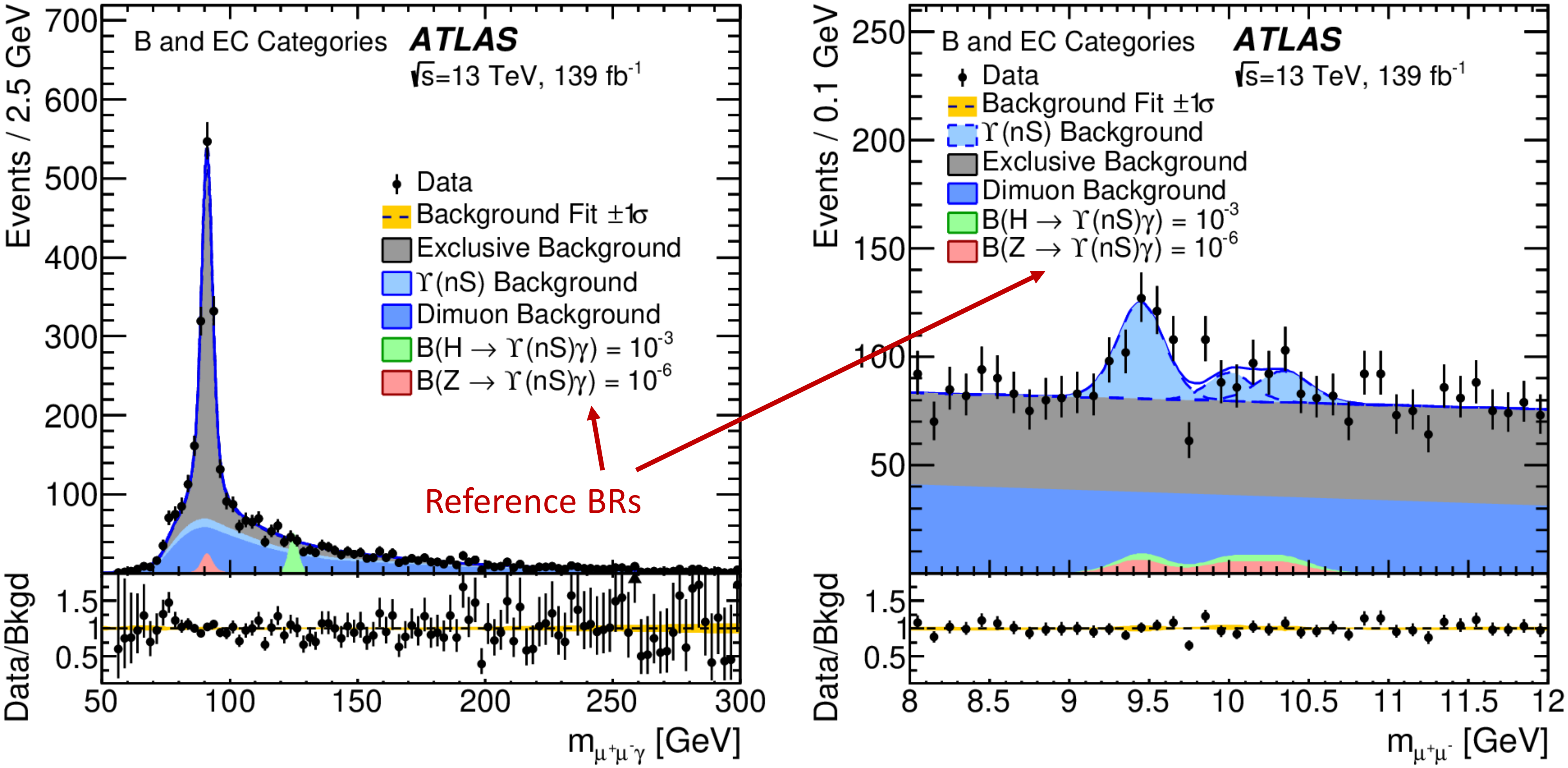

$H(Z) \rightarrow \Upsilon(nS)\gamma$: Fit in Separate B and EC Categories

EPJC 83 (2023) 781

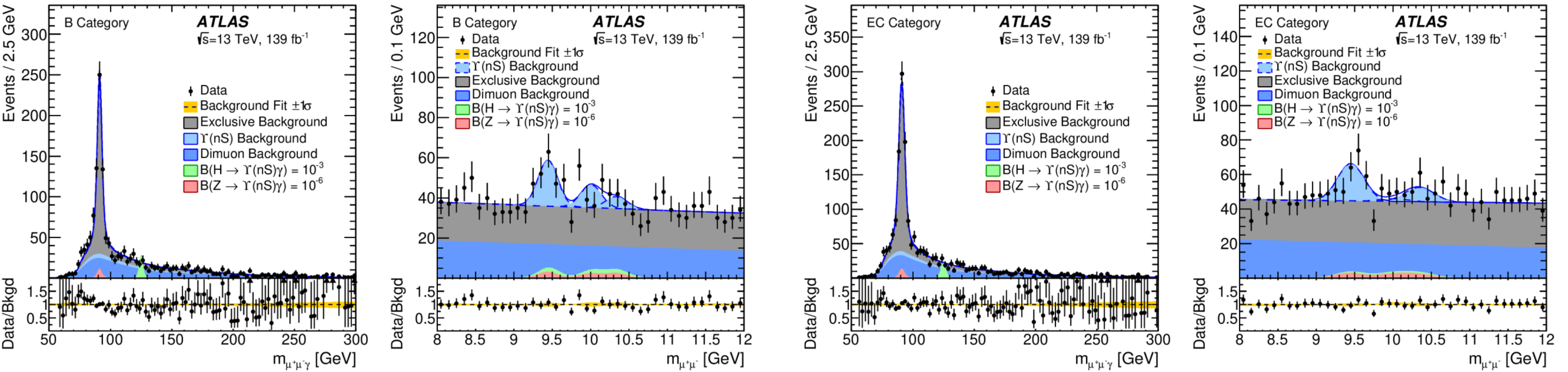

$H(Z) \rightarrow \Upsilon(nS)\gamma$: Barrel Category Projections

[*EPJC* 83 (2023) 781]

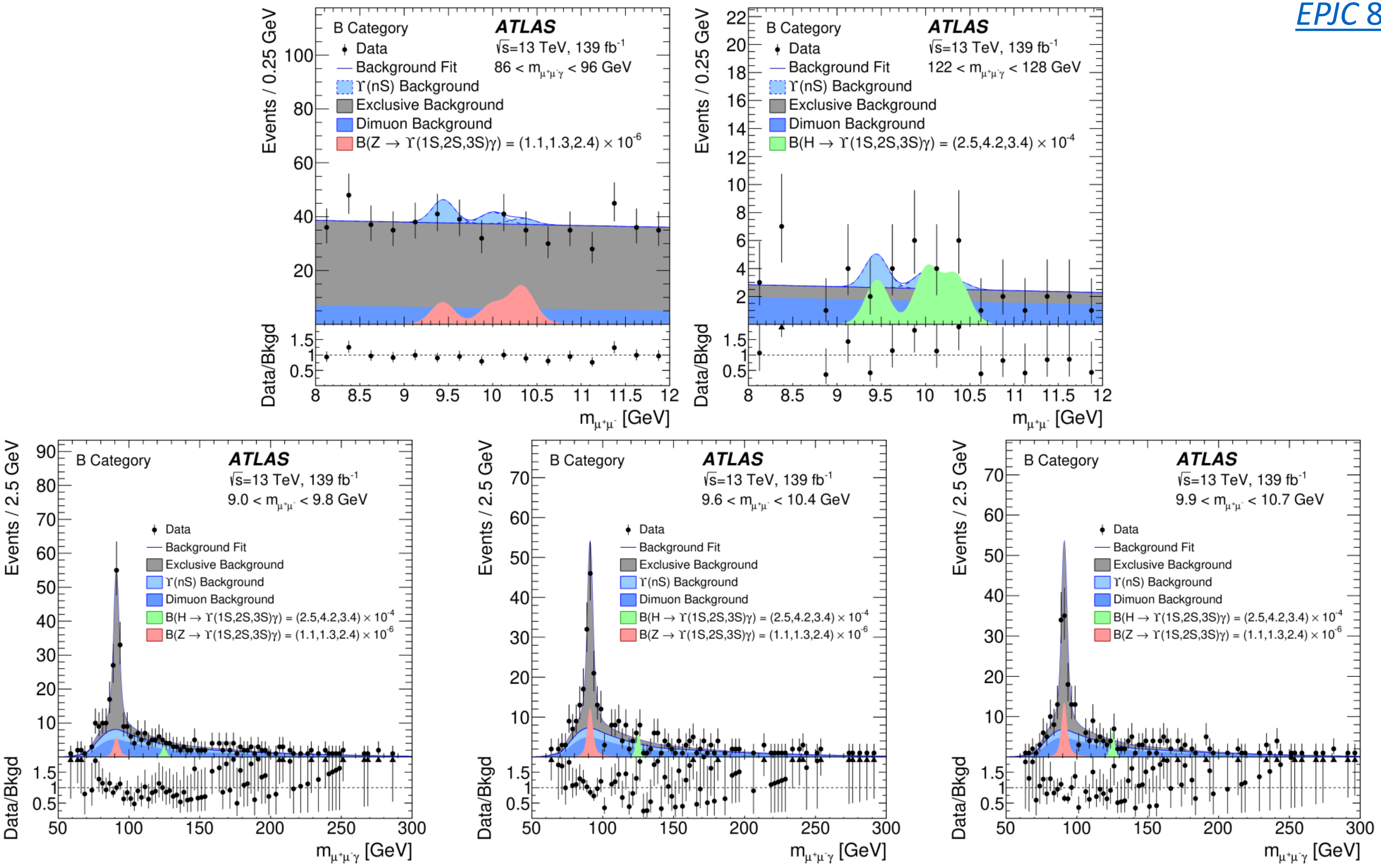

$H(Z) \rightarrow \Upsilon(nS)\gamma$: Endcap Category Projections

[EPJC 83 (2023) 781]

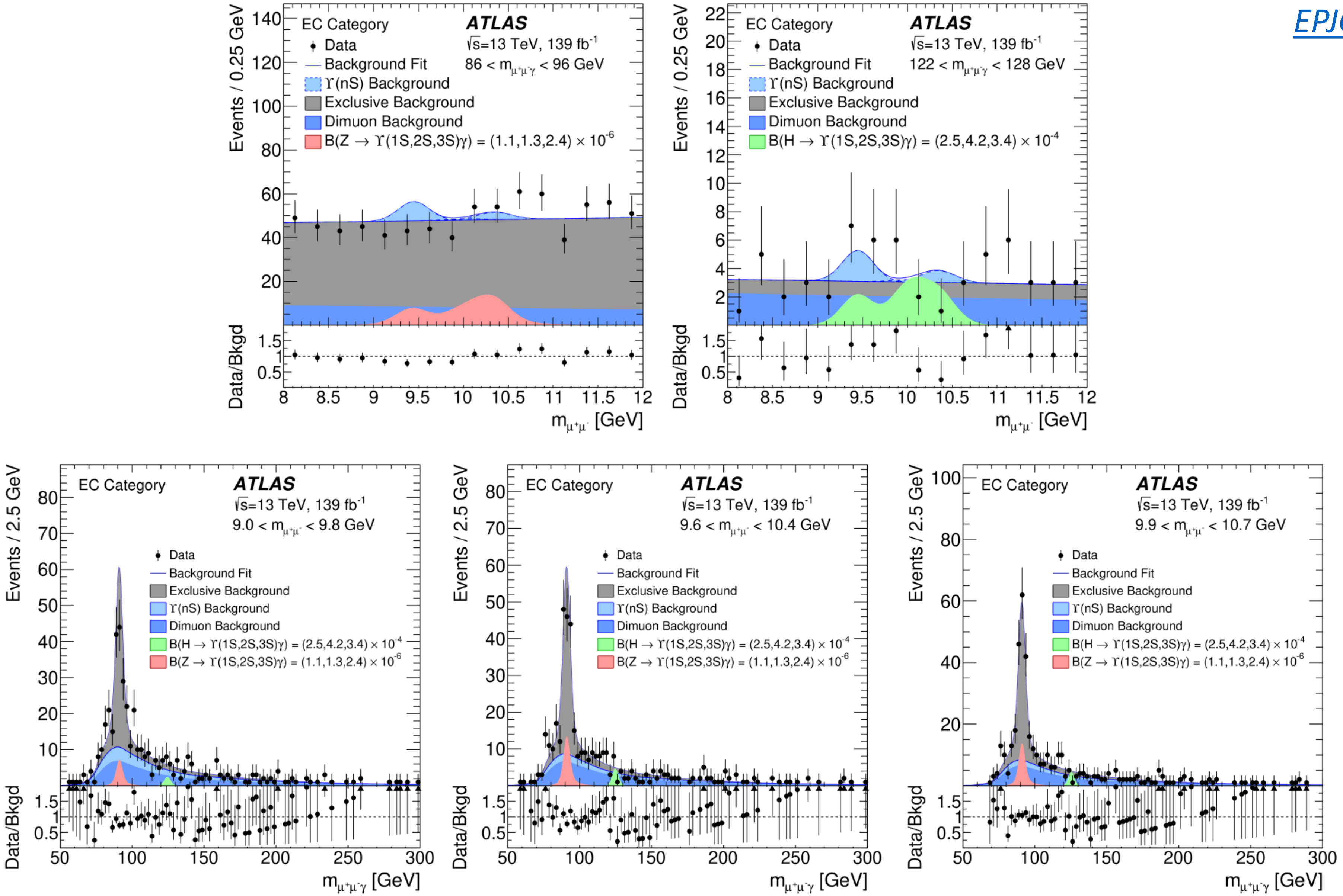

$H(Z) \rightarrow Q\gamma$: Limits and Observed Events

Category	$m_{\mu^+\mu^-}$ range [GeV]	Observed (expected) background $m_{\mu^+\mu^-\gamma}$ range [GeV] 86–96		122–128		Z signal for $\mathcal{B} = 10^{-6}$	H signal for $\mathcal{B} = 10^{-3}$
Inclusive	2.9–3.3	198	(185.6 ± 5.9)	61	(59.1 ± 1.6)	49.3 ± 2.4	87.8 ± 6.1
Inclusive	3.5–3.9	83	(82.5 ± 4.0)	21	(22.9 ± 0.9)	6.5 ± 0.3	11.8 ± 0.8
Barrel	9.0–9.8	125	(125.3 ± 4.7)	12	(11.6 ± 0.6)	11.4 ± 0.6	20.2 ± 1.4
Barrel	9.6–10.4	118	(121.9 ± 4.6)	14	(10.7 ± 0.6)	8.8 ± 0.4	15.3 ± 1.1
Barrel	9.9–10.7	102	(119.9 ± 4.5)	11	(10.2 ± 0.6)	10.1 ± 0.5	17.4 ± 1.2
Endcap	9.0–9.8	133	(162.9 ± 5.7)	16	(13.6 ± 0.7)	15.5 ± 0.8	20.5 ± 1.4
Endcap	9.6–10.4	150	(157.1 ± 5.6)	11	(11.7 ± 0.5)	11.7 ± 0.6	15.8 ± 1.1
Endcap	9.9–10.7	171	(156.7 ± 5.8)	7	(11.4 ± 0.6)	13.5 ± 0.7	17.6 ± 1.2

Observed and Expected Events

	95% CL upper limits					
	Branching fraction				$\sigma \times \mathcal{B}$	
Decay channel	Higgs boson [10^{-4}] Expected	Higgs boson [10^{-4}] Observed	Z boson [10^{-6}] Expected	Z boson [10^{-6}] Observed	Higgs boson [fb] Observed	Z boson [fb] Observed
$J/\psi\,\gamma$	$1.8^{+0.8}_{-0.5}$	2.0	$0.7^{+0.3}_{-0.2}$	1.2	11	69
$\psi(2S)\,\gamma$	$8.1^{+3.6}_{-2.3}$	10.5	$3.0^{+1.3}_{-0.8}$	2.4	58	142
$\Upsilon(1S)\,\gamma$	$2.7^{+1.2}_{-0.8}$	2.5	$1.6^{+0.6}_{-0.4}$	1.1	14	62
$\Upsilon(2S)\,\gamma$	$3.4^{+1.5}_{-1.0}$	4.2	$2.1^{+0.8}_{-0.6}$	1.3	24	74
$\Upsilon(3S)\,\gamma$	$3.0^{+1.3}_{-0.8}$	3.4	$1.9^{+0.8}_{-0.5}$	2.4	19	143

Observed and Expected Limits

EPJC 83 (2023) 781

$H(Z) \rightarrow Q\gamma$: CMS Results

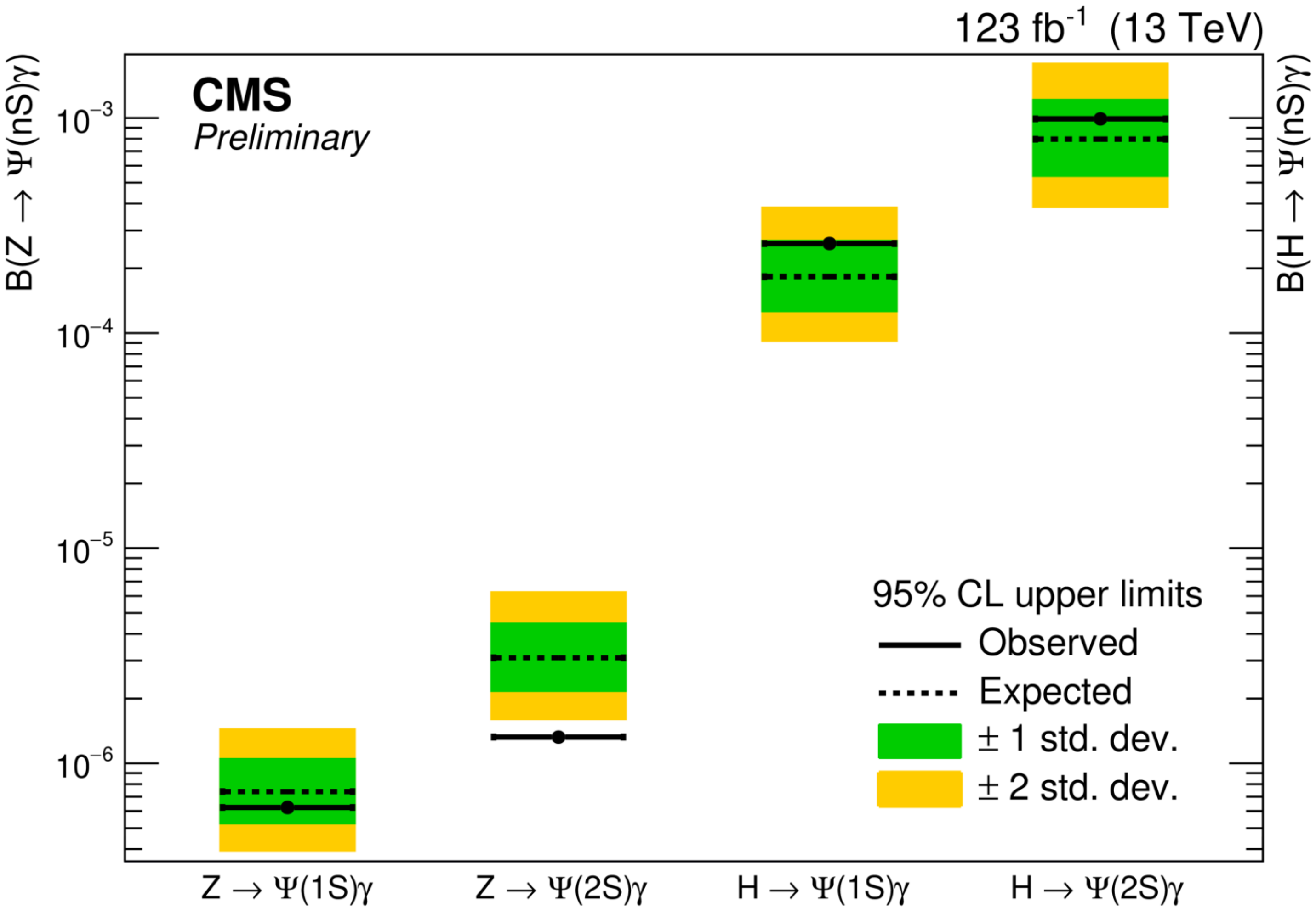

CMS-PAS-SMP-22-012

$W^{\pm} \rightarrow (\pi^{\pm}, K^{\pm}, \rho^{\pm})\gamma$: Strategy

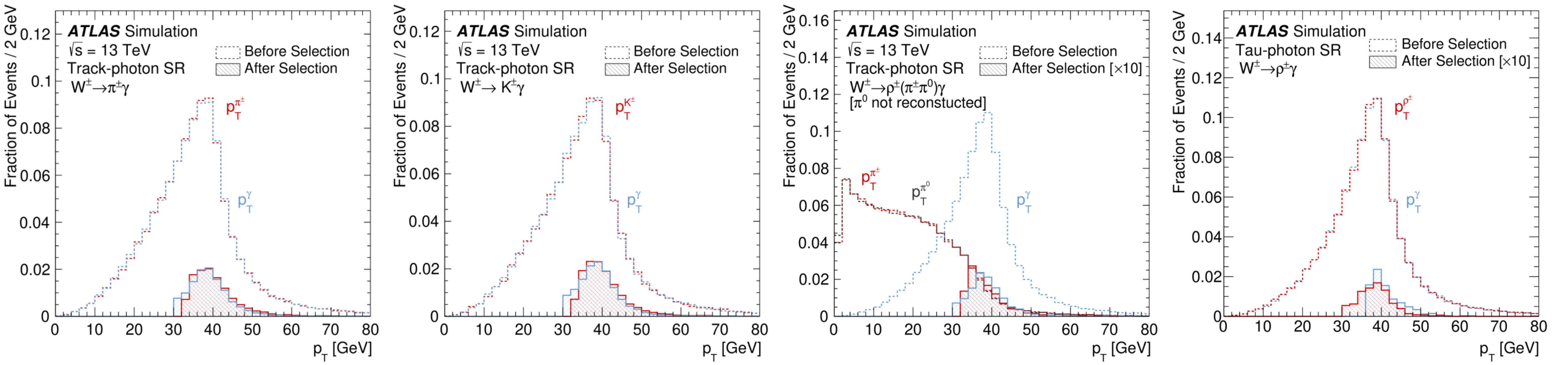

- Signal shapes: (Sum of two Voigtians) × efficiency factor
  - Exception: $W^{\pm} \rightarrow \rho^{\pm}\gamma$ (track + photon) modelled with smoothed MC template

2.7 – 3.1% Resolution

Total Signal Efficiency		
$W^{\pm} \rightarrow \pi^{\pm}\gamma$	$W^{\pm} \rightarrow K^{\pm}\gamma$	$W^{\pm} \rightarrow \rho^{\pm}\gamma$
5.0%	5.5%	0.5% (0.3%)

- Background is multi-jet and γ+jet sources
  - Use non-parametric data-driven background model

- Small contribution from $Z \rightarrow e^{+}e^{-}$ modelled with simulation
  - Suppress using TRT to identify $e^{\pm}$

arXiv:2309.15887

$W^{\pm} \to (\pi^{\pm}, K^{\pm}, \rho^{\pm})\gamma$: Signal Modelling

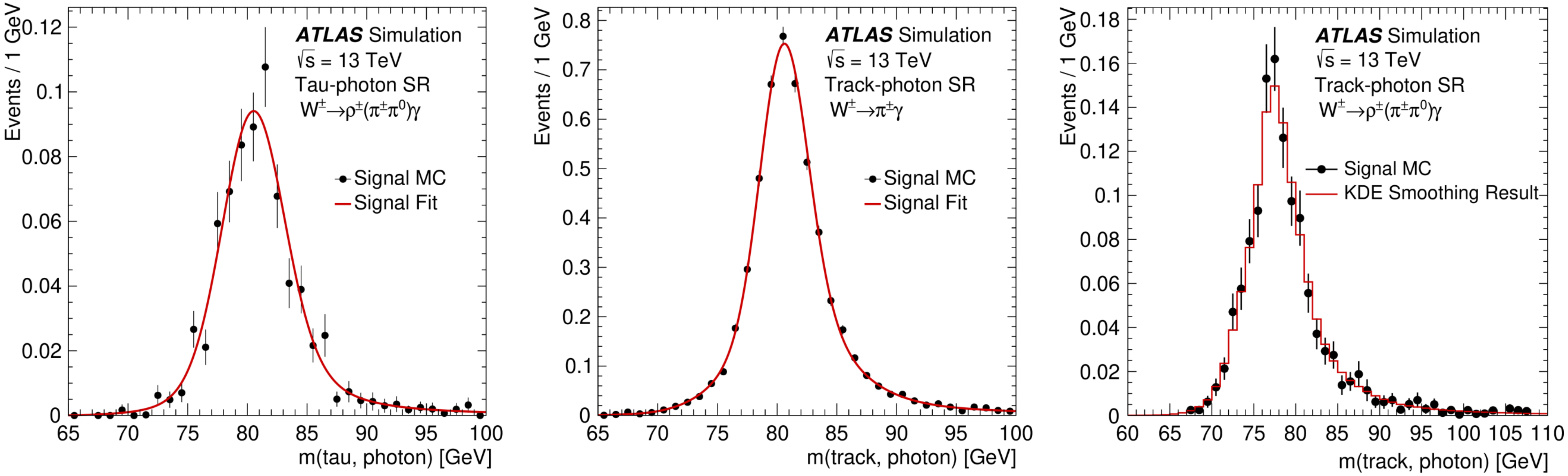

- Model with analytical fits to simulated events
  - $W \to (\pi^{\pm}, K^{\pm})\gamma$ shapes are identical
  - $W \to \rho^{\pm}\gamma$ in track + photon category is modelled with smoothed template from simulation

arXiv:2309.15887

$W^{\pm} \rightarrow (\pi^{\pm}, K^{\pm}, \rho^{\pm})\gamma$: Background Sampling Schemes

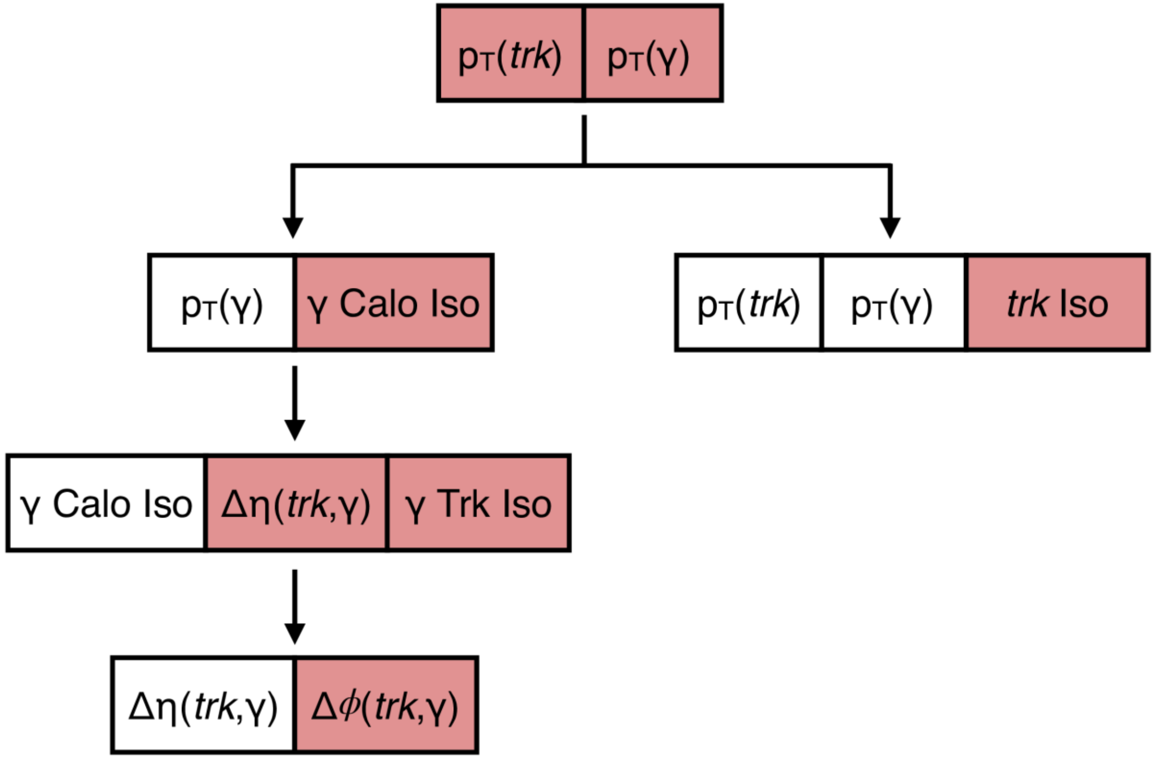

Track + Photon Category

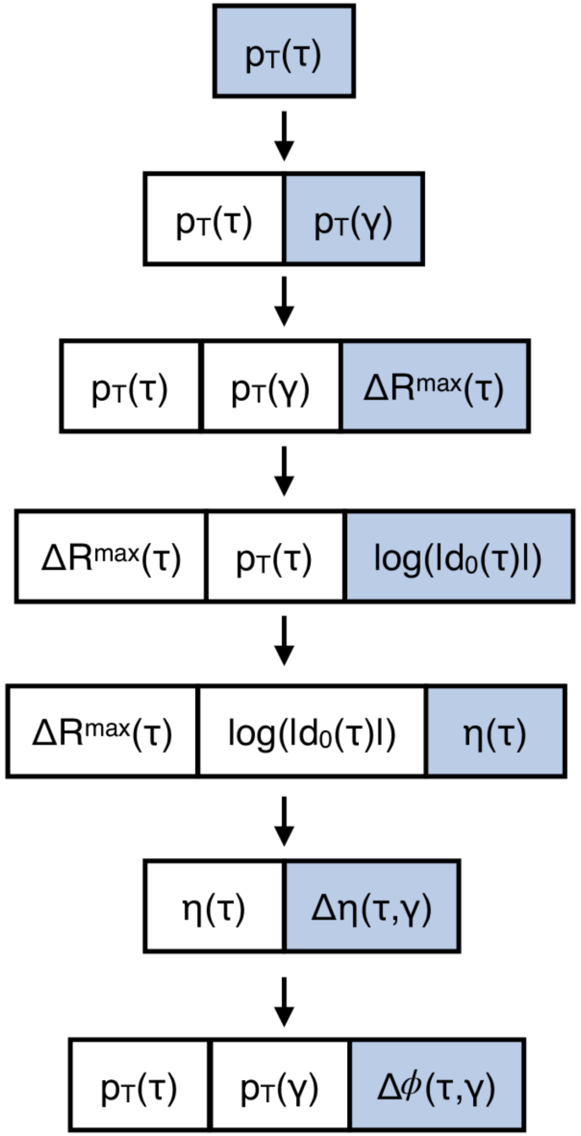

τ + Photon Category

arXiv:2309.15887

$W^{\pm} \rightarrow (\pi^{\pm}, K^{\pm}, \rho^{\pm})\gamma$: Background Validation

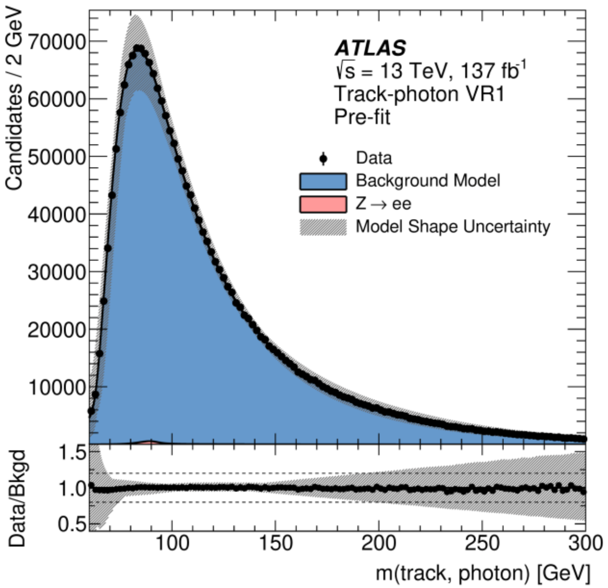

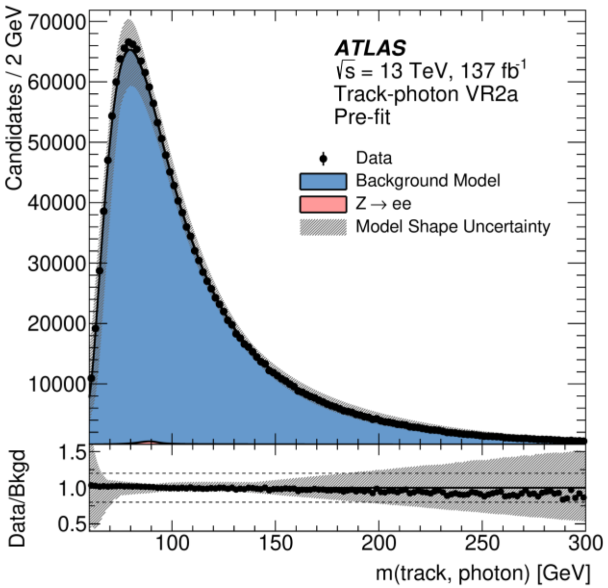

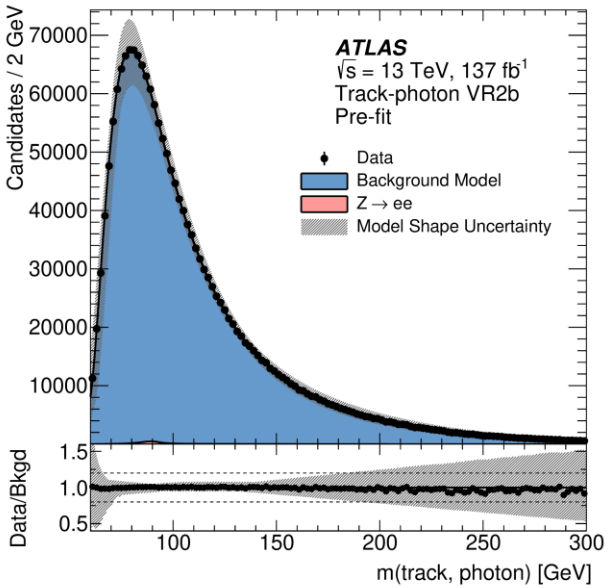

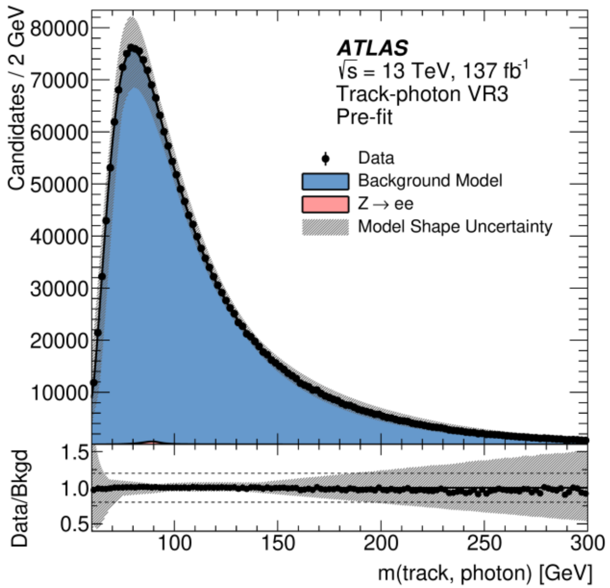

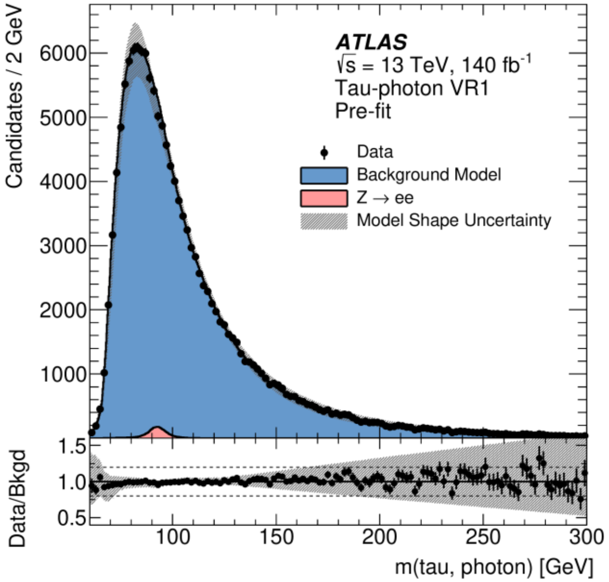

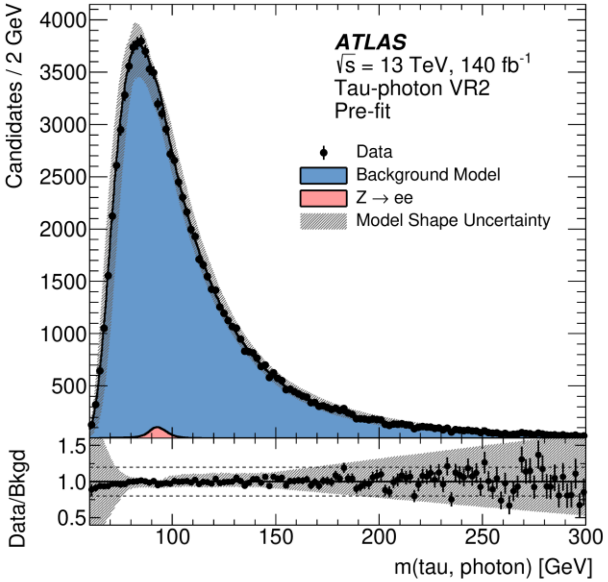

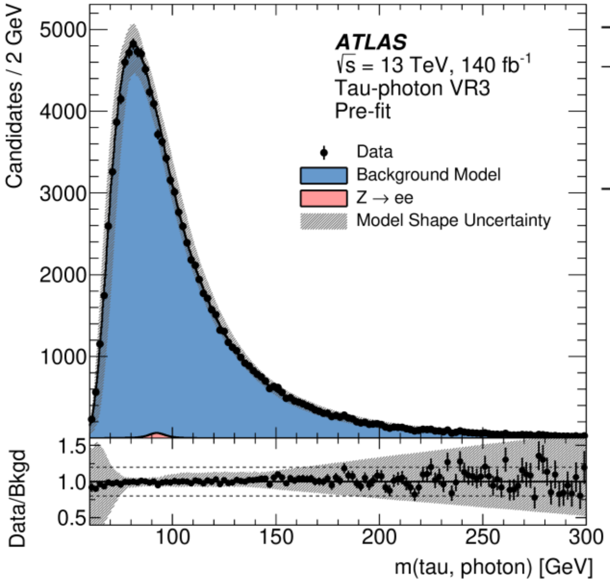

Track-photon		Tau-photon	
VR1	$p_{\mathrm{T}}(M) > 33\,GeV$	VR1	$p_{\mathrm{T}}(M) > 30\,GeV$
VR2a	Photon calorimeter isolation	VR2	$\Delta R_{\tau_{\mathrm{had}}} < 0.065$
VR2b	Photon track isolation	VR3	$\log\|d_0\| < -1.2$
VR3	Meson isolation		

arXiv:2309.15887

$W^{\pm} \rightarrow (\pi^{\pm}, K^{\pm}, \rho^{\pm})\gamma$: Results 2

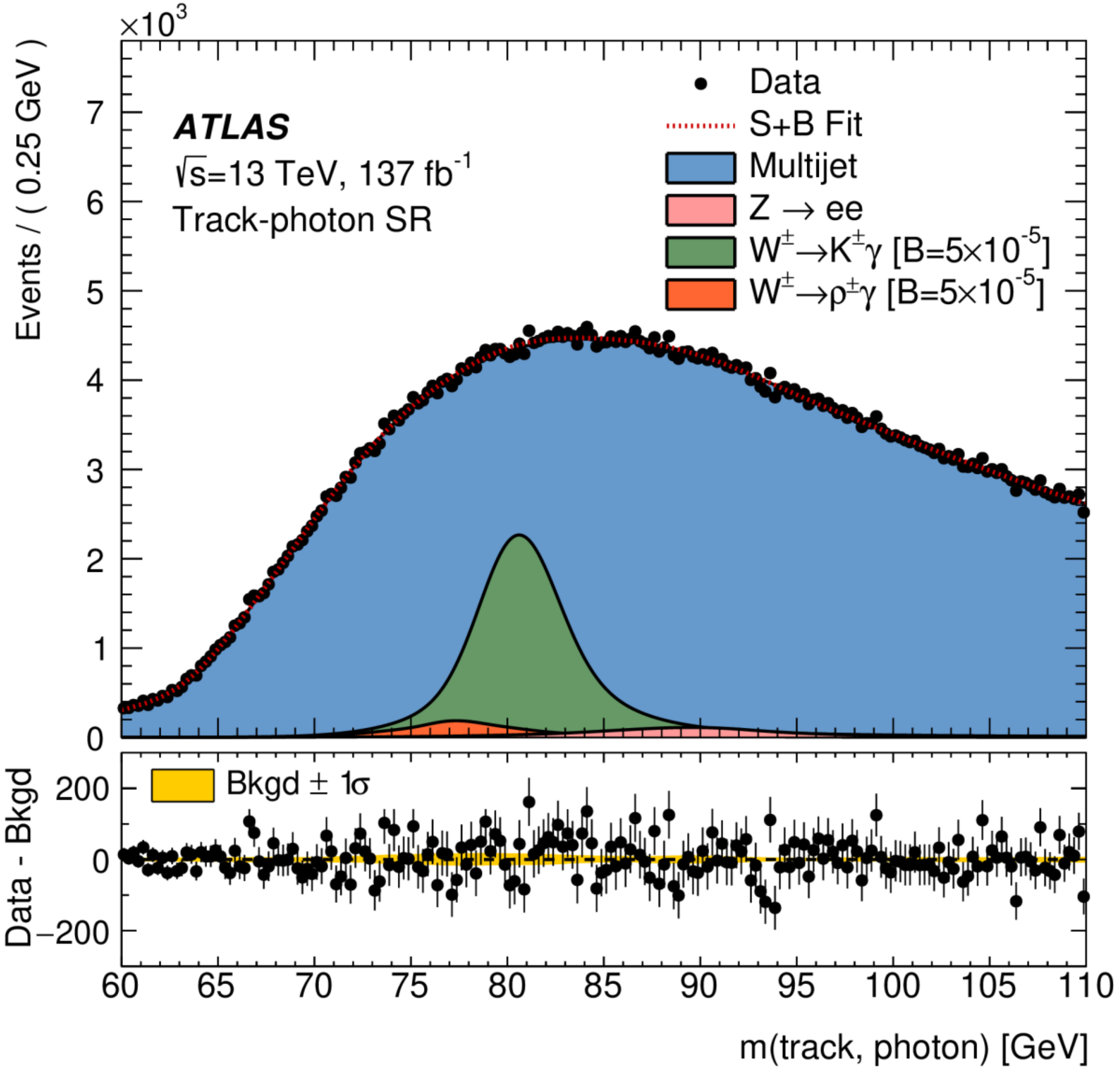

	Number of events	
	Track-photon SR	Tau-photon SR
Multijet	632000 ± 2200	43200 ± 600
$Z \rightarrow e^+e^-$	6100 ± 1500	-200 ± 400
$W^{\pm} \rightarrow \pi^{\pm}/K^{\pm}\gamma$	1000 ± 800	–
$W^{\pm} \rightarrow \rho^{\pm}\gamma$	-100 ± 400	-90 ± 240
Data	638962	42918

arXiv:2309.15887